Reprogramming Immune Cells in situ

A Targeted LNP Delivery Technology Utilizing IVT mRNA

Lemgart, Viktor T.

Publication date:
2023

Document Version
Publisher's PDF, also known as Version of record

sanofi

Reprogramming Immune Cells *in situ*

A Targeted LNP Delivery Technology Utilizing IVT mRNA

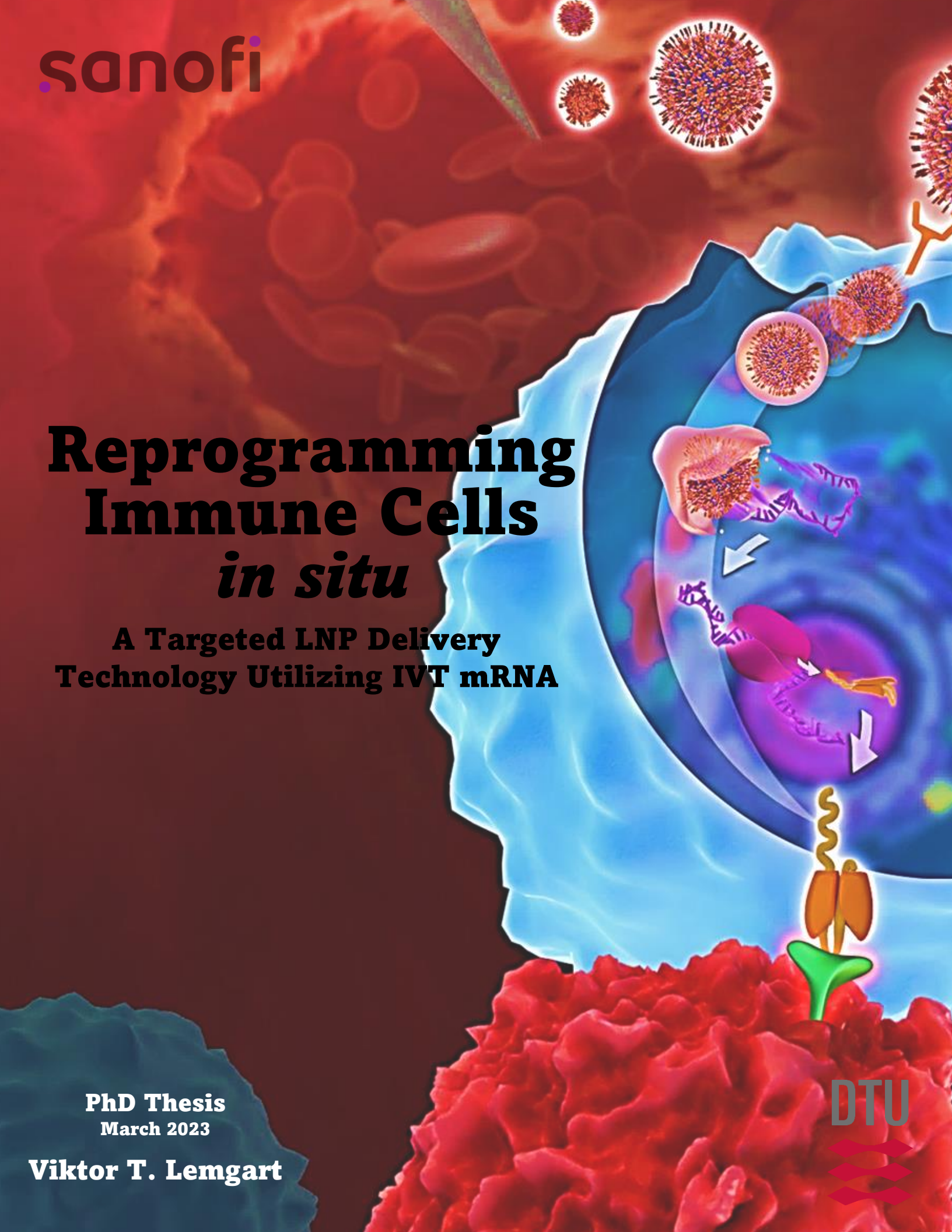

PhD Thesis
March 2023

Viktor T. Lemgart

DTU

THIS PAGE IS INTENTIONALLY LEFT BLANK
TO MATCH PAGINATION OF PRINTED THESIS

Tidal Therapeutics (a Sanofi Company)
350 Water Street, Cambridge,
MA 02141, USA

Technical University of Denmark
Department of Health Technology
Colloids and Biological Interfaces (CBIO) Group
Produktionstorvet, building 423,
2800 Kongens Lyngby, Denmark

Student number: s163695
Phone: +1 (857)-919-1935 // +45 21433235
Email: viklem@dtu.dk // viktor.lemgart@sanofi.com

Preface

March 31st, 2023

Boston, MA, USA

This dissertation is submitted as part of the requirements for obtaining a PhD degree from the Technical University of Denmark (DTU). The research described within this thesis was conducted between May 2021 and March 2023 at Tidal Therapeutics (a Sanofi Company) located in Cambridge, MA, USA.

From Tidal Therapeutics, Ulrik Nielsen served as the primary supervisor on the project with initial co-supervision by Austin Boesch followed by co-supervision by Andrew Sawyer. From DTU, Thomas Lars Andresen initially served as the primary supervisor followed by Anders Elias Hansen.

The thesis is divided into four chapters consisting of a theoretical introduction chapter (Chapter I), which will lay the foundation for the research conducted herein, two project chapters (Chapter II and III) describing some of the research conducted during the PhD, and a conclusion and future directions chapter (Chapter IV), which will summarize the research and discuss the time ahead for the platform and the individual projects. Researchers who have contributed significantly to the research described will be acknowledged in the individual chapters. All references will be compiled at the end of the dissertation.

A substantial part of my research throughout the last two years has involved the development of a clinical drug candidate with a leading focus on CAR design and engineering, which due to legal reasons will not be disclosed herein. However, I hope to soon follow this drug into the clinic and see how it may benefit cancer patients for whom other treatments may not promote disease regression. Additionally, substantial work on targeting strategies for reprogramming other immune cells than T-cells has been carried out but will also not be included herein as it would disclose proprietary data.

This PhD journey is one of few that combines research conducted in academia, a biotech startup, and *Big Pharma*.

Enjoy,

Viktor T. Lemgart

Acknowledgment

In the past two years, I have had the privilege of conducting my PhD research under Ulrik Nielsen. First, as part of a 10-person biotech startup company, Tidal Therapeutics, conducting novel drug development and research, and later as part of a 100.000-person *Big Pharma* company, Sanofi, with a focus on accelerating a lead drug candidate toward the clinic. Ulrik has been an outstanding mentor whom with very few words are able to say a lot and I am thankful for the experience I have gained under Ulrik and trust that we will be working together in the future.

I also wish to thank Austin Boesch who have been a great advisor and taught me valuable skills within the field of protein engineering. Additionally, I express my gratitude to Andrew Sawyer who have advised me toward the end of my PhD and have given me significant insights into project management and how to advance a drug toward clinical trials. I feel honored to have worked alongside Daryl Drummond and William Kuhlman throughout the last few years as they have helped me gain a greater understanding of the field thanks to their extensive scientific knowledge. Finally, I want to thank the entire Tidal team who have worked tirelessly toward one common goal – to develop medicines that one day can benefit cancer patients worldwide. Outside of Tidal, I want to express my gratitude to Yannis Hara who gave me the opportunity to contribute to scientific projects related to sickle cell anemia, which resulted in three publications.

On the non-scientific side, my appreciation goes to my family for their support and understanding of my dedication to the work. Particularly, I want to thank my little nephew, Luka, who always manages to put a smile on my face. I hope that he one day will be inspired to read the work described here. I wish to express how thankful I am for my friends, Gustav, Marcus, and Magnus that despite being on another continent continue being supportive and are an important part of my life. I also want to take this opportunity to thank my friend Mike, whom besides being a fantastic colleague at Tidal, showed me the beauty of New England and became my source to cultural enrichment while in the United States.

Finally, I want to express my appreciation to the love of my life, Victoria, for her unwavering support and encouragement throughout this project. Having been on this adventure with you has been nothing less than incredible and I cannot wait for the many ahead.

Abstract

Cancer immunotherapy has become a standard pillar of cancer treatment throughout the last decade. Immune checkpoint inhibitors (ICIs) and adoptive cell therapies (ACTs) such as tumor-infiltrating lymphocytes, tumor-specific T-cell receptor-modified T-cells, and chimeric antigen receptor (CAR)-engineered T-cells have proven successful in initiating an immunologic response against various cancers. Unfortunately, not all patients respond to ICIs and ACTs requires cumbersome and expensive processes.

For currently approved CAR-T therapies, T-cells are first extracted from the patient by leukapheresis followed by being transduced with lentivirus that encodes the CAR. CAR-expressing T-cells are then expanded over a two-week period before finally being re-administrated to the patient. Besides the substantial manufacturing costs associated with this therapy, CAR-T cells often cause toxicity-related side effects upon infusion.

This thesis aims to develop a strategy that allows for the generation of transient CAR-transfected T-cells *in situ* to treat hematological malignancies and thus overcome the limitations associated with currently approved CAR-T therapies. The technology uses in vitro transcribed synthetic mRNA that is formulated in lipid nanoparticles (LNPs) as a systemically injectable drug. The LNPs are directed to circulating T-cells via an antibody-based targeting moiety to transiently express disease-specific receptors, thereby bypassing the need to extract, culture, and reinfuse lymphocytes into patients. The thesis then aims to demonstrate the broad applicability of the technology beyond hematological malignancies by targeting other immune cell subsets to overcome solid tumors.

First, we demonstrate that the technology can be used to deliver reporter mRNA specifically to human T-cells. We then show that the platform enables specific delivery of functional CAR-encoding mRNA to circulating T-cells directly *in vivo*. Finally, we extend the application of the technology to reprogram T-cells to become bi-specific T-cell engager-secreting factories, thereby reducing solid tumor burden in mice.

Overall, this thesis demonstrates the development and potential applications of a novel groundbreaking immunotherapeutic technology. This technology holds strong promise to be employed in the clinic to treat various cancers and thus improve the lives of patients worldwide.

Resumé (Abstract in Danish)

Cancerimmunterapi er igennem det seneste årti blevet en velimplementeret type af kræftbehandling. Immune checkpoint-inhibitorer (ICI'er) og adoptive celleterapier såsom tumor-infiltrerende lymfocytter, tumor-specifikke T-celle-receptor-modificerede T-celler og chimeric antigen-receptor (CAR)-konstruerede T-celler har vist sig at være vellykkede i initieringen af et immunologisk respons mod forskellige kræftformer. Desværre reagerer ikke alle patienter på ICI'er, og adoptiv celleoverførsel er en omstændig og dyr proces.

For nuværende godkendte CAR-T-terapier ekstraheres T-celler først fra patienten ved leukaferese efterfulgt af at blive transduceret med lentivirus, der koder for CAR. CAR-udtrykkende T-celler ekpanderes derefter over en periode på ca. to uger, før de endelig administreres til patienten. Udover de betydelige produktionsomkostninger, der er forbundet med denne type af terapi, forårsager CAR-T-celler ofte toksicitetsrelaterede bivirkninger ved infusion.

Denne afhandling har til formål at udvikle en strategi, der muliggør genereringen af transiente CAR-transfekterede T-celler *in situ* til at behandle hæmatologiske kræftsygdomme og dermed overkomme begrænsningerne forbundet med godkendte CAR-T-terapier. Teknologien bruger in vitro transskriberet syntetisk mRNA, der er formuleret i lipid nanopartikler (LNP'er) som et systemisk injicerbart lægemiddel. LNP'erne er rettet mod cirkulerende T-celler via en antistofbaseret modalitet, der muligør transient ekspression af sygdomsspecifikke receptorer og derved omgås behovet for at ekstrahere, dyrke og genadministrere T-celler til patienter. Afhandlingen har derudover til formål at demonstrere den brede anvendelighed af teknologien ud over hæmatologiske kræftsygdomme ved at transfektere andre immunceller til behandling af solide tumorer.

Først demonstrerer vi, at teknologien kan bruges til at levere reporter mRNA til human T-celler. Vi viser derefter at platformen can anvendes til at levere funktionelt CAR-kodende mRNA til cirkulerende T-celler direkte *in vivo*. Afslutningsvis udvider vi brugen af platformen til at omprogrammere T-celler til at blive bi-specifikke T-celle engager-producerende fabrikker og derved behandle solide tumorer.

Samlet set demonstrerer denne afhandling udviklingen og potentielle anvendelser af en ny banebrydende immunoterapeutisk teknologi. Teknologien forventes at blive implementeret i klinikken til behandling af forskellige kræftformer og dermed forbedre livet for patienter verden over.

List of contributions

The PhD research described herein significantly contributed to a USD160 million acquisition deal and toward the development of a clinical drug candidate to treat hematological malignancies. Additionally, the author presented the work conducted at mRNA-, LNP-, cell therapy-, and oncology-focused conferences and discussed it on panel debates with expert leaders in the field. Finally, in addition to the publications listed below, a patent application and a publication for the lead drug candidate will be submitted.

Projects and related contributions included in this thesis:

i. **Viktor T Lemgart**, Allison Caron, Ralston Augspurg, Samantha Stewart, Michael Monte, Carrington Mcleod, Laura Strauss, Sanjana Kulkarni, William Kuhlman, Aaron Griset, Eyoung Shin, Christopher Borges, Andrew Sawyer, Austin Boesch, Ulrik Nielsen, Daryl Drummond
Using targeted LNPs to specifically deliver CAR mRNA to human T-cells in vivo
Manuscript ready for submission.

ii. **Viktor T Lemgart**, Ralston Augspurg, Allison Caron, Carrington Mcleod, Brandon Quido, Samantha Stewart, Michael Monte, Rasmus Münter, Unnur Jóna Björgvinsdóttir, Doha Ghannam, Andrew Sawyer, Ulrik Nielsen, Austin Boesch, Daryl Drummond
Reprogramming murine T-cells in situ to secrete and capture anti-tumoral BiTEs utilizing IVT mRNA
Manuscript ready for submission.

Other projects with related contributions not included in this thesis:

i. Yannis Hara, **Viktor T Lemgart**, Nis Halland, Kiana Mahdaviani, Jean-Antoine Ribeil, Samuel Lessard, Alexandra Hicks, David R Light.
SGK1 Inhibition Induces Fetal Hemoglobin Expression and Delays Polymerization in Sickle Erythroid Cells
Published, Blood Advances. DOI: 10.1182/bloodadvances.2022008710

ii. Yannis Hara, Emily Kawabata, **Viktor T Lemgart**, Paola G Bronson, Alexandra Hicks, Sriram Krishnamoorthy, Nicholas Watkins, Robert Peters, David J Roberts, Emanuele Di Angelantonio, John Danesh, William Astle, Dirk S Paul, Samuel Lessard, Adam S Butterworth.
Inhibition of MRP1 Induces Fetal Hemoglobin through NRF2 Activation to Protect Human Erythroid Cells from Sickling
Conference abstract, American Society of Hematology.

iii. Yannis Hara, Emily Kawabata, **Viktor T. Lemgart**, Paola G. Bronson, Alexandra Hicks, Robert Peters, Sriram Krishnamoorthy, Jean-Antoine Ribeil, Lisa J. Schmunk, Jennifer Eglinton, Nicholas A. Watkins, David J. Roberts, Emanuele Di Angelantonio, John Danesh, William J. Astle, Dirk S. Paul, Samuel Lessard, Adam S. Butterworth.
Genomic discovery and functional validation of MRP1 as a novel fetal hemoglobin modulator and potential therapeutic target in sickle cell disease
Manuscript in review, Nature.

iv. Yannis Hara, **Viktor T. Lemgart**, Samuel Lessard, Courtney J. Mercadante, Jean-Antoine Ribeil, Alexandra Hicks, Pauline Rimmele, David R. Light
AMPKβ1 Activators Induce Fetal Hemoglobin in Human Erythroid Cells and Sickle Mice Through Noncanonical Nrf2 Pathway
Manuscript in review, Science Translational Medicine.

Abbreviations

ABC	Accelerated blood clearance
ACT	Adoptive cell therapy
APC	Allophycocyanin
ApoE	Apolipoprotein E
ATCC	American Type Culture Collection
BiTE	Bi-specific T-cell engager
CAR	Chimeric antigen receptor
CMC	Chemistry, manufacturing, and controls
circRNA	Circular RNA
COVID-19	Coronavirus disease 2019
CRS	Cytokine release syndrome
CTLA4	Cytotoxic T lymphocyte antigen 4
DAMP	Damage-associated molecular pattern
DC	Dendritic cell
DLS	Dynamic light scattering
dsRNA	Double-stranded RNA
EphA2	Ephrin receptor A2
EPR	Enhanced permeability and retention
Fab	Fragment antigen-binding
Fluc	Firefly luciferase
GFP	Enhanced green fluorescent protein
ICI	Immune checkpoint inhibitor

IL	Interleukin
IFN	Interferon
Ig	Immunoglobulin
ITAM	Immunoreceptor tyrosine-based activation motif
IV	Intravenous
IVIS	In vivo imaging system
IVT	In vitro transcription
JAK	Janus kinase
LNP	Lipid nanoparticle
mAb	Monoclonal antibody
mRNA	messenger RNA
NHL	Non-Hodgkin lymphoma
ORF	Open reading frame
PEG	Polyethylene glycol
PD-1	Programmed cell death protein 1
PD-L1	Programmed death-ligand 1
PDI	Polydispersity index
polyA	Polyadenylated
RNA	Ribonucleic acid
RPMI	Roswell Park Memorial Institute
saRNA	Self-amplifying RNA
SC	Subcutaneous
scFv	Single-chain variable fragment

siRNA	Small interfering RNA
STAT	Signal transducer and activator of transcription
TCR	T cell receptor
TIL	Tumor-infiltrating lymphocyte
TLR	Toll-like receptor
TME	Tumor microenvironment
TRUCK	T-cell redirected for universal cytokine-mediated killing
UTR	Untranslated region
VHH	Variable domain of heavy-chain antibody

Table of Contents

Table of Figures

Table of Supplemental Figures

Chapter I | Introduction

I.1 | The past and the presence of cancer immunotherapy

The utilization of a patient's own immune system to selectively target cancer cells, known as cancer immunotherapy, has become a standard pillar of cancer treatment [1, 2]. Several strategies for modulating the immune system into fighting off cancerous cells have already been approved by regulatory agencies while new therapies are still being developed [3]. Two approaches, where clinically approved therapies currently exist, include immune checkpoint inhibitors (ICIs) and adoptive cell therapies (ACTs) [2]. Immune checkpoint therapy involves blocking various immune system checkpoints that cancer cells use to evade the recognition and elimination by the immune system's healthy T-cells. Programmed cell death 1 (PD1) and cytotoxic T lymphocyte antigen 4 (CTLA4) are two well-studied T-cell immune checkpoints, and the discovery that these could be targeted with ICIs in patients with melanoma ultimately earned pioneers James P. Allison and Tasuku Honjo the Nobel Prize in Physiology or Medicine in 2018 [3-5]. Before the approval of the first ICI in 2011 (ipilimumab, an anti-CTLA4 antibody), it was unimaginable that complete remission, being the complete disappearance of all visible metastases, could be achieved in 20% of patients with melanoma. However, this is the case today in melanoma patients treated with ICIs where long-term remission is observed even after treatment discontinuation [6, 7]. Additionally, seven FDA-approved monoclonal antibodies (mAbs) that target PD1 or its ligand PDL1 have demonstrated unprecedented clinical efficacy in several cancer types including non-small cell lung cancer, renal cell carcinoma, and metastatic melanoma [8, 9].

Unfortunately, not all cancer types respond well to ICIs and the population of cancer patients where ICI treatment does not result in a complete response, either by patients having required or primary resistance, still constitutes the majority [6, 10, 11].

Another strategy used to modulate the immune system to attack cancer cells is to treat patients directly with modified effector cells [12]. Here, cells are first harvested from the patient, then either modified or directly cultured and expanded *ex vivo* before finally being reinfused into the host [13, 14]. Tumor-infiltrating lymphocytes (TILs), tumor-specific T-cell receptor (TCR)-modified T-cells, and chimeric antigen receptor (CAR)-engineered T-cells are types of modified immune cells that, upon transfer into the patient, initiate an immunologic response against the cancer cells [14-16]. However, though often proven very potent and efficacious, ACT-based strategies often come with their own set of challenges related to product safety, reproducibility, costly and time-consuming manufacturing, and the need for patient preconditioning therapy such as lymphodepleting chemotherapy resulting in increased risk and difficulties in reaching a broad patient population [17-19]. But what if we did not have to extract the patient's cells to modify them? What if we could deliver a message to the immune system to instruct it to make the necessary changes directly in its own environment – *in situ* – to fight the tumor cells? First, this would help circumvent the *ex vivo* manipulation and reinfusion of engineered cells, which is often associated with severe toxicities [20, 21]. Second, this could allow for significantly driving down the treatment costs compared to the current costly therapies and thus make it available to a broader patient population [22]. Developing such groundbreaking strategies is the scope of this thesis.

However, to better define novel strategies for developing improved immunotherapies an understanding of the interaction between cancer and the immune system is first required. In the following sections, we will scratch the surface of how the interplay between the development of cancer and the healthy immune system functions.

I.2 | How does cancer become cancer?

In 2000, Douglas Hanahan and Robert Weinberg proposed a set of functional capabilities acquired by normal human cells that allow them to become malignant tumors. These capabilities became known as the first generation of the *Hallmarks of Cancer* and constituted the acquired ability of cells to sustain proliferative signaling, evade growth suppressors, resist cell death, enable replicative immortality, induce angiogenesis, and activate invasion and metastasis [23]. In 2011, after a decade of progress in understanding the underlying cancer-related biology, Hanahan and Weinberg proposed *the next generation* of hallmarks [24]. The improved understanding of the biological complexity of tumor formation led to the proposition of two *emerging* hallmarks and two *enabling characteristics*, which included the ability to evade immune destruction and reprogramming cellular metabolism as the emerging hallmarks and the instability and mutations in the genome and tumor-promoting inflammation as the enabling characteristics. Finally, in 2022, Hanahan proposed *new dimensions* for the hallmarks [25]. Here, Hanahan proposed four additional *emerging hallmarks* and *enabling characteristics* that involved unlocking phenotypic plasticity, senescent cells, non-mutational epigenetic reprogramming, and polymorphic microbiomes. Overall, through more than two decades of research, these generations of the first proposed

and now widely accepted hallmarks, emphasize how the understanding of the underlying cancer biology continuously advances.

Having laid out some of the principles for tumor cell development through the *Hallmarks of Cancer* it is important to note the paradox that some of these same principles also enable the immune system to generate a response resulting in cancer cell elimination [26]. One concept that provides an explanation for how and why the immune system can elicit a T-cell response resulting in tumor cell recognition and eradication, is known as the *Cancer-Immunity Cycle* and was proposed by Daniel Chen and Ira Mellman in 2013 (Figure I-1) [27]. The Cancer-Immunity Cycle is a seven-step cyclic process that can be self-propagating starting and ending with the death of a cancer cell resulting in the release of neoantigens. After cancer cell antigens are released (step 1), antigen-presenting cells will capture, process, and present the antigens on MHCI or MHCII molecules (step 2) to T-cells in the lymph node (step 3). If the specific cancer cell-derived antigen is viewed as foreign by the T-cell and if central tolerance has been incomplete, the recognition will result in priming and activation of a cancer antigen-specific effector T-cell response. The activated effector T-cells then traffic to (step 4) and infiltrate (step 5) the tumor, followed by the specific recognition of the neoantigen presented on MHCI through the TCR (step 6), and finally resulting in target cancer cell killing (step 7). Hereafter, additional neoantigens can be released (step 1) and the cycle can repeat, which increases the breadth of the response. Needless to say, in cancer patients, the cycle described above does not perform optimally.

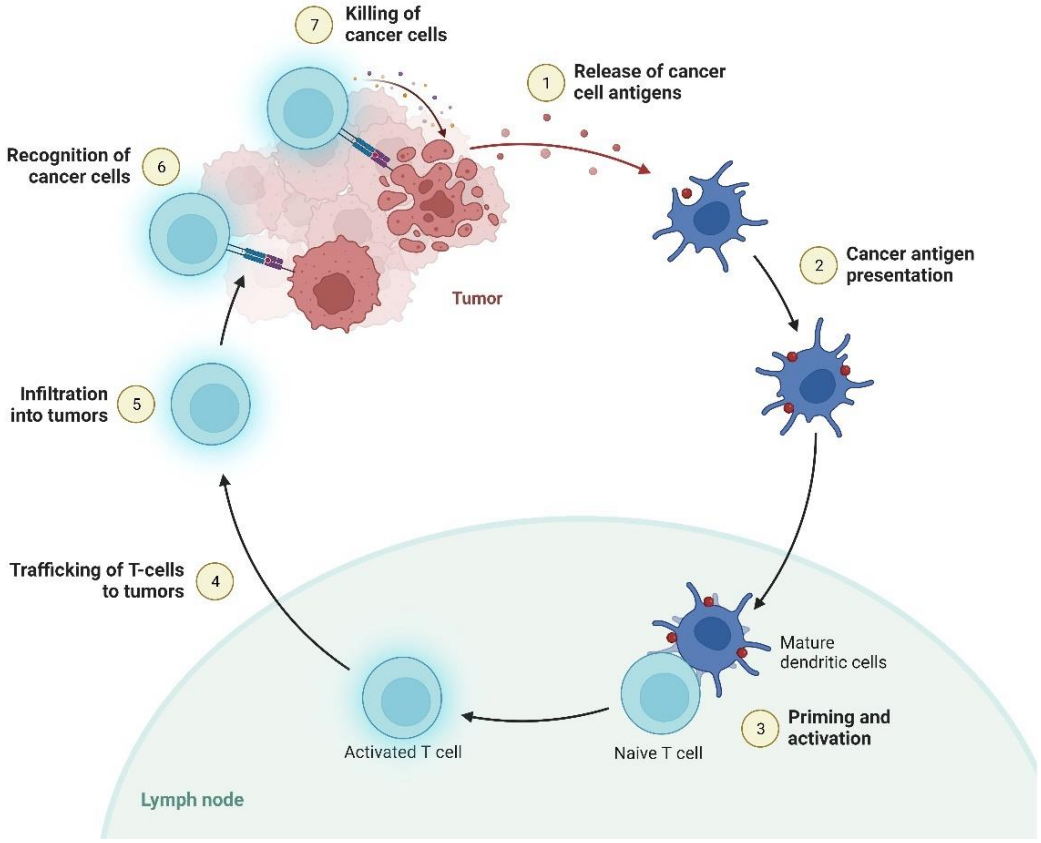

Figure I-1. The Cancer-Immunity Cycle.

In the same review where the Cancer-Immunity Cycle is conceptualized, Chen and Mellman provide examples of how certain therapies can affect different steps of the cycle [27]. One example constitutes how chemo- and radiation therapy can promote step 1 of the cycle. Broadly, exogenous stimuli such as chemotherapy and radiation result in the release of damage-associated molecular patterns (DAMPs), which can directly elicit host immune responses [28]. Another example included in the conceptualization by Chen and Mellman describes how cancer vaccines can accelerate anti-cancer immunity by promoting cycle step 2 [27]. Here, antigen-presenting cells such as immature dendritic cells (DCs) can be

targeted with vaccines to initiate a tumor-specific T-cell response. Several engineering strategies for DC-based vaccines exist and include tumor-associated antigens or neoantigens encoded and delivered as mRNA, synthesized as peptides, or viral vectors [29, 30]. As a third example, Chen and Mellman describe how IL-2 therapy is part of cycle step 3 [27]. It has previously been shown that IL-2 is required for the generation of robust T-cell responses and T-cell survival [31]. Thus, therapeutic strategies involving the administration of IL-2 have been investigated. However, IL-2 immunotherapy has been shown to have critical drawbacks such as short half-life *in vivo* and severe toxicity at the therapeutic dosage [32]. Two final therapeutic examples of how the Cancer-Immunity Cycle can be targeted include the engineering and administration of CAR-T cells to directly recognize and kill cancer cells to promote step 6 of the cycle and the blocking of PD1 using anti-PD1 antibodies to remove the inhibition of cancer cell killing by T-cells at cycle step 7 [27].

Since this review was published in 2013, cancer immunotherapy has continued to revolutionize the field of oncology, which has led to a rapid increase in the number of novel immunotherapeutic strategies [33-35]. By improving our understanding of the inherent cancer-related immune biology these strategies can help further improve current treatments.

I.3 | Changing the game of immunotherapy treatments

As briefly introduced, CAR-T cells constitute a type of adoptive cell immunotherapy that can be used to enhance the immune response against tumor cells [16]. CAR-T therapy has truly been a game changer in the treatment of B-cell acute lymphoblastic leukemia and B-

cell lymphoma since its first approvals of tisagenlecleucel (Kymriah, Novartis) and axicabtagene ciloleucel (Yescarta, Kite), respectively, in 2017 [36, 37]. Prior to the introduction of CAR-T cells in the clinic, the prognosis for most patients with these B-cell malignancies was poor and patients often relapsed or were refractory to previous treatments. However, initial clinical studies using autologous CAR-T cells showed complete remission in patients that had been unresponsive to other cancer treatments [38, 39]. Today, a total of six CAR-T therapies have been approved by the FDA for use in the USA [40-43].

CARs are synthetic receptors that, independently of MHC presentation, can recognize native cell surface antigens [16, 44]. They are generally composed of four domains; the antigen recognition domain, the hinge domain, a transmembrane region, and one or multiple intracellular signaling domains (Figure I-2a) [45]. The antigen recognition domain or the binding domain is commonly comprised of a single-chain variable fragment (scFv) derived from a mAb. The complementarity-determining regions (CDRs) of the scFv determine where on the target antigen the CAR binds [46]. Studies have shown that the distance between the CAR-T cell surface and the specific epitope that the scFv recognizes is important in the design of the hinge and in establishing the optimal hinge length. Short CAR hinges are more effective in binding membrane-distal epitopes whereas longer hinges allow better access to epitopes that are proximal to the target cell membrane [47, 48]. The transmembrane domain serves as an anchor of the CAR in the T-cell membrane and consists of a hydrophobic α helix. Both the hinge and the transmembrane domain are often derived from CD8α or CD28 [46, 49]. The intracellular portion of the CAR contains the functional domains that initiate T-cell activation upon antigen recognition. By incorporating a CD3ζ-

derived domain containing immunoreceptor tyrosine-based activation motifs (ITAMs) into the construct, CAR-mediated signaling mimics that of the endogenous T-cell antigen receptor (TCR) [50]. Following the binding of the target antigen the ITAMs become phosphorylated, which starts the downstream signaling cascade leading to T-cell activation [51]. CAR constructs containing a single intracellular CD3ζ domain became recognized as the first generation of CARs (Figure I-2b). Second-generation CARs, incorporating a CD28- or 4-1BB-derived co-stimulatory domain, were then developed based on the understanding of a co-stimulatory signal required for optimal activation in physiological T-cell responses. The introduction of one of these co-stimulatory molecules significantly improves IL-2 secretion, T-cell proliferation, and target cell killing over the first generation of constructs [52]. The third generation of CARs is engineered by incorporating multiple co-stimulatory domains (e.g., both CD28 and 4-1BB) to enhance cytokine potency and CAR-mediated killing [53]. Enhanced antitumor activity with the fourth-generation CARs, also known as T-cells redirected for universal cytokine-mediated killing (TRUCKs), is achieved by including a transgene that allows for increased cytokine secretion [54, 55]. Finally, with the latest advancement in CAR designs, the fifth generation, introduces a fragment of the IL-2 receptor β (IL-2Rβ). Upon binding, the IL-2Rβ fragment mediates activation of the JAK/STAT pathway, which promotes T-cell proliferation and increases the persistence of CAR-T cells [56, 57].

Although CAR-T therapy has proven to be revolutionary in cancer treatment with impressive clinical responses against hematological malignancies, barriers still remain to increasing the therapeutic response and limit the CAR-T cell-associated toxicities. The most

commonly observed side effect of CAR-T therapy is cytokine release syndrome (CRS) also known as “cytokine storm”. CRS is a consequence of CAR-T cell activation upon target engagement, which results in the release of large amounts of cytokines such as IL-6, IL-10, and IFN-γ [58, 59]. Clinically, CRS can range from patients having mild fever and headache to severe cases where patients may experience cardiac dysfunction or multiorgan system failure, which possibly can progress to death [60, 61]. Another toxicity that is commonly observed after CAR-T cell therapy is immune effector cell-associated neurotoxicity syndrome (ICANS). Similar to CRS, ICANS vary in severity where critically affected patients may experience seizures and cerebral edema [36].

Besides the toxicities observed in the treatment of hematological malignancies, another limitation of CAR-T therapy is the lack of efficacy observed in solid tumor treatments. The absence of tumor-specific antigens, the immunosuppressive tumor microenvironment (TME), and the limited trafficking of CAR-T cells to the tumor site are some of the pivotal challenges in the fight against solid tumors [62, 63].

Finally, the costs associated with CAR-T treatments provide a significant limitation for reaching a broad patient population. With tisagenlecleucel and axicabtagene ciloleucel being marketed at more than USD350,000 per infusion, excluding the costs associated with the monitoring of disease status, additional procedures, and extended hospitalization stays, these potentially lifesaving treatments are inaccessible for most patients [64, 65].

Thus, developing the next generation of CAR-T therapies is necessary to not just change the game against cancer but for the clinicians and patients to win it.

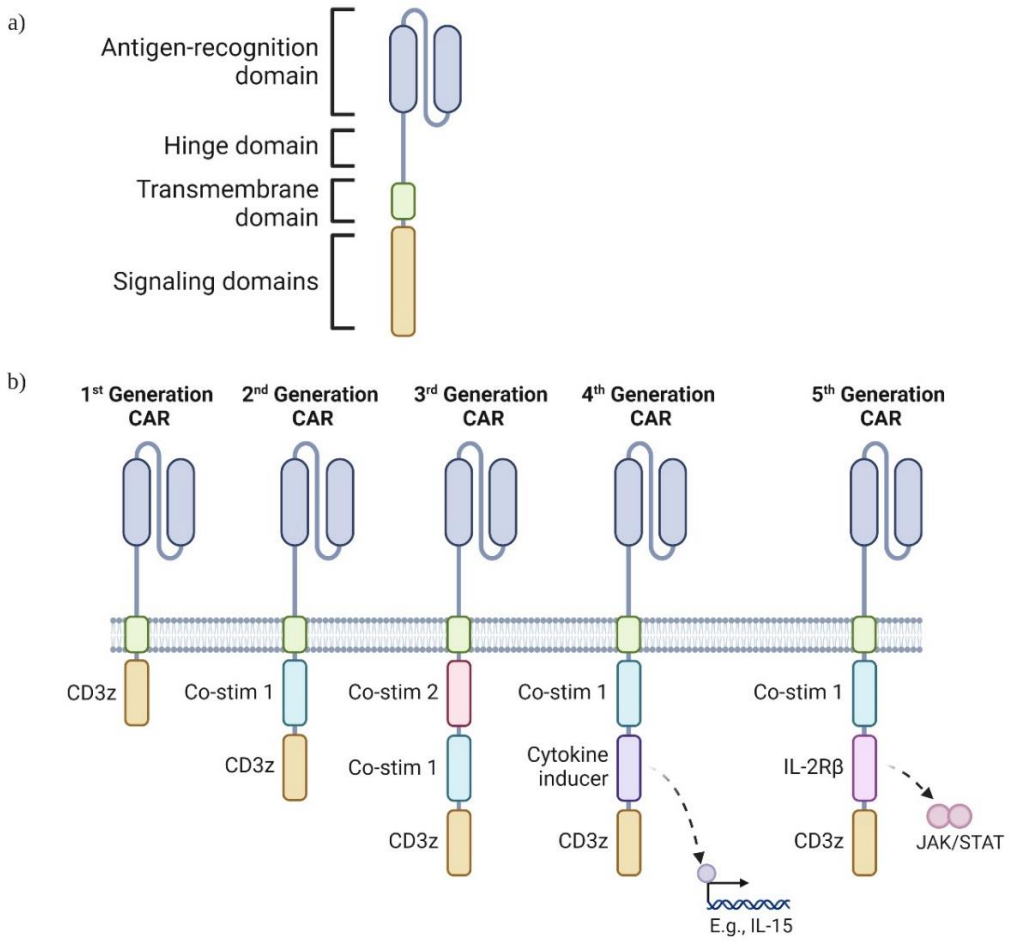

Figure I-2. Structure and generations of Chimeric Antigen Receptors.

a) The general composition of a CAR. b) The current generations of CAR designs. CAR, chimeric antigen receptor; co-stim, co-stimulatory domain. Created with BioRender.com.

I.4 | mRNA therapeutics - a new class of drugs

In December 2019, a novel coronavirus named SARS-CoV-2 causing coronavirus disease 2019 (COVID-19) started spreading globally. This lead the World Health Organization to declare a pandemic on March 12, 2020 [66]. Before the end of the same year, two vaccines were approved by the FDA through emergency use authorization in the United States [67].

Both vaccines, developed by Pfizer/BioNTech and Moderna, respectively, relied on the delivery and translation of messenger RNA (mRNA) into its encoding viral spike protein to elicit the desired immune response and thus prevent COVID-19 [68, 69]. This did not only result in billions of administered doses worldwide, but it also sparked interest in mRNA as a means of delivering therapeutic proteins. The authorization of the two COVID-19 vaccines underlined the potential of developing mRNA-based drugs due to the high efficacy rates, short timeframe from target identification to clinical use, and the convincing safety profile [67, 70-73]. However, the development of mRNA therapeutics presents challenges that are different from those of mRNA vaccines. As previously reviewed by Rohner et. al., one of the key challenges in the clinical development of mRNA therapeutics versus vaccines is related to the required protein expression levels [70]. To address this challenge, various optimization strategies can be employed. In the following paragraphs, we will turn our attention to how increased protein expression can be achieved through modifications of various components of the mRNA (Figure I-3).

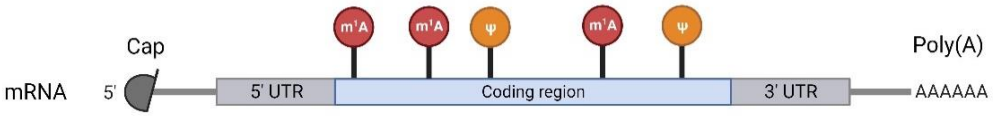

Figure I-3. IVT mRNA optimization strategies.

Therapeutic mRNAs, containing various regulatory elements, can be modified to achieve increased stability and translation and to decrease unwanted immunogenic reactions. UTR, untranslated region; m^1A, N1-methyladenosine; Ψ, pseudouridine. Created with BioRender.com.

While immunization using vaccines only requires minimal protein production due to its reliance on the immune system to amplify the desired response through cell-mediated and humoral responses, mRNA therapeutics require up to 1,000-fold higher levels of protein expression to reach a therapeutic threshold [74-76]. To increase the total protein expression in the cell, several strategies around optimizing the individual components of the mRNA have been developed. These components include the cap, the 5' and 3' untranslated regions (UTRs), the open reading frame (ORF), and the polyadenylated (poly(A)) tail [77-80]. The process by which mRNA is synthetically produced is known as in vitro transcription (IVT) [81]. As the name suggests, this process involves mimicking the cell's natural ability to transcribe DNA into mRNA using RNA polymerase enzymes [82]. IVT utilizes a DNA template encoding the sequence of interest which is transcribed following the addition of RNA polymerases derived from bacteriophages, such as T7 or SP6 [83]. Just like in a living cell, the polymerases selectively recognize the promoter region in the DNA template, catalyzing and initiating transcription. The result from this process is naked RNA transcripts where additional steps are taken to cap and polyadenylate the RNA molecules at the 5'- and 3'-end, respectively. The 5'-cap is vital for mRNA stability, translation, and self- versus non-self identification [82, 84] whereas the length of the 3'-poly(A) tail has been shown to be an important physiological determinant for translation efficiency and mRNA stability [85, 86]. UTRs are known to affect translation in eukaryotic cells and data suggests that optimal UTRs may vary depending on the cell type. Therefore, several UTR modifications have been proposed to increase protein expression [87, 88]. The ORF, marked by start and stop codons, encodes the protein of interest [89]. Here, the codon composition may affect translation efficiency where codons that are more frequently found in nature generally

increase translational yield as opposed to rare codons [90]. However, this is found to be highly dependent on the protein of interest and the desired application. As it is well known that RNA activates cells of the innate immune system by stimulating Toll-like receptor (TLR) 3, TLR7, and TLR8, the IVT process may incorporate naturally occurring modified nucleosides such as pseudouridine, N1-methyladenosine, or N1-methylpseudouridine. Studies have demonstrated that by integrating modified nucleosides into the transcript the TLR-mediated immunogenic response can be significantly reduced [91, 92]. Overall, by implementing the various mRNA modifications in the IVT process, the kinetic profile of the encoded protein can be modulated and altered as desired for the specific application [89]. Finally, one major contaminant in the IVT mRNA that may play a role in reducing protein expression levels is double-stranded RNA (dsRNA). Upon internalization from the extracellular space into the cytoplasm or endosome, cells sense dsRNA as a foreign invader, a pathogen-associated molecule pattern (PAMP), which triggers the activation of enzymes leading to inhibition of protein synthesis [93]. Additionally, dsRNA is recognized by TLR3, retinoic acid-inducible gene I (RIG-I), and melanoma differentiation-associated protein 5 (MDA5), which leads to the secretion of cytokines and elicitation of an often undesired immune response [94]. Several methods have been explored for the removal of dsRNA after the IVT process resulting in a purified mRNA product [93, 95-97].

However, achieving the desired purity and required level of protein expression to reach a therapeutic threshold only helps overcome *one* of the challenges associated with the development of mRNA therapeutics. Another challenge in the clinical development of mRNA

therapeutics constitutes achieving the desired delivery specificity. Thus, not just reaching the required level of protein expression, but getting it in the right place [70].

I.5 | mRNA delivery mediated by lipid nanoparticles

mRNA does not possess favorable characteristics to function as an individual therapeutic drug. The molecule must cross the cell membrane to reach the cytoplasm and become available for translation by the ribosome. Due to mRNA's relatively large size (1-15 kb) in comparison to other types of RNA (e.g., siRNA) and its overall negative charge, crossing the cell membrane, which is made up of a lipid bilayer and also maintains a negative potential, is an improbable task [98]. Additionally, prior to reaching the target tissue or cell, the naked mRNA is likely to be degraded by abundant levels of extracellular ribonucleases present in the skin and blood [99].

Apart from mRNA, another valuable tool that became increasingly known to the public following the success of the Pfizer/BioNTech and Moderna COVID-19 vaccines was lipid nanoparticles, abbreviated LNPs [100]. Both vaccines utilized LNPs to deliver the viral protein-encoding mRNA. Generally, LNP formulations consist of four main components including an ionizable lipid enabling endosomal escape, a helper lipid that resembles the lipids in the cell membrane and contributes to the stability and delivery efficiency, cholesterol that creates stability of the LNP, and a polyethylene glycol (PEG)-lipid that reduces protein absorption in circulation [100-103].

Ionizable lipids, consisting of a polar head group, a hydrophobic tail region, and a linker between the two domains, are designed to contain a neutral charge at physiological pH but to become protonated at low pH [100, 104]. Once trapped in the cells' endosome where the pH is decreased compared to the extracellular environment, the ionizable lipid becomes positively charged. This likely enables membrane destabilization and allows for the LNP and mRNA cargo to escape and become available for translation in the cytoplasm [105, 106]. Various strategies for designing and optimizing ionizable lipids to enhance cell-mediated uptake and drive endosomal escape have been explored. One such optimized lipid was MC3, which became a key component of the systemically delivered siRNA drug, Onpattro, which was approved in 2018 to treat hereditary transthyretin-mediated amyloidosis [107, 108]. Further improvement of the biodegradability by introducing cleavable ester bonds have shown to increase delivery efficacy and lead to faster elimination in circulation *in vivo* and thus improve tolerability [109]. This is the case for the lipids SM-102 and ALC-0315, which are the ionizable lipids used in the Moderna and Pfizer/BioNTech COVID-19 vaccines, respectively [100]. Several other ionizable lipid types have been explored for RNA delivery. Through appropriate lipid design, these can be engineered to modulate the LNPs' pharmacokinetic and pharmacodynamic profiles, their ability to transfect specific cell subsets, and their capability of driving endosomal escape for specific disease applications [104, 110-115].

Active targeting for cell specificity

The liver is the primary organ of LNP accumulation following systemic administration. After intravenous (IV) administration, PEG-lipids start to dissociate from the LNP surface followed by the recruitment of apolipoprotein E (ApoE) to the exposed LNP. ApoE is the main constituent that upon association with the LNP forms what is known as the LNP protein corona [116, 117]. Upon reaching the liver, LNPs extravasate through fenestrated endothelium and bind to ApoE-binding receptors on hepatocytes, such as the low-density lipoprotein receptor, which mediate uptake and thus clearance of LNPs [107, 118]. Additionally, tissue-resident macrophages of the liver, Kupffer cells, being part of the mononuclear phagocyte system (also known as the reticuloendothelial system) can play an important role in the elimination of LNPs [119, 120]. Though the delivery of mRNA to the cells of the liver has therapeutic potential, as demonstrated by the FDA approval of Onpattro, many diseases, such as most cancers, would benefit from non-liver targeting [101, 121]. Thus, to achieve clinically relevant tissue- and cell-specific delivery, improved delivery systems are required.

Specific tissue- and cell-targeting LNPs can be achieved by modifying the lipids and the composition of the formulation or by introducing targeting ligands that are conjugated to the LNP surface [121, 122]. Herein, passive targeting refers to strategies involving optimization of the lipid composition whereas active targeting refers to LNPs incorporating chemically conjugated specific targeting moieties.

Passive targeting strategies often involve regulating the size and the charge of the LNP. This can be achieved by changing the composition of the four lipid types used in the

formulation or by incorporating additional lipids that may alter the biodistribution of the LNP. Such strategies have been explored by several groups [123-131]. However, when successful, these strategies may only result in tissue-specific accumulation and not in cell-specific uptake.

To achieve cell-specific nucleic acid delivery various active targeting strategies can be utilized [121, 122, 132]. One such strategy involves relying on the specificity of antibodies. Here, an antibody-based targeting moiety (e.g., Ig, Fab, scFv, or VHH) with specificity for a chosen target on a cell of interest (e.g. a specific receptor on an immune cell) can be conjugated to a PEG lipid and incorporated into the surface of the LNP, thereby allowing for cell-specific uptake (Figure I-4) [130, 131, 133-137].

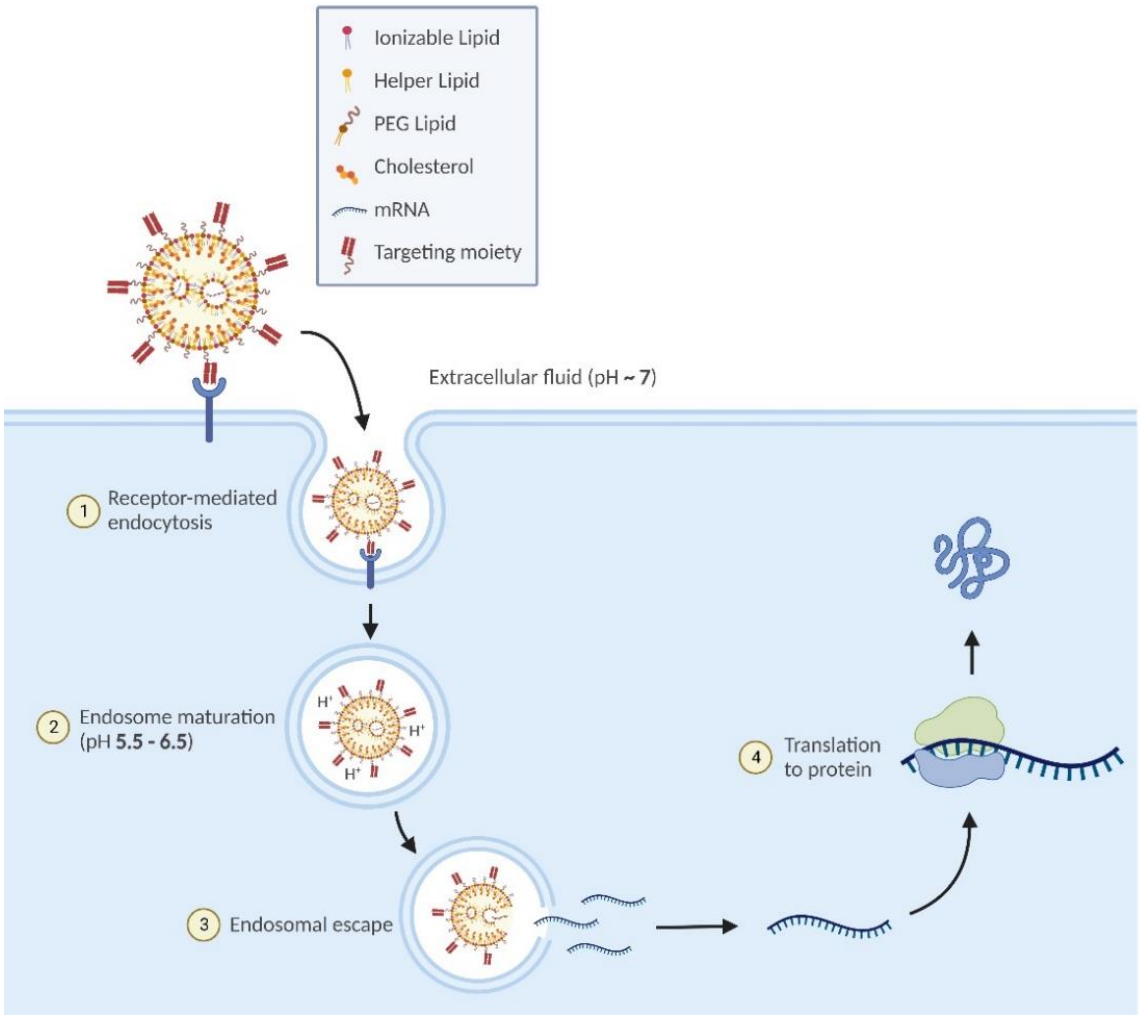

Figure I-4. An active targeting approach utilizing LNPs to deliver mRNA.

An antibody-based targeting moiety allows for receptor-mediated uptake of the LNP into the cell of interest (1). Upon maturation of the endosome the pH decreases resulting in protonation of the ionizable lipid (2) and leading to endosomal escape of the mRNA (3). The mRNA, now in the cytoplasm, is then available for translation by the ribosome into the encoded protein (4). PEG, polyethylene glycol; mRNA, messenger RNA. Created with BioRender.com.

I.6 | Developing a platform for reprogramming immune cells directly *in vivo*

In this thesis I have, in collaboration with Tidal Therapeutics (a Sanofi Company), developed a targeted LNP platform that can deliver therapeutic mRNA directly *in vivo* to specific immune cell subsets of interest and thereby modulate the immune response to treat cancers in a multifaceted way. The developed technology is based on previous research conducted in the laboratory of Mathias Stephan from the Fred Hutchinson Cancer Center in Seattle [138-140]. The excitement around this type of technology was exemplified by the acquisition of Tidal Therapeutics by Sanofi in 2021 for an upfront payment of USD 160 million and up to USD 310 million upon achievement of certain milestones [141]. Additionally, several other companies, such as Capstan Therapeutics, Sana Biotechnology, Umoja BioPharma, Interius BioTherapeutics, Turn Biotechnologies, and Moderna, are currently pursuing similar *in vivo*-based cell therapy strategies [142].

Applications of the platform established herein involve the delivery of CAR-encoding mRNA to human T-cells to fight hematological malignancies (Chapter II) and the delivery of Bi-specific T-cell Engager (BiTE)-encoding mRNA to murine T-cells to treat solid tumors (Chapter III). As mentioned above, the development of novel immunotherapeutic strategies based on the steps of the Cancer-Immunity Cycle to elicit a desired anti-cancer immune response is likely to prove beneficial for cancer patients [35]. The two novel approaches described herein can affect the Cancer-Immunity Cycle at various steps and overall show an effective anti-cancer immune response (Figure I-5). In *Chapter II* we show that the platform enables the reprogramming of T-cells to express a CAR against a specific tumor cell antigen, leading to recognition of its target (step 6) and thereby CAR-mediated

target cell killing (step 7). In *Chapter III* we demonstrate how the platform can be utilized to reprogram T-cells to become BiTE-secreting factories. Here, secreted BiTEs enable T-cell engagement with target tumor cells (step 6) and similarly mediate target cell killing (step 7). This merely demonstrates how the immediate steps of the Cancer-Immunity Cycle might be affected. However, the T-cell reprogramming strategies described in the following chapters may have a self-propagating effect that upon initial cancer cell killing leads to neoantigen release (step 1) and thus initiates a new round of the Cancer-Immunity Cycle increasing the possibility of tumor regression and anti-cancer immunity.

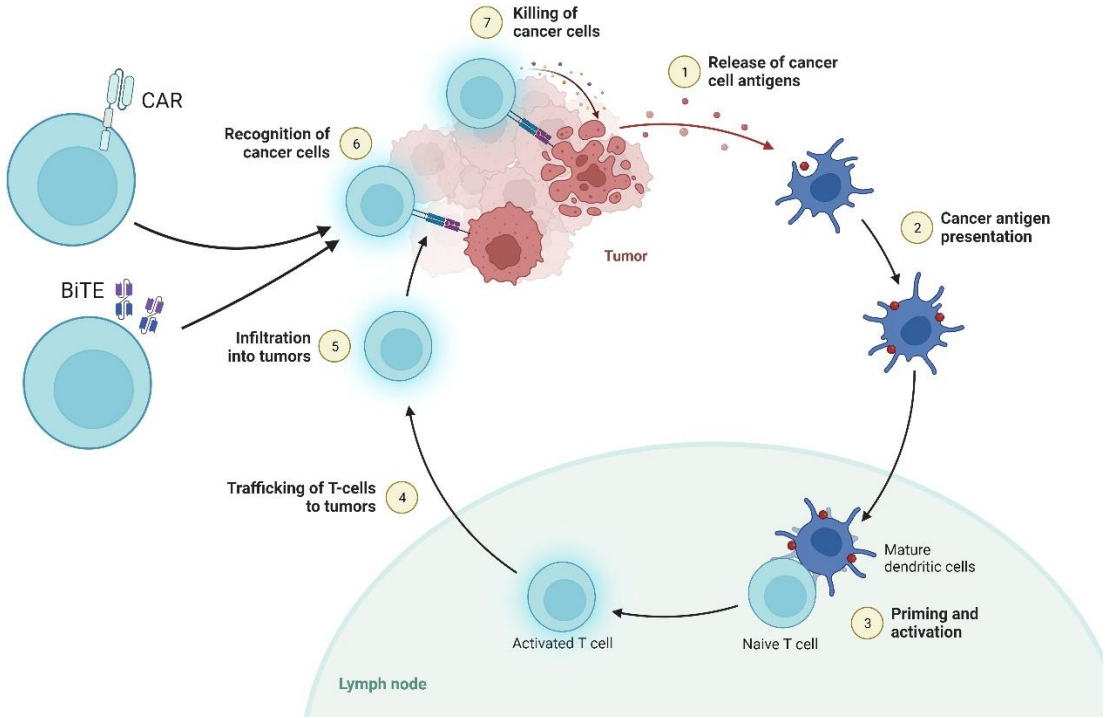

Figure I-5. Overview of how the Cancer-Immunity Cycle can be targeted with various strategies utilizing the Tidal platform.

CAR- and BiTE-reprogrammed T-cells can be achieved using the Tidal technology. CAR T-cells and BiTEs facilitate the specific recognition of tumor cells and mediate tumor cell killing (Step 6 and 7). CAR, chimeric antigen receptor; BiTE, bi-specific T-cell engager. Created with BioRender.com.

Chapter II | Using targeted LNPs to specifically deliver CAR mRNA to human T-cells *in vivo*

Authors:

Viktor T Lemgart[1,2,*], Allison Caron[1], Ralston Augspurg[1], Samantha Stewart[1], Michael Monte[1], Carrington Mcleod[1], Laura Strauss[1], Sanjana Kulkarni[1], William Kuhlman[1], Aaron Griset[1], Eyoung Shin[1], Christopher Borges[1], Andrew Sawyer[1], Austin Boesch[1], Ulrik Nielsen[1], Daryl Drummond[1,*]

Affiliations:

[1] Tidal Therapeutics (a Sanofi Company), Sanofi, Cambridge, MA, USA

[2] Department of Health Technology, Technical University of Denmark, Lyngby, Denmark

[*] Corresponding author

The purpose of this chapter is to demonstrate the use of Tidal's LNP-mRNA platform with the goal to develop a first-in-class targeted LNP that specifically delivers CAR-encoding mRNA to T-cells directly *in vivo* to treat hematological malignancies. As our lead drug candidate comprises a proprietary ionizable lipid, a proprietary targeting moiety, and a proprietary CAR sequence, the research described in this chapter exploits previously disclosed lipids, antibody sequences, and CAR designs. Additionally, some of the data shown in this chapter will involve a proprietary target that will not be disclosed herein.

Ralston Augspurg and Michael Monte kindly formulated and characterized the LNPs used herein.

II.1 | Abstract

Ex vivo chimeric antigen receptor (CAR) T-cell therapy has proven successful in patients with hematologic malignancies, but its broad application is still facing significant challenges due to current approaches requiring elaborate and expensive techniques to engineer and manufacture T-cells. Here, we demonstrate a platform, using antibody-targeted lipid nanoparticles (LNPs) encapsulating mRNA to reprogram circulating human T-cells *in vivo*, thus overcoming these barriers. We show that the approach can be utilized to deliver CAR-encoding mRNA specifically to $CD3^+$ or $CD8^+$ T-cell subsets through an antibody-derived targeting moiety, thereby enabling transient functional CAR expression. The targeted LNP formulation allows for repeated dosing strategies while circumventing off-cell target mRNA delivery. We further demonstrate that the delivery of mRNA encoding clinically relevant CARs can drive specific target cell killing *in vitro*. Collectively, our approach holds strong promise for becoming a broadly applicable CAR-T treatment for hematologic malignancies while being a highly adaptable platform for other diseases.

II.2 | Introduction

Genetic modification of T-cells with chimeric antigen receptors (CARs) to target specific diseases has shown impressive clinical responses in patients with hematologic malignancies [16]. However, several barriers remain to make this therapy available to a broader patient population. Currently, CAR-T cell therapy production is carried out *ex vivo*, including genetic modification of the patient's T-cells in culture before infusing the cells back into the patient [143]. The *ex vivo* methods required to generate sufficient numbers of

tumor-specific T-cells are complex thereby hindering widespread application to treat cancer patients [139]. Additionally, two CAR-T therapies approved by the U.S. Food and Drug Administration (FDA) are priced at USD373,000 (Yescarta, Kite) and USD475,000 (Kymriah, Novartis), making it economically challenging to provide this personalized treatment to the millions of cancer patients worldwide [144]. Finally, CAR T-cell therapy has related acute and chronic toxicities that must be overcome when developing new drugs to treat cancer patients [145]. The onset of immune activation, known as cytokine release syndrome (CRS), is the most prevalent adverse effect following CAR T-cell infusion. Additionally, other side effects reported in patients receiving CAR T-cells include the development of neurological toxicities, on-target/off-tumor recognition, anaphylaxis, and insertional oncogenesis [146-148]. To overcome these significant challenges and limitations, more innovative strategies are required to program T-cells to express CARs.

In-vitro transcribed (IVT) mRNA has, in recent years, proven as a promising technology to express desired proteins in cells, making it a promising alternative to DNA-based products. By utilizing IVT mRNA researchers allow for transient protein expression without causing integration into the genome [149, 150]. However, to function *in vivo*, effective and stable delivery platforms, protecting the mRNA from degradation and allowing for cellular uptake, are required [100]. One such delivery system that has entered the clinic and proven successful is lipid nanoparticles (LNPs) [98, 105, 151]. Remarkably, the recent authorization of two coronavirus disease 2019 (COVID-19) vaccines [68, 152] utilizing LNPs to deliver mRNA stands out as noticeable examples. However, to date, the use and design of

LNPs for systemic delivery have mainly allowed for cellular uptake by hepatocytes and Kupffer cells of the liver [153, 154].

Here, we describe a novel approach to selectively reprogram human T-cells *in vitro* and *in vivo* by specifically delivering IVT mRNA via antibody-targeted LNPs. We demonstrate the clinical relevance of the platform by showing specific CAR-encoding mRNA delivery *in vitro* and *in vivo* and report functional CAR-mediated cancer cell killing *in vitro* as well as B-cell aplasia *in vivo*.

II.3 | Methods

LNP preparation

LNPs were prepared in a similar fashion to previously published reports [155]. Briefly, LNPs were formulated with an encapsulated mRNA payload and lipid blend by mixing an aqueous mRNA solution and an ethanolic lipid solution using an in-line microfluidic mixing process. The lipid components DLin-KC3-DMA (Organix Inc, Massachusetts, US), Cholesterol (Dishman, NL), Distearoylphosphatidylcholine (DSPC, Avanti Polar Lipids, Alabama, US), and 1,2-Dipalmitoyl-rac-glycero-3-methylpolyoxyethylene glycol-2000 (DPG-PEG2000, NOF America Corporation, New York, US) were dissolved in anhydrous ethanol. mRNA and lipid solutions were mixed using a NanoAssemblr Ignite microfluidic mixing device and NxGen mixing cartridge from Precision Nanosystems Inc. (British Columbia, Canada). Following mixing, ethanol removal and buffer exchange was performed on the resulting LNP suspension using a discontinuous diafiltration process. LNPs were

recovered from the centrifugal device and stored at 4°C for short-term use. Otherwise, LNP solutions were spiked with a 49 wt% sucrose stock solution to reach a final sucrose concentration of 9.8 wt%. LNPs were then frozen and kept at -80°C for long-term storage.

CAR design and mRNA production

The anti-human CD20 antibody VH and VL sequences were derived from public sources (Leu-16 PMID11809933). The CD20 antibody and the anti-human antibody against an undisclosed target were encoded into CAR cassettes as scFvs in the VH/VL orientation with a 3x or 4x(G4S) linker between the variable heavy and light chains. The anti-CD20 Leu-16 CAR construct was built with an N-terminal FLAG-tag variant (DYKAKE) that can bind the M1 antibody clone with high affinity in the absence of calcium (PMID9237191). The CAR cassettes including a CD28 or CD8 hinge, CD28 or CD8 transmembrane domain and CD28 and CD3z intracellular signaling domains were based on sequences from the previously reported CAR constructs and signaling domains (PMID2974162, PMID31011207). Herein, these CAR constructs will be referred to as CD20 CAR and CAR X, respectively.

mRNA was produced by Trilink Biotechnologies (California, US). Briefly, mRNA encoding a second generation CD20 CAR or CAR X with CD28 co-stimulatory and CD3zeta signaling domains were in vitro-transcribed, poly-A tailed, and capped (CleanCap) (Trilink Biotechnologies, California, US).

Targeting moiety design and production

For the CD3- and CD8-targeting Fabs, in both the human heavy and light chain constant domains, the native interchain disulfide-forming cysteines were mutated to serine. Additionally, similar mutations to a previous report [156] were introduced into both the heavy and light chains to enable a stabilized disulfide linkage while avoiding DSPE-PEG-maleimide conjugation. At the end of the human CH1, the human IgG1 hinge was used up to the first natural cysteine followed by a 6-his tag (EPKSSDKTHTCHHHHHH), enabling conjugation to DSPE-PEG-maleimide and purification by IMAC.

Variable heavy and light chain amino acid sequences for anti-human CD3 (Clone: SP34-2) and CD8 (Clone: TRX2) were derived from public sources. Fabs were produced in HEK, purified by IMAC, and formulated into PBS by Biointron (Taizhou, China).

Targeting moiety conjugation and post-insertion

Antibody conjugation to DSPE-PEG was done similary to previously published reports [157, 158]. DSPE-PEG(2k)-Fab conjugate was then combined with base LNPs and placed in a ThermoMixer (Eppendorf, Hamburg, Germany) at 37°C at 300 rpm for 4 hours, followed by storage at 4°C until use.

LNP characterization

The LNPs were characterized to determine the average hydrodynamic diameter, zeta potential, and mRNA content (total and dye-accessible). The hydrodynamic diameter was determined by dynamic light scattering (DLS) using a Zetasizer model ZEN3600 (Malvern Pananalytical, Malvern, UK). The zeta potential was measured in 5 mM pH 5.5 MES buffer and 5 mM pH 7.4 HEPES buffer by laser Doppler electrophoresis using the Zetasizer.

RNA content of the nanoparticles was measured using Quant-iT RiboGreen RNA Assay Kit (Thermo Fisher, Massachusetts, US). Dye-accessible RNA, which includes both non-incorporated RNA and RNA that is near the surface of the nanoparticle, was measured by diluting the nanoparticles to approximately 1 µg/mL mRNA using HEPES buffered saline, and then adding Quant-iT reagent to the mixture. Total RNA content was measured by diluting the particles to 1 µg/mL mRNA using HEPES buffered saline, disrupting the nanoparticles by heating them to 60°C for 30 minutes in HEPES buffered saline containing 0.5% Triton, and then adding Quant-iT reagent. RNA was quantified by measuring fluorescence at 485/535 nm, and concentration was determined relative to a contemporaneously run RNA standard curve.

Cell lines and quantification of target surface marker

The CD20-positive human B-cell lymphoblast line, Raji, the CD20-negative B-cell leukemia line, Nalm6, and the CD20-negative lymphoblast cell line, K562, were purchased from American Type Culture Collection (ATCC, Maryland, US) and were maintained according

to the manufacturer's recommendations. A Quantibrite™ PE kit (BD Biosciences, New Jersey, US) was used to quantify the number of CD20 molecules per cell, respectively, on each cell line following the manufacturer's instructions.

CD3- and CD8-dependent uptake in isolated T-cells *in vitro*

$CD3^+$ or $CD8^+$ T-cells were isolated from human PBMCs using human CD3 or CD8 T-cell negative magnetic isolation kits (StemCell Technologies, Vancouver, Canada). Prior to LNP treatment, isolated T-cells were seeded into 96-well round bottom plates at a concentration of $1x10^6$ cells/mL (100K cells per well). Cells were then treated by adding targeted LNPs encapsulating mRNA to the cells followed by mixing by pipetting and incubating at 37°C.

Cells were washed in phosphate buffer saline (PBS) containing 0.5% BSA and 0.1% NaN_3 (FACS buffer) for cytometry analysis. After washing, cells were stained with CD4-, CD3-, and CD8-antibodies. For CD20 CAR detection, an M1 antibody conjugated in-house to AF488 was used. CAR X-expression was detected using an indirect staining method with a target antigen followed by a secondary stain using an anti-target antibody conjugated to APC. All stains were performed at 4°C for 30 minutes prior to washing and resuspending in FACS buffer. Stained cells were acquired by flow cytometry on a Symphony (BD Biosciences, New Jersey, US) running FACSDiva software and further analyzed in FlowJo. Dead cells were excluded from analysis by using eFluor780 fixable viability dye (Thermo Fisher, Massachusetts, US).

Microscopy

Microscopy of human $CD8^+$ T-cells was performed on a Nikon TiE microscope with a 60X objective and analyzed on (Fiji Is Just) ImageJ software. Briefly, isolated $CD8^+$ T-cells transfected with CD3- or CD8-targeted GFP/DiI LNPs for 24 hours were stained with NucBlue™ Live ReadyProbes™ (Thermo Fisher, Massachusetts, US) for 20 minutes at 37°C before washing and resuspending in Live Cell Imaging Solution (Thermo Fisher, Massachusetts, US) for microscopic analysis.

Cytokine profiling with MSD

Cytokine secretion *in vitro* was analyzed by MSD (Meso Scale Diagnostics, Maryland, US). Supernatants were pulled from the culture at the 24-hour time point and a custom U-PLEX assay was used for the detection of human TNF-alpha, IFN-gamma, and IL-10 following the manufacturer's instructions. For *in vivo* analysis, blood was drawn at the respective time points into 300 µL Microvette 100 EDTA tubes and centrifuged at 500 x g for 10 minutes. Plasma was then collected and analyzed using a custom U-PLEX assay for the detection of human TNF-alpha, IFN-gamma, and IL-10 following the manufacturer's instructions.

Signature T-cell gene analysis using NanoString technology

Gene expression profiles of LNP-transfected human $CD8^+$ T-cells were assessed using nCounter CAR-T Characterization Panel (NanoString Technologies, Washington, US), characterizing 780 human CAR T-related genes. Briefly, $CD8^+$ T-cells were isolated and transfected as described above. Cells were lysed using Buffer RLT (Qiagen, Hilden, Germany), and cell lysates were treated with Proteinase K (Thermo Fisher, Massachusetts, US) prior to hybridization following the manufacturer's instructions.

In vivo CAR reprogramming in humanized NSG mice

For reprogramming T-cells in vivo, 0.3 mg/kg mRNA encapsulated in LNPs was administered intravenously through the tail vein of 10-week-old female NSG mice engrafted with human PBMCs. Blood was collected into EDTA-coated collection tubes and red blood cells (RBCs) were lysed using Versalyse (Beckman Coulter, California, US). Cells were washed in FACS buffer and stained with human CD45-, CD4-, CD3-, CD8-, and CD20-antibodies, murine CD45-antibodies, and CAR X-staining reagents as described above. Cells were washed twice in FACS buffer and acquired by flow cytometry on a Symphony (BD Biosciences, New Jersey, US) running FACSDiva software and further analyzed in FlowJo. Dead cells were excluded from analysis by using eFluor780 fixable viability dye (Thermo Fisher, Massachusetts, US).

Spleens, livers, lungs, and bone marrow were first excised, weighed, and processed to single-cell suspensions before staining and acquiring by flow cytometry as described above.

Flow Cytometry-based cytotoxicity assay

Raji, Nalm6, and K562 cells were stained with Cell Trace Violet proliferation dye (CTV) (Thermo Fisher, Massachusetts, US) following the manufacturer's protocol. Briefly, target cells were incubated with CTV for 20 minutes at room temperature prior to washing and co-culturing. $CD8^+$ T-cells were isolated and transfected as described above and washed after 4 hours of incubation to remove unbound LNPs. Transfected $CD8^+$ T-cells were then co-cultured with CTV-stained target cells at varying effector-to-target cells ratios in T-cell media (RPMI-1640, 10% FBS, and 50 ng/mL recombinant human IL-2) in a 96-well flat-bottom plate for 48 hours. After 48 hours of co-culture, cells were stained with eFluor780 fixable viability dye (Thermo Fisher, Massachusetts, US) to assess the level of cytotoxicity and with CD69-BUV395 (BD Biosciences, New Jersey, US) to quantify the level of activation. Cells were washed twice in FACS buffer and acquired by flow cytometry on a Symphony (BD Biosciences, New Jersey, US) running FACSDiva software and further analyzed in FlowJo (BD Biosciences, New Jersey, US). For T-cell phenotyping, cells were stained with CD95-BUV395 (BD Biosciences, New Jersey, US), CD3-BUV737 (BD Biosciences, New Jersey, US), CD62L-BV605 (Biolegend, California, US), CD45RO-BV711 (Biolegend, California, US), CD19-BV785 (Biolegend, California, US), CD45RA-AF488 (Biolegend, California, US), CCR7-PE (Biolegend, California, US), and PD1-APC (Biolegend, California, US).

IncuCyte Cytotoxicity assay

The IncuCyte NucLight Red Lentivirus reagent (Sartorius, Gottingen, Germany) was used to transduce Raji, Nalm6, and K562 cells following the manufacturer's protocol. Transduced NucLight Red positive cells were selected for using puromycin and >95% purity was confirmed by flow cytometry prior to co-culture assays. $CD8^+$ T-cells were isolated and transfected as described above. Unbound LNPs were removed by washing in PBS 4 hours post-transfection. Transfected T-cells were then co-cultured with NucLight Red Lentivirus transduced Raji, Nalm6, or K562 cells at varying effector-to-target cell ratios in T-cell media (RPMI-1640, 10% FBS and 50 ng/mL recombinant human IL-2) in a 96-well flat-bottom plate. Cancer cell killing was monitored in the SX5 IncuCyte every 3 hours. The level of cytotoxicity was quantified by normalizing the count of red cells to the initial time point.

Study approval

All animal procedures were performed in accordance with the National Institutes of Health Guide for the Care and Use of Laboratory Animals and were approved but the CRADL Institutional Animal Care and Use Committee (AICUC). Whole blood was collected from healthy adult (>18 years) donors in heparin Vacutainer® tubes under an approved protocol for Sanofi following informed consent prior to the blood draw.

Statistical analysis

Statistical significance, comparing two samples, was evaluated using Student's *t* test. Analysis of variance (ANOVA) was used to evaluate statistical significance for multiple comparisons followed by Dunnett's posttest to compare all groups against a single control. Statistical analysis was performed using GraphPad Prism. Error bars indicate the standard deviation (SD), or the standard error of the mean (SEM) as specified in the figure legend. A p value less than 0.05 was considered to be statistically significant.

II.4 | Results

We hypothesized that CAR-encoding mRNA could be encapsulated in LNPs and through an antibody-based targeting moiety directed toward $CD3^+$ or $CD8^+$ T-cells mediating functional CAR expression directly *in vivo* (Figure II-1). First, LNPs were formulated and characterized, evaluating the size, polydispersity (PDI), and zeta potential after the various formulation steps (Figure II-2a-c). Additionally, the mRNA recovery levels were evaluated using the RiboGreen assay kit to ensure sufficient encapsulation of mRNA into the LNPs (Figure II-2d).

To study whether the formulated LNPs could get to and deliver a functional mRNA payload to human T-cells we incorporated a traceable DiI dye into the LNPs and used a reporter mRNA encoding GFP. DiI-LNPs encapsulating GFP mRNA were inserted with an anti-CD3 or anti-CD8 targeting Fab conjugated to DSPE-PEG and added to primary T-cells at different dose levels evaluating the LNP-association and GFP expression by Flow

Cytometry after 24 hours (Figure II-3a). The targeted LNPs were shown to bind and transfect human primary T-cells in a dose-dependent manner with more than 70% of T-cells showing GFP expression 24 hours after adding CD3-targeted LNPs (Figure II-3b-f).

Next, we investigated how the chosen targeting moieties inserted into the LNPs in combination with the various selected CARs would affect the profile of the T-cells. An upregulation in the early activation marker, CD69, and elevated cytokine release of IFN-gamma, TNF-alpha, and IL-10, was observed upon transfection with the CD3-targeted LNPs in comparison to the CD8-targeted LNPs (Figure II-4a-e). To study how the two targeting moieties would affect the gene expression of the T-cells we performed a NanoString gene expression analysis of the transfected T-cells (Figure II-4f-i). We observed that a wide range of genes related to T-cell activation, exhaustion, and type 1 and 2 interferon signaling were significantly upregulated in T-cells transfected with CD3-targeted LNPs. No upregulation in these signature genes was observed in T-cells transfected with CD8-targeted LNPs when compared to untreated T-cells.

Having observed high expression of our GFP mRNA payload in isolated T-cells, we next wanted to investigate the level of specificity of our platform in a translational context. Here we developed an *ex vivo* experiment, transfecting human whole blood and evaluating the expression efficiency by Flow Cytometry (Figure II-5). In addition to investigating the transfection efficiency and specificity, we included nine healthy donors in this experiment to study the uptake variability across donors. A high level of LNP association was observed in the Granulocyte and B-cell population but with no detection of GFP expression. As expected, our CD3-targeted LNPs were able to transfect both $CD4^+$ and $CD8^+$ T-cells while

no GFP expression was observed in the $CD4^+$ T-cell population transfected with the CD8-targeted LNPs. We observed a variation in transfection efficiency among the donors evaluated, but all nine donors showed a high degree of specificity as no GFP expression could be observed in off-target cell populations.

To demonstrate the translatability of the platform and to study whether the targeted LNPs could be used to reprogram T-cells into CAR T-cells, a clinically relevant CAR construct against CD20 (Clone: Leu16, [159]) and a CAR construct against an undisclosed target, were encoded in mRNAs and formulated into targeting LNPs. These CAR-encapsulating LNPs showed similar characteristics to LNPs encapsulating reporter mRNA (Figure II-2a-d). From *in vitro* experiments, we were able to detect expression of both CARs on the surface of primary T-cells in a dose-dependent manner (Figure II-6a-b) and for up to 72 hours (Figure II-6c-d) when transfected with either CD3- or CD8-targeting LNPs. Additionally, the cytokine release between the two CARs was investigated. Here, we observed that the elevated levels of cytokines secreted were triggered by the CD3-targeting moiety and not the CARs (Figure II-6e-g). However, the CD20-targeting CAR, Leu16, also showed elevated cytokine levels when encapsulated in the CD8-targeting LNPs in comparison to CAR X.

Following promising data *in vitro* we next investigated whether we were in fact able to deliver the mRNA payload to the specific T-cell subsets *in vivo*. Here, NSG mice were engrafted with human PBMCs and intravenously injected with a clinically relevant dose of LNPs (0.3 mg/kg) (Figure II-7a). 24 hours after treatment, translated mCherry reporter protein could be observed in $CD8^+$ T-cells for both CD3- and CD8-targeting LNPs and in

$CD4^+$ T-cells for CD3-targeting LNPs in bone marrow, liver, lung, blood, and spleen (Figure II-7b-k). Additionally, we evaluated CAR X expression in $CD8^+$ T-cells in various organs (Figure II-7l-p) and successfully observed CAR reprogramming in bone marrow, lung, spleen, and whole blood while no CAR expression was observed in the liver. Similar to our *in vitro* studies, CD3-targeting LNPs showed superior transfection to the CD8-targeting LNPs in all organs evaluated. Finally, a trend showing a decrease in human $CD20^+$ B-cells could be observed in mice treated with CAR X mRNA, indicating functional B-cell aplasia *in vivo* (Supplemental Figure II-2).

The killing capacity of the mRNA-encoding CARs was further studied in cytotoxicity experiments *in vitro*. Here, we observed efficient killing of target-expressing cell lines down to low effector-to-target cell ratios while increased killing was absent in a non-target-expressing cancer cell line (Figure II-8a-l). Additionally, a shift from naïve T-cells to central and effector memory phenotypes was observed for isolated $CD8^+$ T-cells transfected with CD3-targeted LNPs in the same cytotoxicity experiment (Figure II-8m).

II.5 | Discussion

Throughout the last decade, clinical results and approvals of CD19 and BCMA chimeric antigen receptor (CAR) T-cells have demonstrated the potential that CAR treatments hold as immunotherapy against cancer [160, 161]. However, current CAR-T cell therapies for B-cell malignancies require elaborate and expensive processes to manufacture engineered T-cells *ex vivo*, which provides a barrier to making them standard-of-care treatments and available to the broad patient population. One solution could be to reprogram the patient's

T-cells to become CAR-T cells directly *in vivo* and thereby overcoming the challenges associated with patient T-cell isolation, genetic modification, and selective expansion *ex vivo*.

Here, we explored an mRNA delivery strategy using targeted lipid nanoparticles (LNPs) to transfect and reprogram human T-cells *in vivo*. We demonstrate that in vitro transcribed (IVT) mRNA encoding two clinically relevant B-cell targeting CARs can be delivered specifically to modify T-cells in human whole blood *ex vivo* in a broad range of donors (Figure II-5). Furthermore, we show that when targeted LNPs are administered systemically to humanized NSG mice *in vivo*, T-cells in circulation are reprogrammed to become CAR-T cells (Figure II-7).

We chose to encapsulate anti-CD20 CAR- and CAR X encoding mRNA payloads in our targeted LNPs based on the clinical success of CAR-T cell therapies against B-cell malignancies [38, 60, 61]. With this, we show that T-cells can be reprogrammed to transiently express a clinically validated CAR using targeted LNPs (Figure II-1). Although only investigated *in vitro*, our data show that the platform can be used to achieve specific killing of target-expressing cancer cell lines down to low effector-to-target cell ratios (Figure II-8). Additional *in vivo* efficacy studies, however, are needed along with optimizing dosing strategies, which our group is currently investigating.

As proof-of-concept, we show that targeting the highly expressed T-cell receptors, CD3 or CD8, is efficient for reprogramming T-cells and for driving CAR-mediated target cancer cell killing. However, as this approach is highly adaptable, our group is also interested in

using the developed platform to explore the targeting of other immune cell types and surface markers to deliver therapeutically relevant mRNA.

In vivo reprogramming of specific cell types such as T lymphocytes is an emerging and rapidly growing field as indicated by several recent published studies [129, 133, 135, 139, 162]. However, to our knowledge, this is the first report demonstrating an antibody-targeted LNP system to specifically deliver CAR-encoding mRNA to various T-cell subsets directly *in vivo* to treat hematological malignancies.

In conclusion, our work demonstrates an efficient and highly adaptable LNP-based platform that can be utilized to specifically deliver relevant mRNA therapeutics to T-cells. The report shows that the approach can be used to reprogram T-cells to become functional cancer-killing CAR-T cells demonstrating one of many applications for which this strategy can be utilized. In general, this platform holds promise for becoming a first-in-class "off-the-shelf" CAR-T cell therapy, overcoming significant economic and biological barriers associated with current approved *ex vivo* CAR-T therapies.

II.6 | Acknowledgements

Funding

The work in this study was supported by Sanofi S.A.

Author contributions

V.T.L., A.S., A.B., U.N., and D.D. conceived of the project and designed experiments. V.T.L., A.C., S.S., C.M., L.S., and S.K. performed experiments. R.A. and M.M. produced the LNPs. V.T.L., A.B., and D.D. interpreted the data. V.T.L. and D.D. wrote the manuscript. All authors reviewed and edited the manuscript.

Competing interests

V.T.L., A.C., R.A., S.S., M.M., C.M., L.S., S.K., W.K., A.G., E.S., C.B., A.S., A.B., U.N., and D.D. were employees of Sanofi at the time of the research, and A.C., S.S., M.M., L.S., W.K., A.G., E.S., C.B., A.S., A.B., U.N., and D.D. are stockholders or hold stock options at Sanofi.

Data and material availability

The authors declare that all data supporting the results of this study are available within the paper and its supplementary information files. Source data collected in this study are available from the corresponding authors upon request.

II.7 | Figures

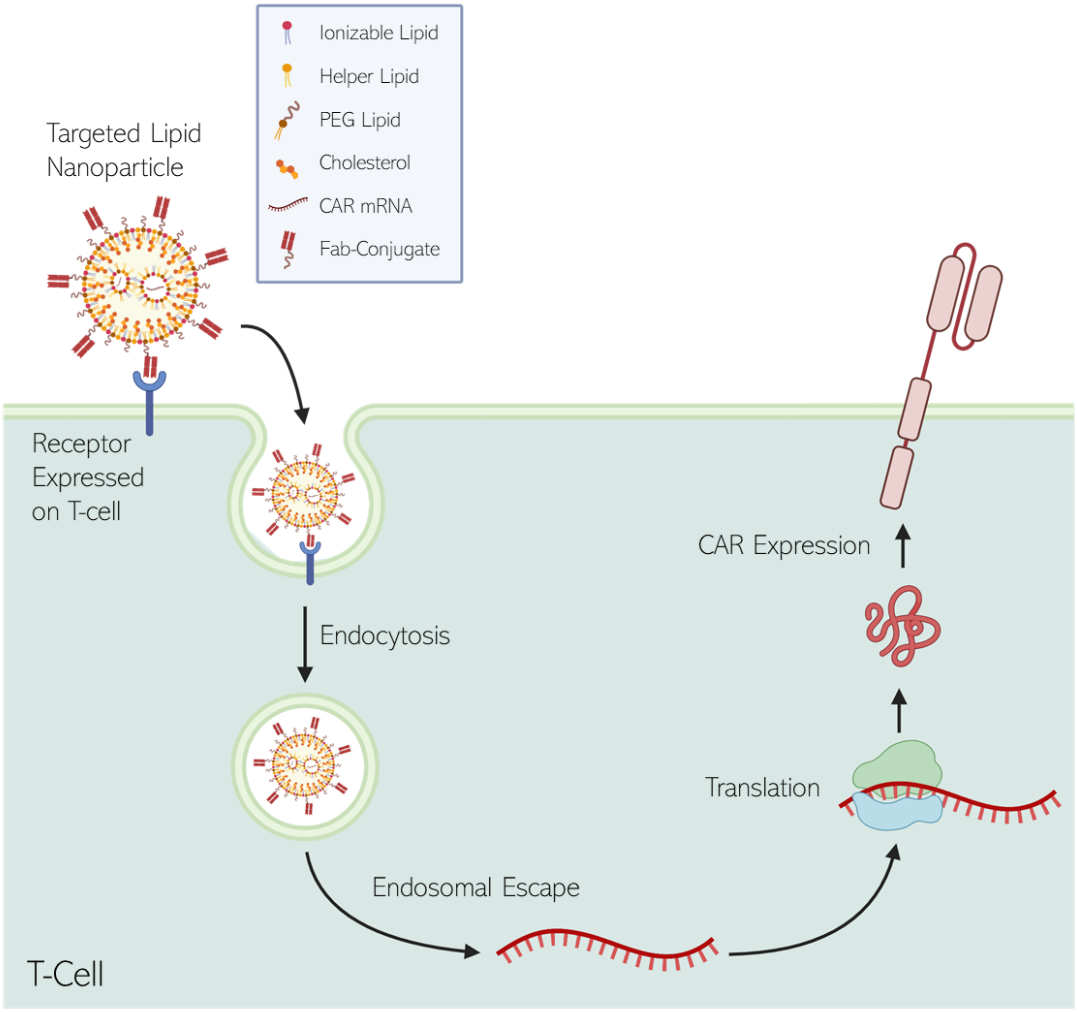

Figure II-1. Concept of reprogramming T-cells into CAR-Ts *in vivo* using targeted LNPs.

LNPs specifically engage with the T-cell through an inserted targeting moiety, which allows for receptor-mediated endocytosis. The ionizable lipid drives endosomal escape of the mRNA payload that then becomes available for translation into the encoding CAR-construct. PEG, polyethylene glycol; CAR, chimeric antigen receptor; LNP, lipid nanoparticle. Created with BioRender.com.

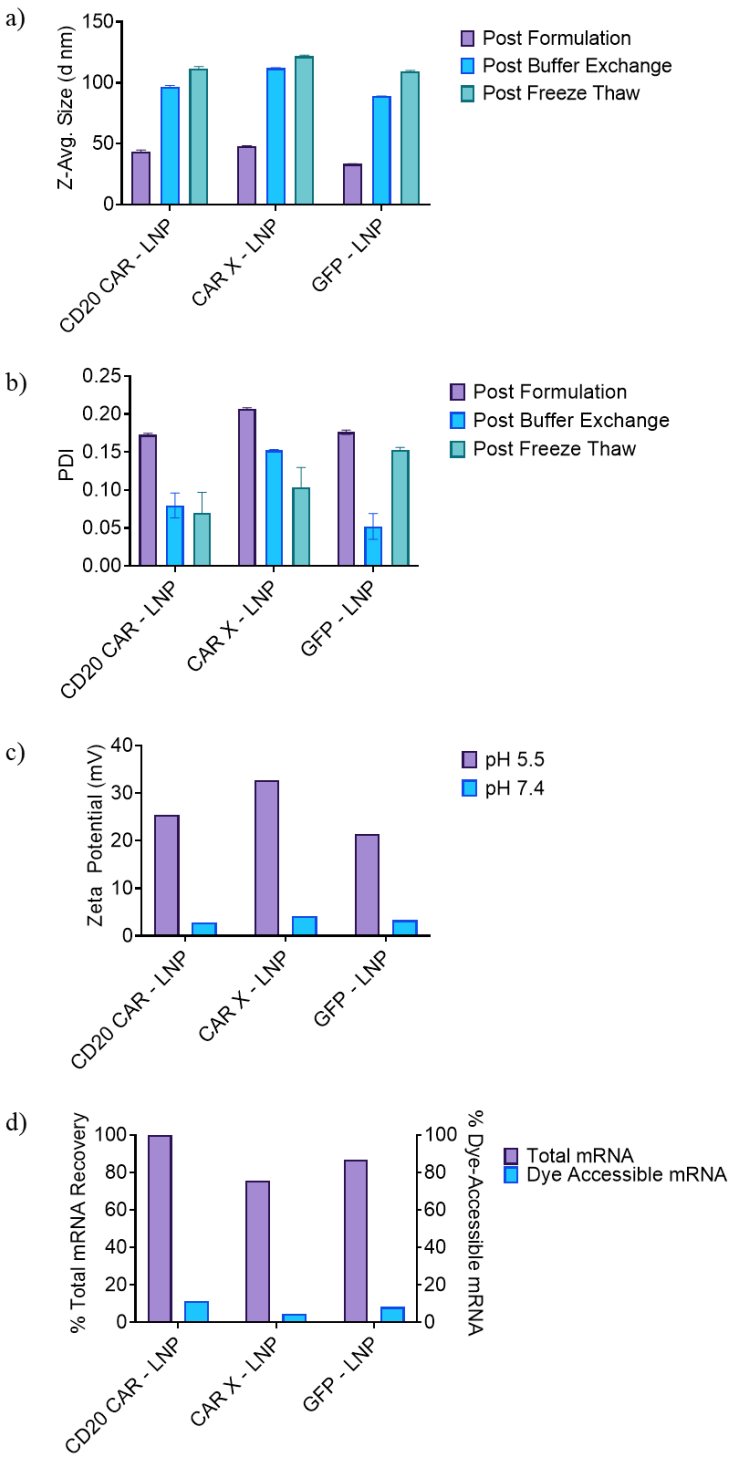

Figure II-2. LNP characterization.

a) The zeta potential, b) size-distribution, and polydispersity index (PDI) was measured using a Zetasizer. c) The RNA encapsulation efficiency was quantified using a Quant-iT RiboGreen RNA Assay Kit. Measurements were performed in triplicate. Means ± SD are depicted. GFP, green fluorescent protein.

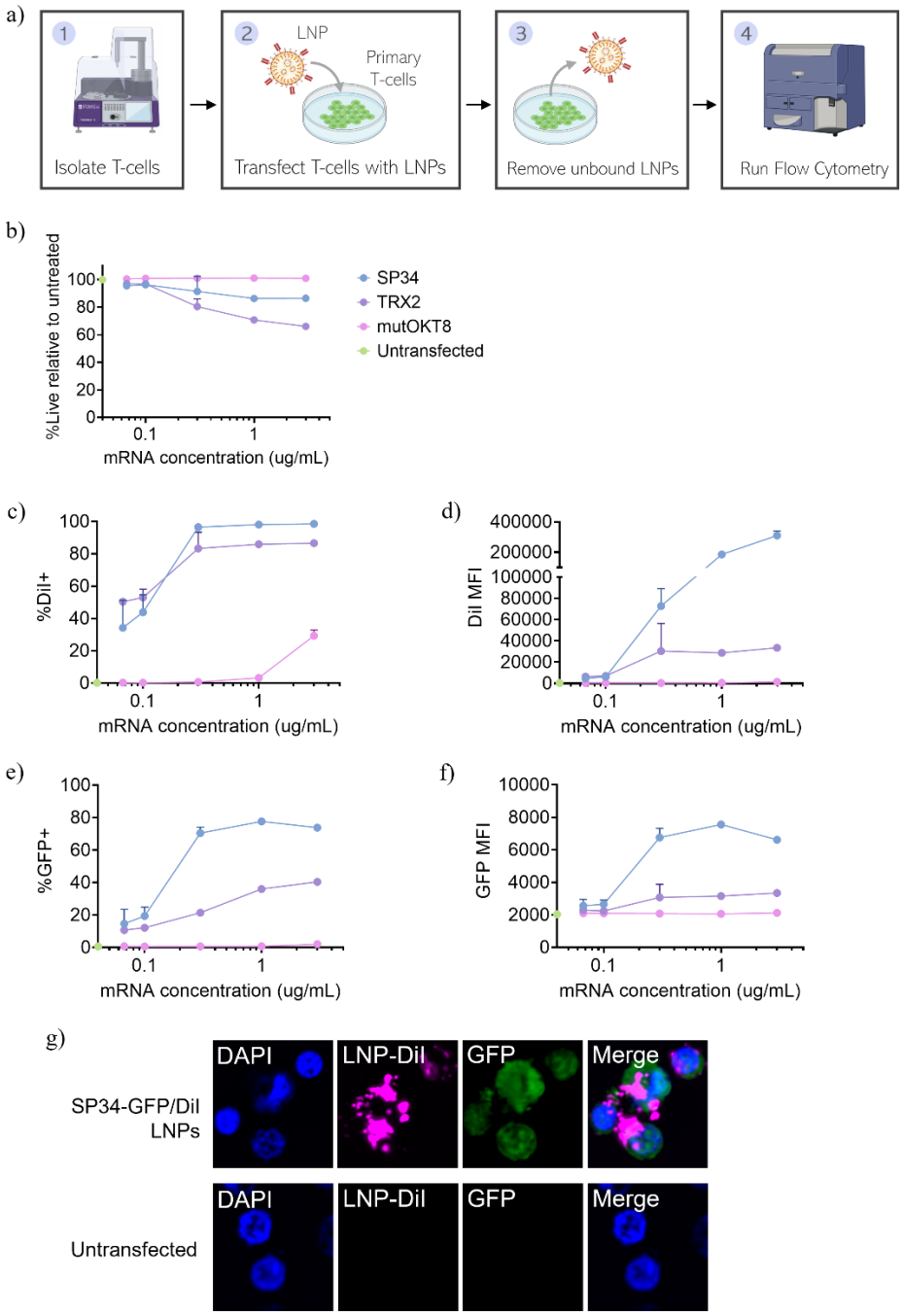

Figure II-3. *In vitro* T-cell targeting and mRNA expression.

a) Illustration of the primary T-cell transfection workflow evaluated by Flow Cytometry. b) The T-cell viability, c-d) LNP association, e-f) and GFP expression was assessed after transfection with anti-CD3 (SP34) or anti-CD8 (TRX2) constructs and compared to a non-targeted LNP control (mutOKT8). g) Microscopy was performed evaluating LNP association (pink) and GFP expression (green) in T-cells transfected with CD3-targeting LNPs. The nuclei were stained with Hoechst (blue). Assays were performed in triplicate. Shown are mean values ± SD. PBMCs, peripheral blood mononuclear cells. Created with BioRender.com.

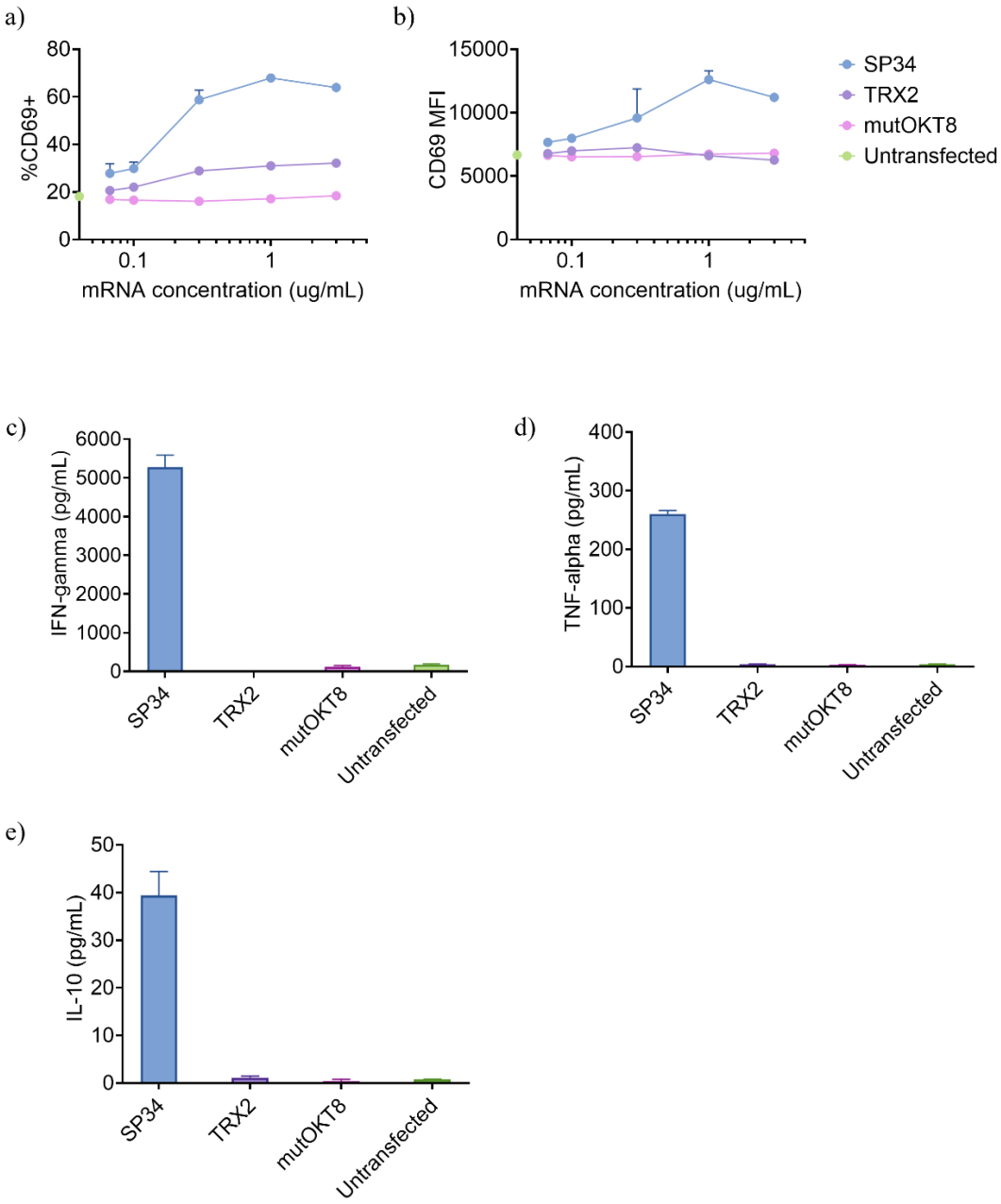
a)
%CD69+
80
60
40
20
0
0.1
1
mRNA concentration (ug/mL)
b)
CD69 MFI
15000
10000
5000
0
0.1
1
mRNA concentration (ug/mL)
SP34
TRX2
mutOKT8
Untransfected
c)
IFN-gamma (pg/mL)
6000
5000
4000
3000
2000
1000
0
SP34
TRX2
mutOKT8
Untransfected
d)
TNF-alpha (pg/mL)
400
300
200
100
0
SP34
TRX2
mutOKT8
Untransfected
e)
IL-10 (pg/mL)
50
40
30
20
10
0
SP34
TRX2
mutOKT8
Untransfected

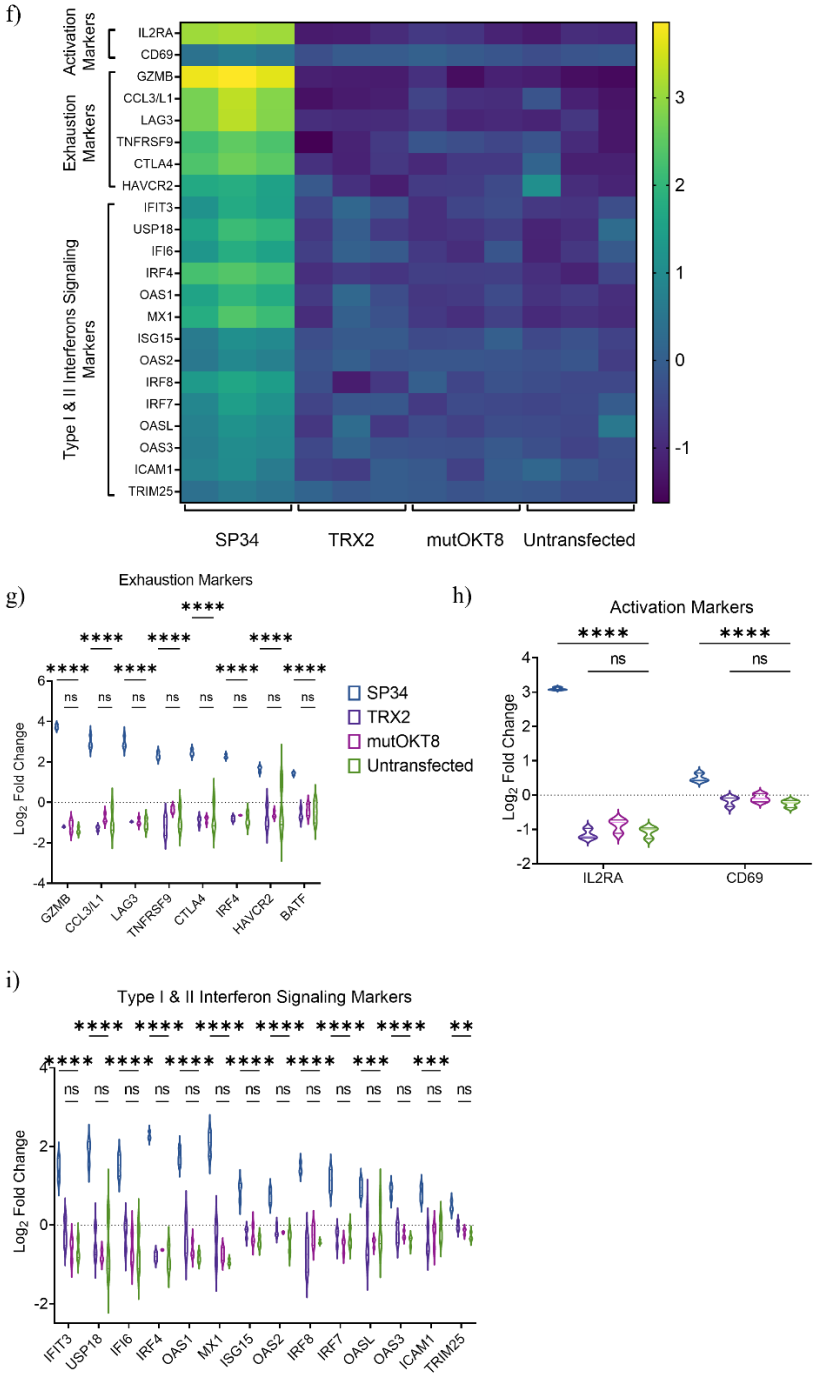

Figure II-4. Effect of LNP-targeting moieties on human T-cells.

a-b) The upregulation of the early activation marker, CD69, secretion of c) IFN-gamma, d) TNF-alpha, and e) IL-10, f-i) and gene regulation evaluated with the Nanostring CAR-T Characterization panel was assessed after transfection with anti-CD3 (SP34) or anti-CD8 (TRX2) constructs and compared to a non-targeted LNP control (mutOKT8). Displayed *p*-values are from two-way ANOVA $p<0.05$. N = 3 biologically independent samples. Data are mean ± SEM.

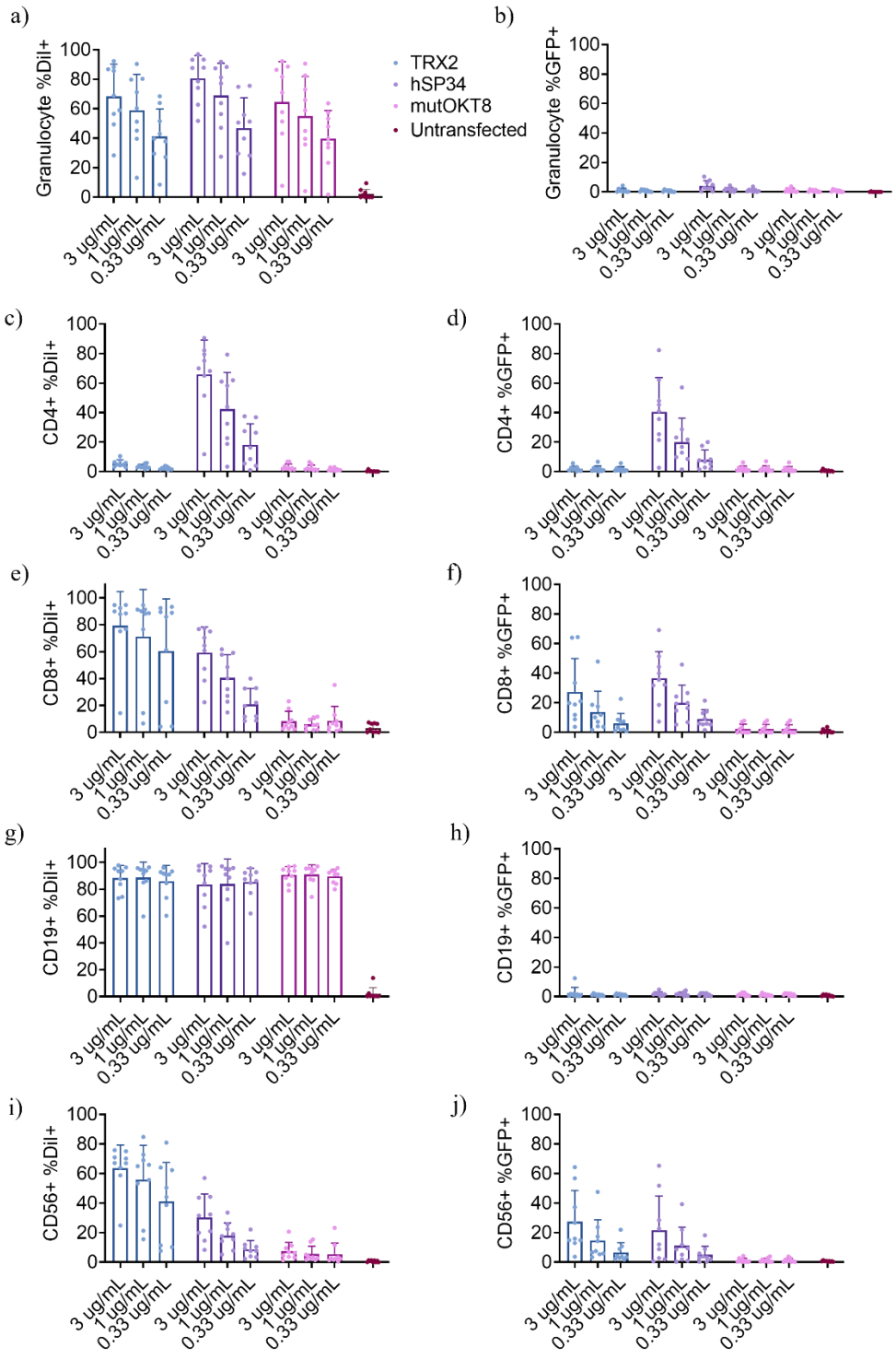

Figure II-5. LNP targeting specificity and efficiency in human whole blood.

LNP association was measured by DiI intensity and transfection efficiency evaluated by GFP expression in a-b) granulocytes, c-d) $CD4^+$ T-cells, e-f) $CD8^+$ T-cells, g-h) B-cells, i-j) and NK cells in human whole blood. N = 9 biologically independent samples. Data are mean ± SEM.

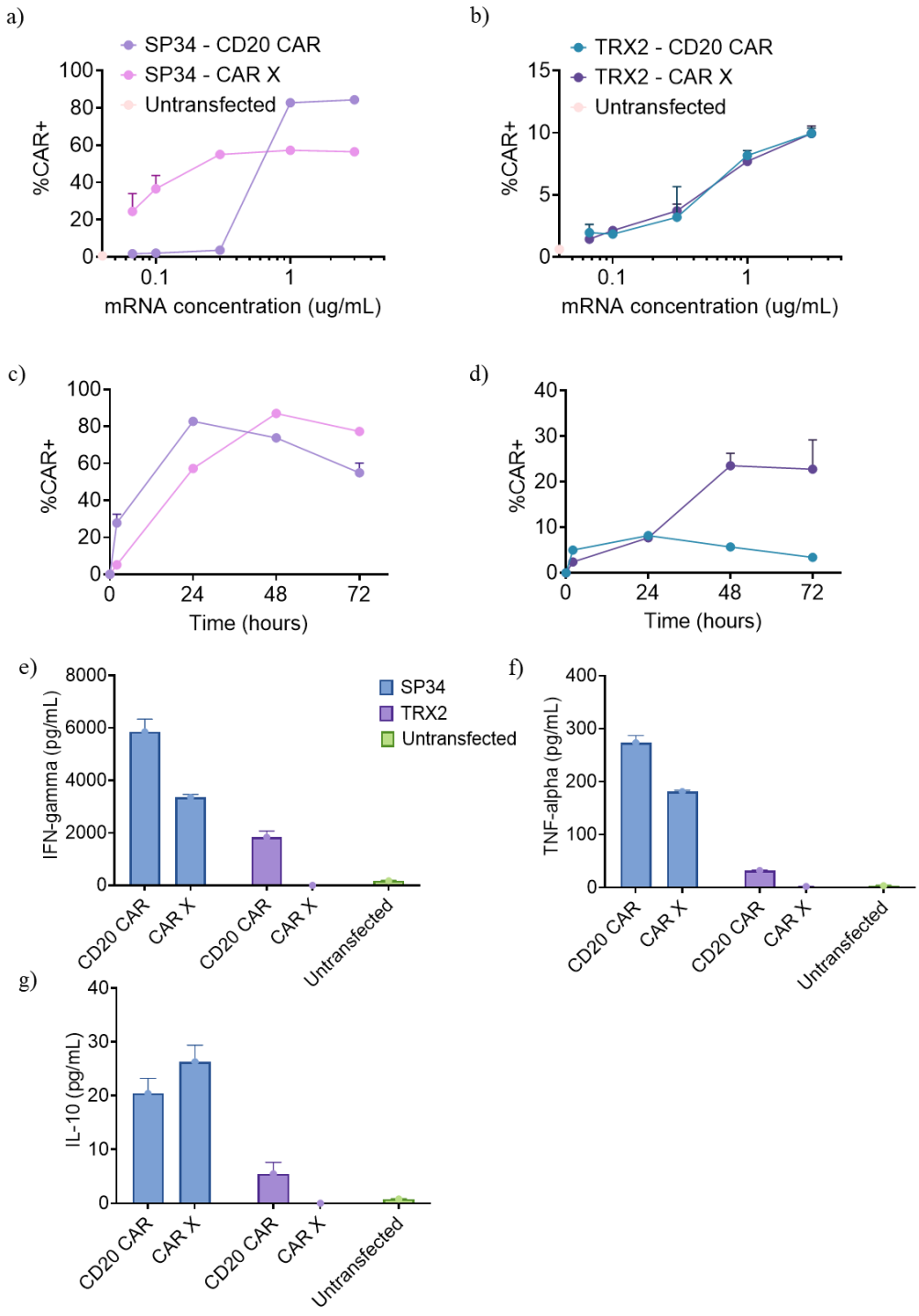

Figure II-6. CAR expression *in vitro*.

a-b) A dose titration c-d) and a time course was performed to evaluate the transfection efficiency of anti-CD20 CAR- and CAR X-encapsulating LNPs, respectively, in primary T-cells. e-g) Cytokine secretion was measured by MSD in supernatants from CAR-transfected T-cells 24 hours post-transfection. Assays were performed in triplicate. Shown are mean values ± SD.

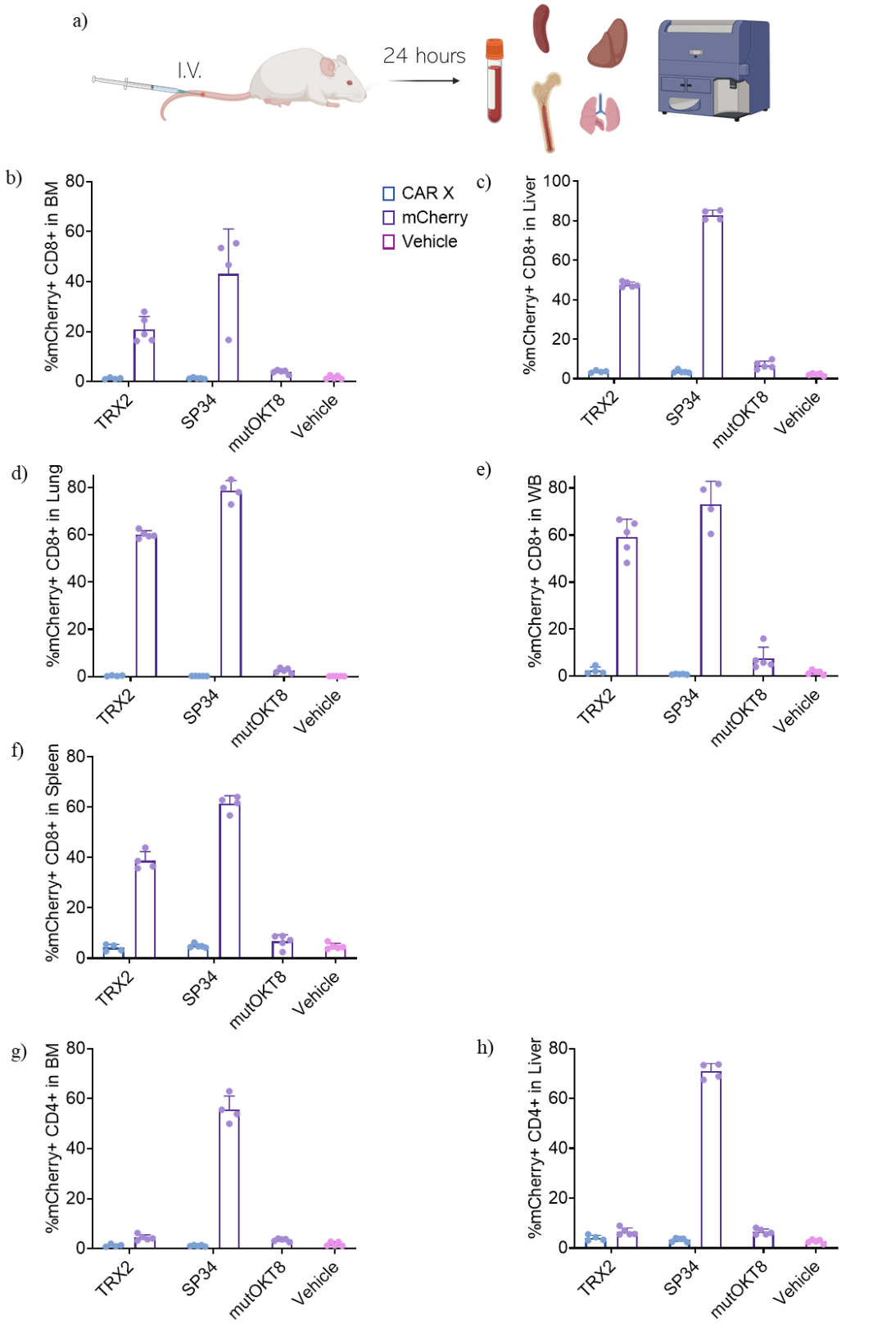
a)
I.V.
24 hours
b)
%mCherry+ CD8+ in BM
CAR X
mCherry
Vehicle
c)
%mCherry+ CD8+ in Liver
d)
%mCherry+ CD8+ in Lung
e)
%mCherry+ CD8+ in WB
f)
%mCherry+ CD8+ in Spleen
g)
%mCherry+ CD4+ in BM
h)
%mCherry+ CD4+ in Liver
TRX2
SP34
mutOKT8
Vehicle

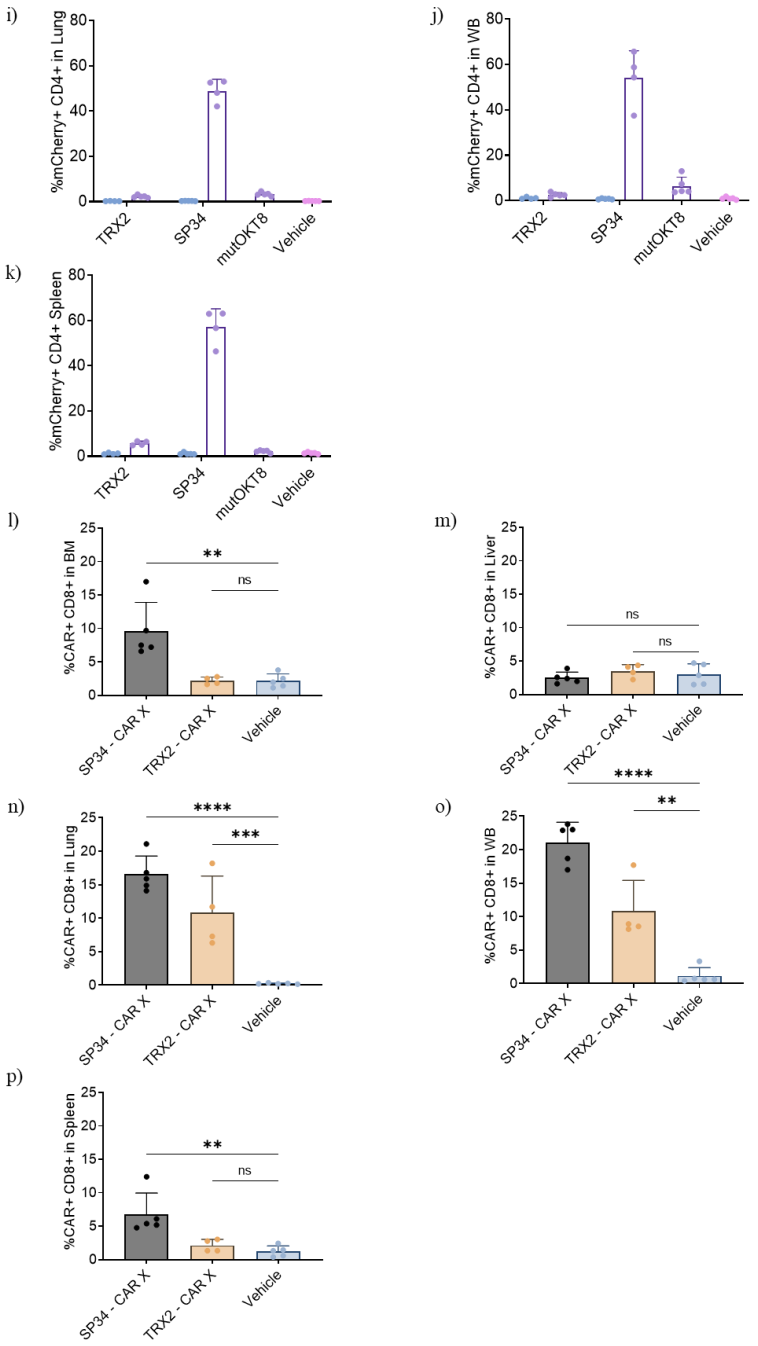

Figure II-7. *In vivo* reprogramming of CAR-T cells mediated by targeted LNPs.

a) Schematic of the *in vivo* workflow illustrating that mice were first intravenously injected, then organs were harvested, processed, and stained before the expression of the mRNA payload was assessed by Flow Cytometry. mCherry expression was evaluated in b-f) $CD8^+$ T-cells g-k) and $CD4^+$ T-cells while the level of CAR expression was assessed in the $CD8^+$ T-cells in the various organs. N = 4, 5 biologically independent mice per condition. Data are mean ± SEM. Displayed *p*-values are from one-way ANOVA $p<0.05$. I.V., intravenous; BM, bone marrow; WB, whole blood. Created with BioRender.com.

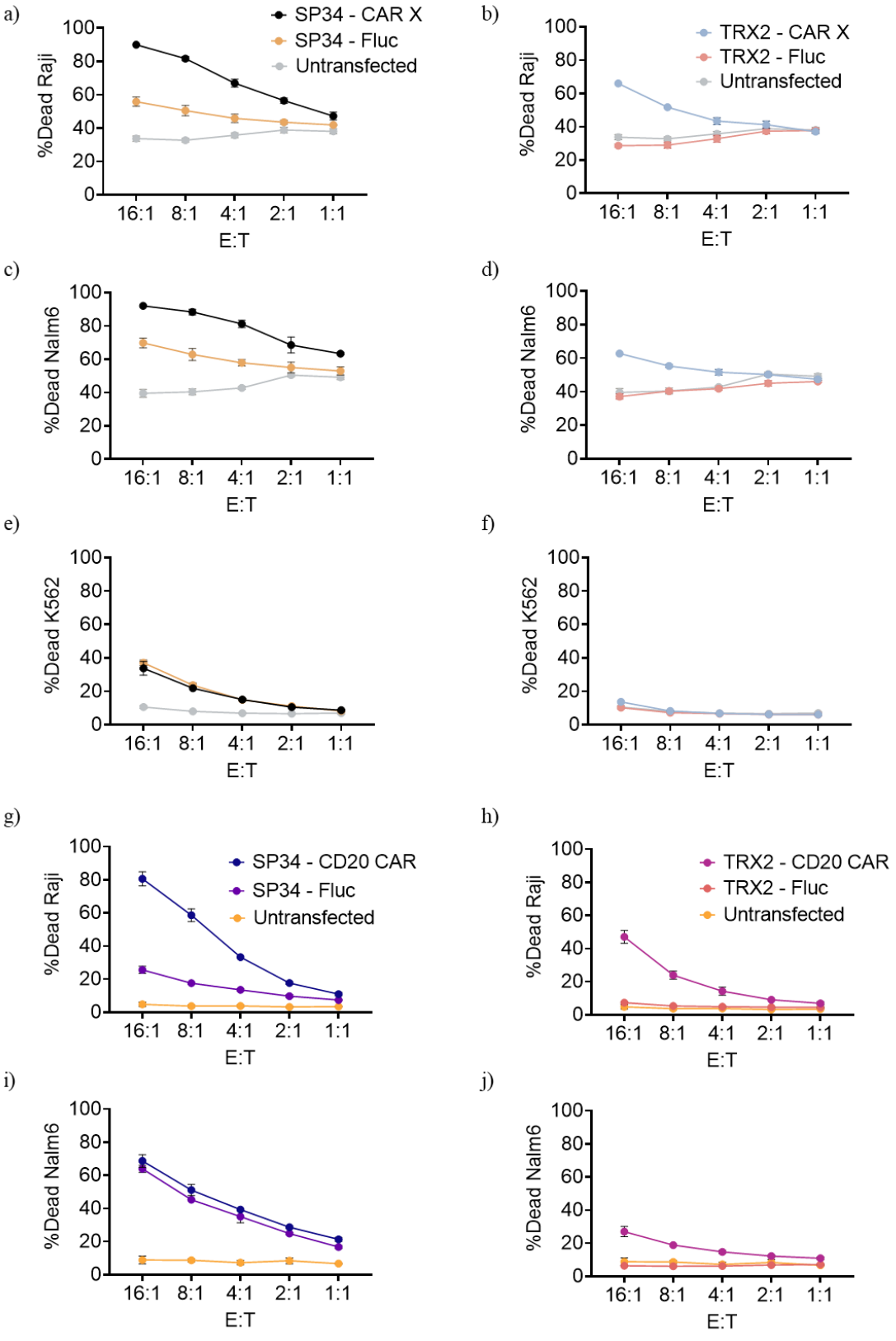
a)
SP34 - CAR X
SP34 - Fluc
Untransfected
%Dead Raji
b)
TRX2 - CAR X
TRX2 - Fluc
Untransfected
%Dead Raji
c)
%Dead Nalm6
d)
%Dead Nalm6
e)
%Dead K562
f)
%Dead K562
g)
SP34 - CD20 CAR
SP34 - Fluc
Untransfected
%Dead Raji
h)
TRX2 - CD20 CAR
TRX2 - Fluc
Untransfected
%Dead Raji
i)
%Dead Nalm6
j)
%Dead Nalm6
100
80
60
40
20
0
16:1
8:1
4:1
2:1
1:1
E:T

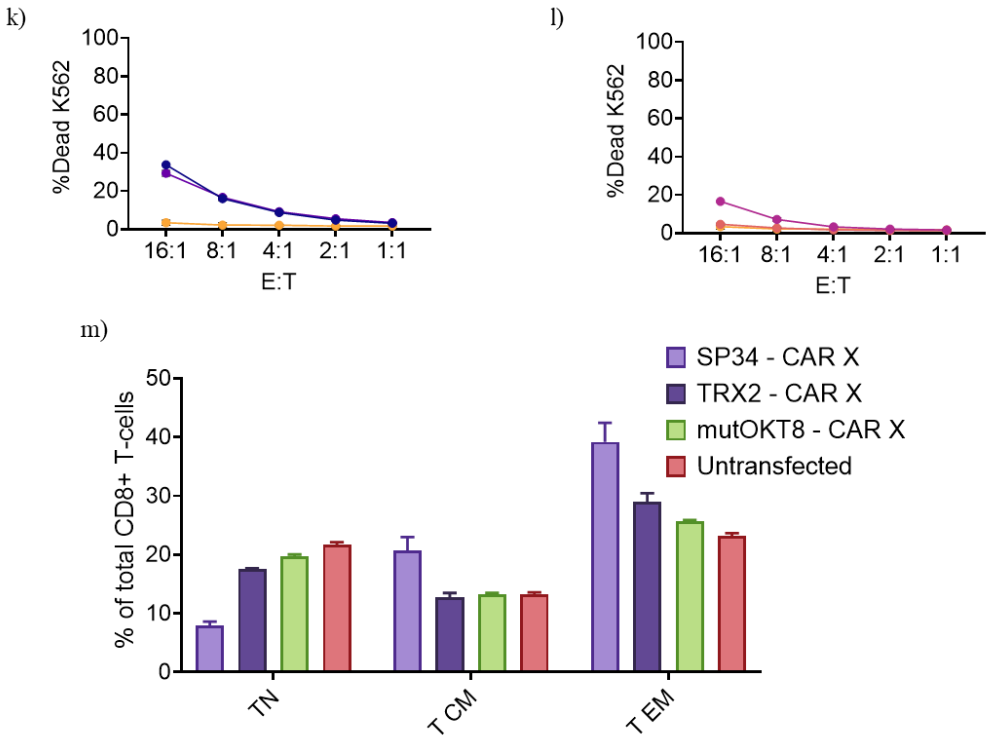

Figure II-8. CAR-specific killing of target cancer cells.

The level of CAR-mediated target cell killing was evaluated against the Raji, Nalm6, and K562 cell lines with a-f) CAR X and, g-l) anti-CD20 CAR constructs, respectively, expressed by primary T-cells via anti-CD3 (SP34) or anti-CD8 (TRX2) targeted LNP delivery. m) Phenotyping of T-cells from cytotoxicity experiment. Naïve T-cells were gated as $CD45RA^{+}$, $CD45RO^{-}$, $CCR7^{+}$, $CD62L^{+}$. Central memory T-cells were gated as $CD45RA^{-}$, $CD45RO^{+}$, $CCR7^{+}$, $CD62L^{+}$. Effector memory T-cells were gated as $CD45RA^{-}$, $CD45RO^{+}$, $CCR7^{-}$, $CD62L^{-}$. Assays were performed in triplicate. Shown are mean values ± SD. TN, naïve T-cells; T CM, central memory T-cells; T EM, effector memory T-cells.

II.8 | Supplemental Figures

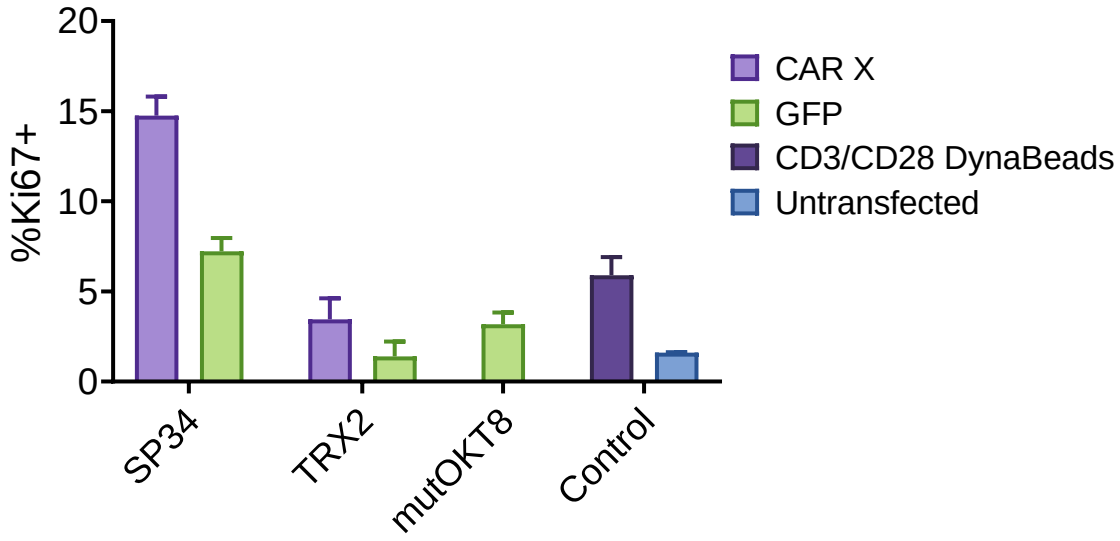

Supplemental Figure II-1. T-cell proliferation after LNP-mediated CAR delivery.

T-cell proliferation was assessed in co-cultured T-cells (E:T = 4:1) by intracellular Ki67 staining and evaluated by Flow Cytometry. Assay was performed in triplicate. Shown are mean values ± SD.

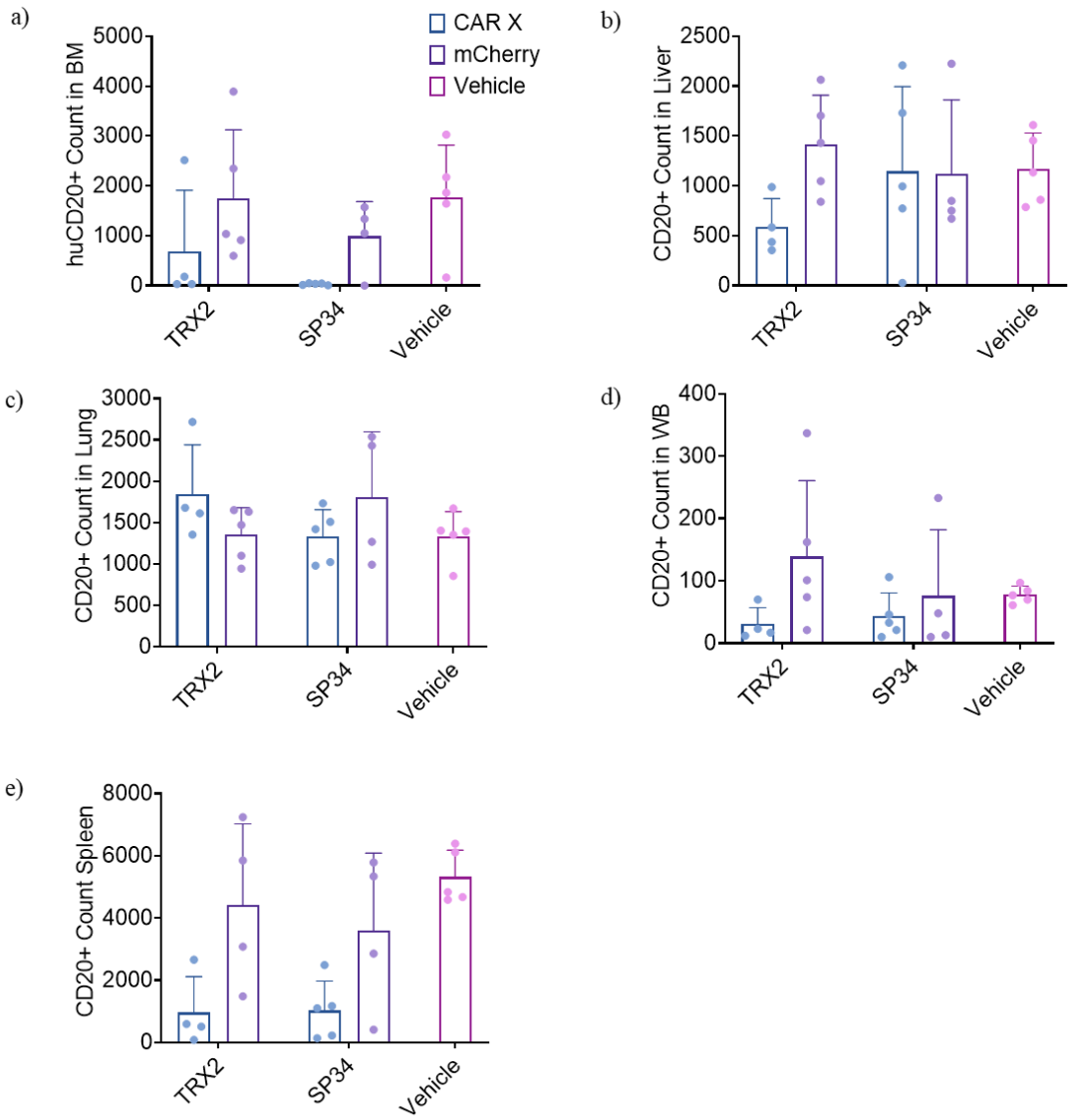

Supplemental Figure II-2. B-cell aplasia *in vivo*.

a-e) Human B-cell counts were evaluated by Flow Cytometry in CAR-treated groups and compared to non-CAR treated groups. N = 4, 5 biologically independent mice per condition. Data are mean ± SEM. BM, bone marrow; WB, whole blood.

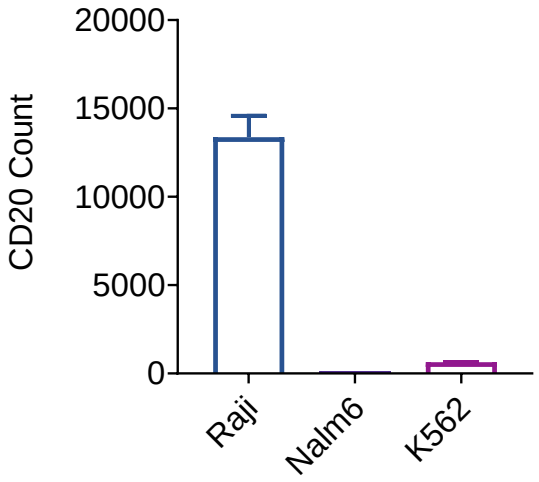

Supplemental Figure II-3. Quantification of CD20 target antigen.

CD20 antigen expression was quantified in target cancer cells by Quantibrite™. Measurements were performed in triplicate. Shown are mean values ± SD.

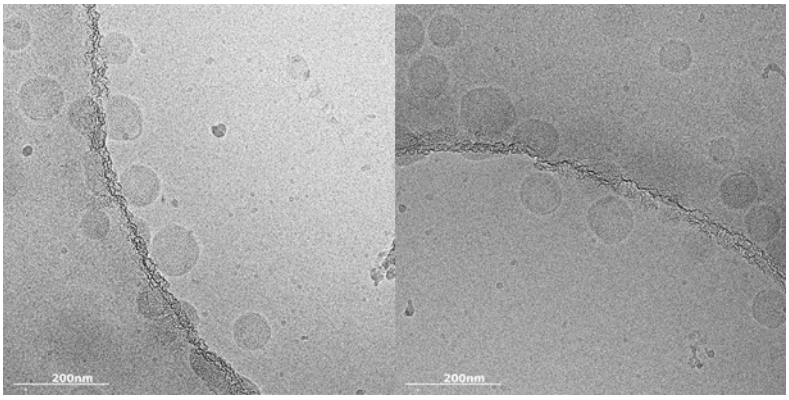

Supplemental Figure II-4. Cryo-TEM images of LNPs.

Cryo-TEM was performed on representative LNPs. Cryo-TEM, transmission electron cryomicroscopy.

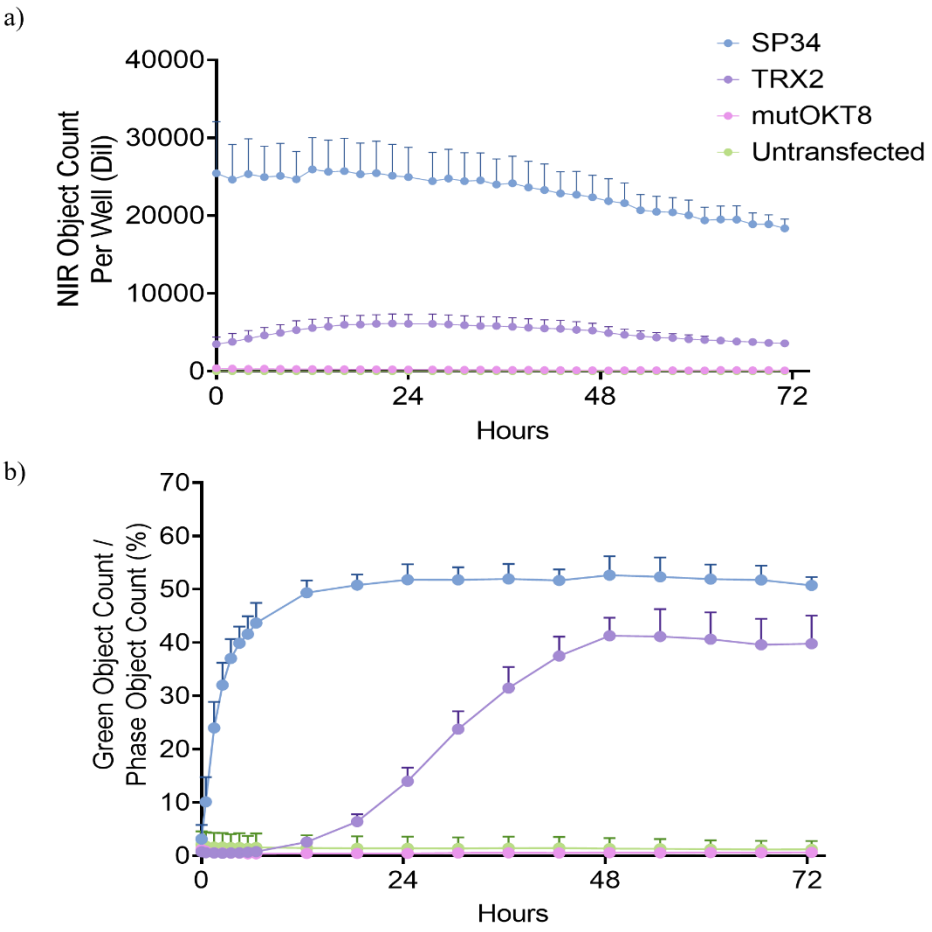

Supplemental Figure II-5. Kinetics of LNP uptake and transfection.

a) The LNP uptake b) and mRNA transfection rates was evaluated over time with the IncuCyte SX5 instrument in T-cells transfected with 1 µg/mL CD3- and CD8-targeting LNPs, respectively**.** Assay was performed in triplicate. Shown are mean values ± SD.

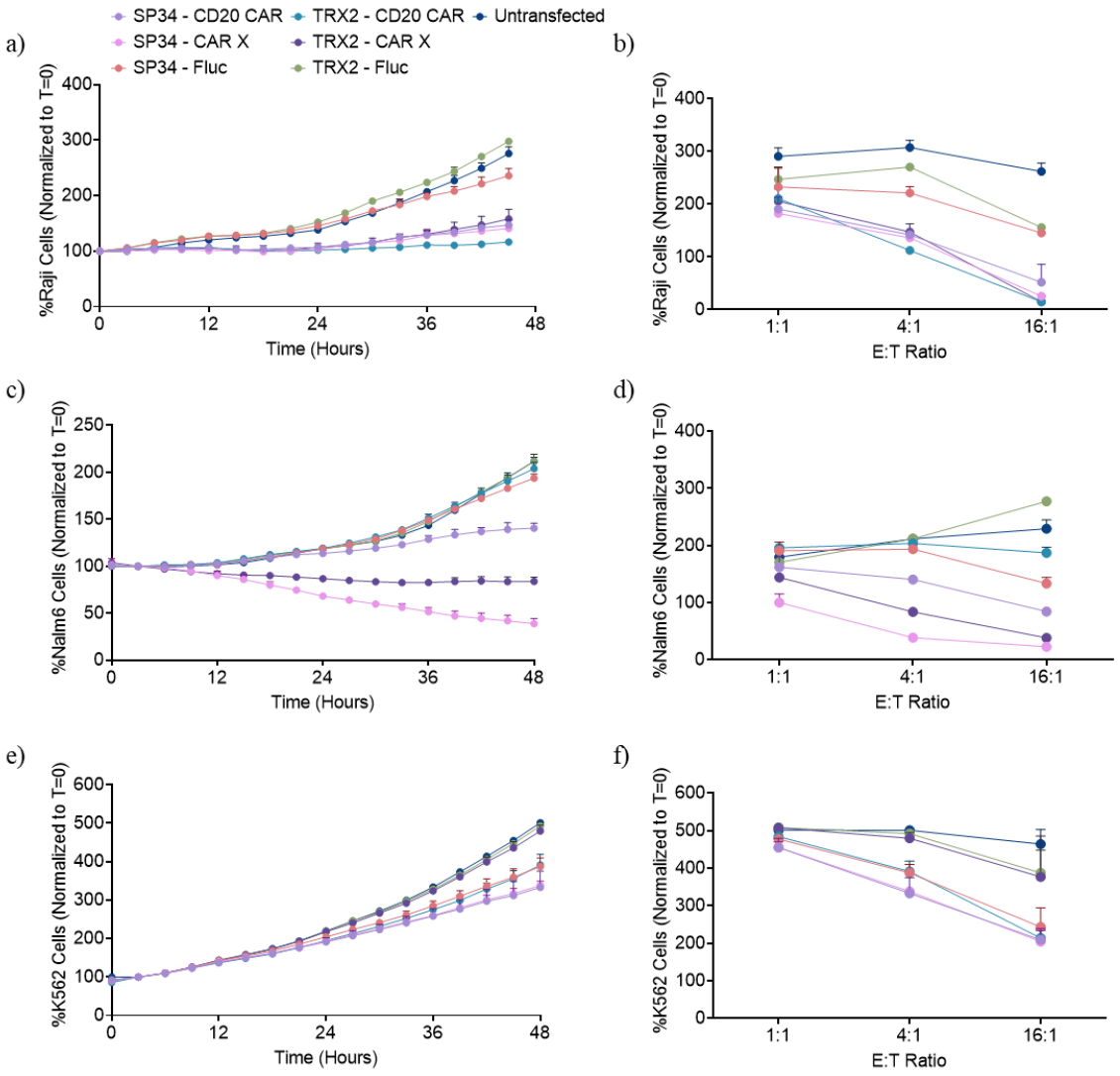

Supplemental Figure II-6. CAR-mediated cytotoxicity over time.

CAR-mediated killing was evaluated over time at various effector-to-target cell ratios in a-b) Raji cells, c-d) Nalm6 cells, e-f) and K562 cells using the IncuCyte SX5 instrument. Assays were performed in triplicate. Shown are mean values ± SD.

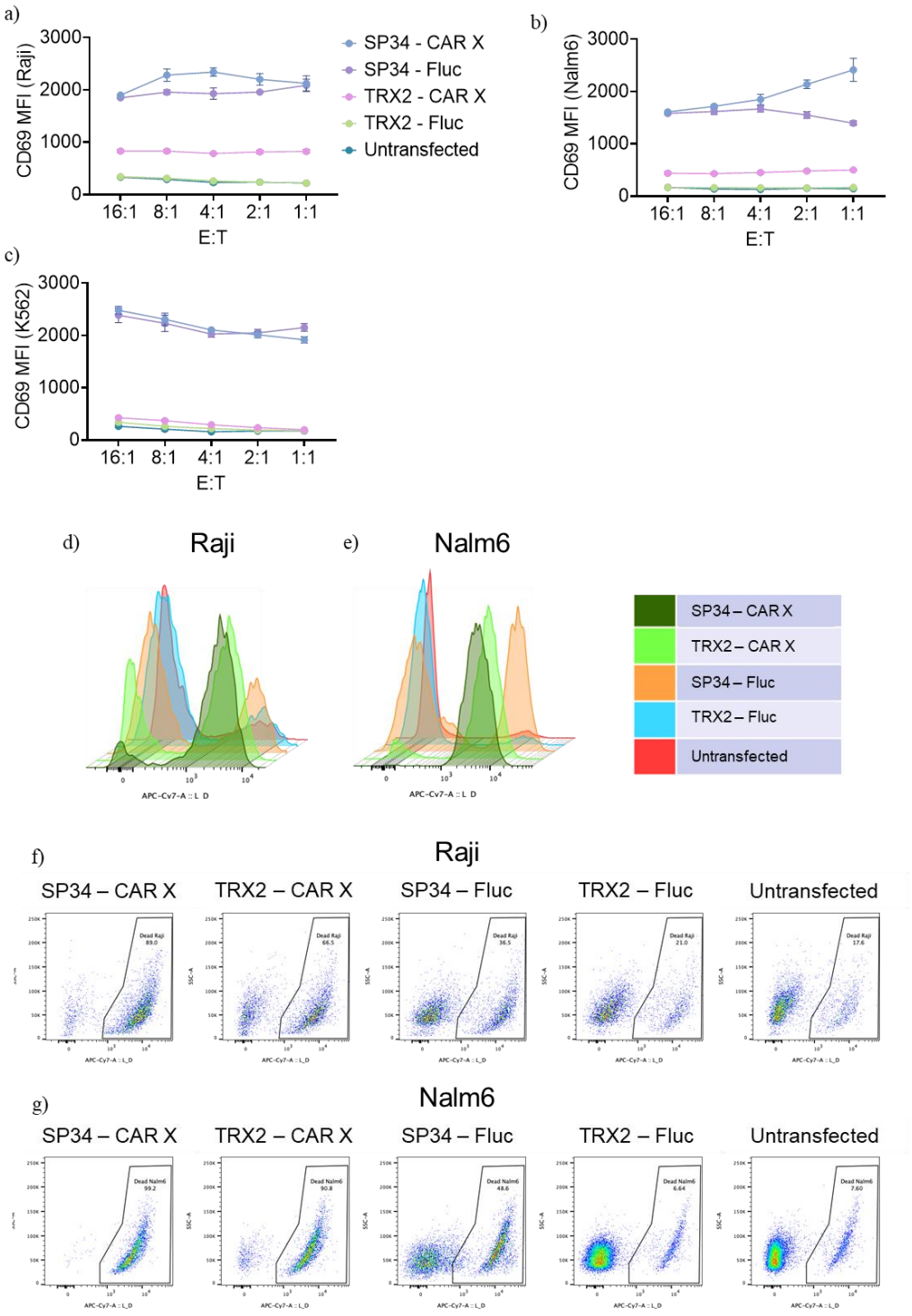

Supplemental Figure II-7. CAR-mediated cytotoxicity in multiple cell lines.

a-c) CD69 expression was assessed in treated T-cells co-cultured with different target cells. CAR-mediated cytotoxicity is shown as d-e) histogram overlays f-g) and Flow Cytometry dot plots. Assays were performed in triplicate. Shown are mean values ± SD.

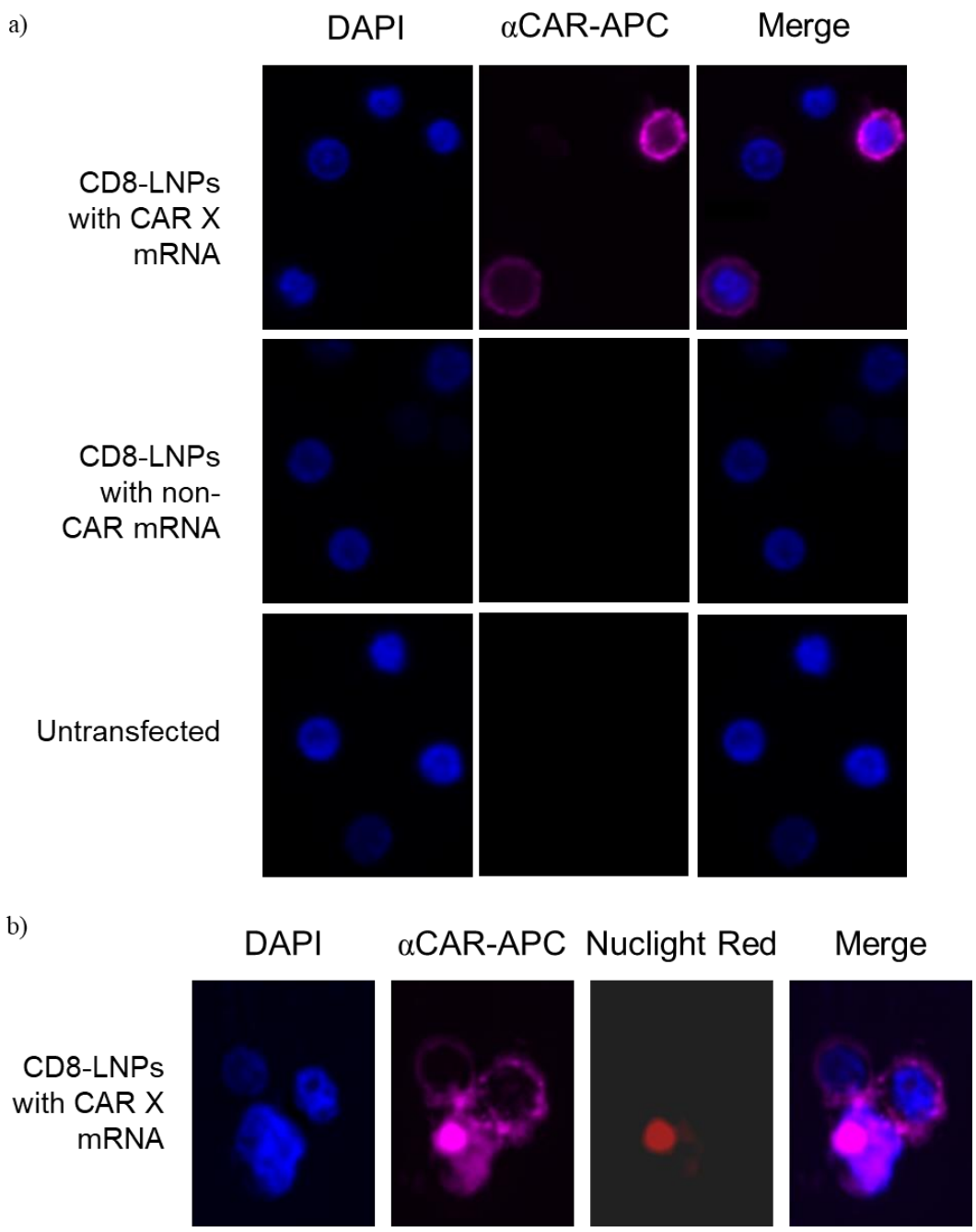

Supplemental Figure II-8. CAR-expression visualized by microscopy.

a-b) Microscopy was performed to visualize CAR expression (pink) and engagement of CAR-T cells with target cells (red). The nuclei were stained with Hoechst (blue).

Chapter III | Reprogramming murine T-cells *in situ* to secrete and capture anti-tumoral BiTEs utilizing IVT mRNA

Authors:

Viktor T Lemgart[1,2,*], Ralston Augspurg[1], Allison Caron[1], Carrington Mcleod[1], Brandon Quido[1], Samantha Stewart[1], Michael Monte[1], Rasmus Münter[2], Unnur Jóna Björgvinsdóttir[2], Doha Ghannam[2], Andrew Sawyer[1], Ulrik Nielsen[1], Austin Boesch[1], Daryl Drummond[1,*]

Affiliations:

[1] Tidal Therapeutics (a Sanofi Company), Sanofi, Cambridge, MA, USA

[2] Department of Health Technology, Technical University of Denmark, Lyngby, Denmark

[*] Corresponding author

The purpose of this chapter is to demonstrate how murine T-cells can be transiently reprogrammed to secrete an anti-tumoral BiTE construct. We explore various targeting strategies against murine T-cells and show how the targeting can affect the phenotype of the cell. We demonstrate that the technology can drive functional BiTE-mediated tumor cell killing and thus tumor regression *in vitro* and *in vivo*.

Ralston Augspurg, Michael Monte, and Rasmus Münter kindly formulated and characterized the LNPs used herein.

III.1 | Abstract

Immunotherapies utilizing bispecific T-cell engagers (BiTEs) have shown great promise in redirecting T-cells against tumor-specific antigens and inducing lysis. However, due to the short half-life of scFvs, current treatment with BiTEs requires continuous infusion to maintain therapeutic serum levels. Additionally, despite the clinical success of blinatumomab, a first-in-class anti-CD19 x CD3 BiTE construct against hematological malignancies, targeting solid tumors with BiTEs remains a major challenge. Here, we develop a platform, using antibody-targeted lipid nanoparticles (LNPs) encapsulating mRNA to reprogram circulating murine T-cells *in vivo*, thus overcoming these barriers. We show that the approach can be utilized to deliver anti-EphA2 x CD3 BiTE-encoding mRNA to T-cells through an antibody-derived targeting moiety, thereby allowing for repeated dosing strategies while circumventing off-cell target mRNA delivery. We further demonstrate that the reprogramming of T-cells to secrete BiTEs can drive functional cytotoxicity against an EphA2-expressing cancer cell line *in vitro* and *in vivo*. Collectively, our approach holds strong promise for becoming a broadly applicable and highly adaptable targeting immunotherapeutic platform for treating solid tumors.

III.2 | Introduction

Targeted immunotherapeutic strategies against cancers have shown tremendous success since first entering the clinic in the 1990s following the approval of the anti-CD20 monoclonal antibody (mAb) rituximab for treating non-Hodgkin lymphoma (NHL) [163]. Having shown promising pre-clinical and clinical results, one such strategy is the use of bispecific T-cell engagers (BiTEs) [164, 165]. BiTEs are a subclass of bispecific antibodies, consisting of two scFvs linked by a peptide chain, simultaneously binding a tumor antigen and a molecule on the T-cell surface to redirect the T-cell to induce tumor cell lysis [166]. Currently, recombinant BiTEs are exogenously administered, and owing to the lack of an Fc portion responsible for neonatal Fc receptor-mediated recycling, the protein has a short half-life and is thus rapidly cleared from circulation [167]. As a result, recombinant BiTEs are administered by continuous intravenous infusion over long periods making the mode of application a drawback of the therapy [163]. In addition, patient exposure to high systemic doses has resulted in severe cytokine release syndrome (CRS) and neurotoxicity [168-170].

Ephrin receptor A2 (EphA2) is a key regulator of tumorigenesis in multiple cancers and previous studies have shown EphA2 to be a promising therapeutic target in various human malignancies [171]. EphA2 is upregulated in human tumor tissue as well as in established cancer cell lines with a relatively low expression in normal tissue. Additionally, elevated receptor expression is often associated with poor prognosis and reduced survival of tumor patients [172-174]. Anti-EphA2 x CD3 BiTEs have been studied previously, e.g. using strategies focused on the administration of the recombinant protein [175] or infusion of ex

vivo genetically modified T-cells secreting the BiTE [176]. Besides the already mentioned drawbacks of exogenously administered BiTEs, ex vivo gene-editing and adoptive T-cell therapy require cumbersome and expensive laboratory processes [177].

In vitro transcribed (IVT) mRNA has, in recent years, proven as a promising technology to express encoding proteins in cells, making it a desirable alternative to DNA-based products. By utilizing IVT mRNA researchers allow for transient protein expression without causing integration into the genome [149, 150]. However, to function *in vivo*, effective and stable delivery platforms, protecting the mRNA from degradation and allowing for cellular uptake, are required [100]. One such delivery system that has entered the clinic and proven successful is lipid nanoparticles (LNPs) [98, 105, 151]. Here, the recent authorization of two coronavirus disease 2019 (COVID-19) vaccines [68, 152] utilizing LNPs to deliver mRNA stands out as noticeable examples. However, specific systemic delivery of mRNA to other cell types than hepatocytes and Kupffer cells of the liver remains a major challenge [153, 154].

Recently, Rurik *et al.* reported mRNA delivery to T-cells *in vivo* via CD5-targeted LNPs to treat cardiac disease [134]. Additionally, Tombácz *et al.* showed mRNA transfection of $CD4^+$ T-cells using CD4-targeted LNPs [133]. Finally, Parayath *et. al.* in the Stephan lab at the Fred Hutchinson Research Center efficiently reprogramed $CD3^+$ and $CD8^+$ T-cells using IVT mRNA encapsulating polymeric nanoparticles [138]. However, to our knowledge, no compelling evidence exists of utilizing targeted LNPs to specifically reprogram various T-cell subsets to secrete and capture BiTEs and thereby achieve an anti-tumoral response.

Here, we describe a novel approach to selectively reprogram subsets of murine T-cells *in vitro* and *in vivo* by delivering IVT mRNA via antibody-targeted LNPs. We demonstrate the clinical relevance of the platform by showing a "secrete-and-capture" strategy, specifically delivering anti-EphA2 x CD3 BiTE-encoding mRNA to T-cells and report functional BiTE-mediated tumor cell killing and tumor regression *in vitro* and *in vivo*, respectively.

III.3 | Materials and methods

mRNA Design and Synthesis

mRNA was produced by Vernal Biosciences (Vermont, US). Briefly, GFP-, Fluc-, and anti-EphA2 x CD3 Bi-specific T-cell Engager (BiTE)-encoding mRNA were in vitro-transcribed, poly-A tailed, and capped (Cap1). Amino acid sequences for anti-mouse CD3 and EphA2 scFvs were derived from public sources (500A2 Genbank AAB81028.1, AAB81027.1; KT3 Genbank AVW80143.1; 2C11 EF063578.1; EphA2 Uniprot P29317). BiTE mRNAs were designed with a mouse kappa chain-derived signal peptide, a 3x(G4S) linker between the VH and VL domain of each binder, a 4x(G4S) linker between the two binders, and a FLAG-tag (Sequence: DYKDDDDK) at the 5' end of the binding region.

Lipid Nanoparticle (LNP) Preparation

LNPs were prepared in a similar fashion to previously published reports [155]. Briefly, LNPs were formulated with an encapsulated mRNA payload and lipid blend by mixing an

aqueous mRNA solution and an ethanolic lipid solution using an in-line microfluidic mixing process. The lipid components DLin-KC3-DMA (Organix Inc, Massachusetts, US), Cholesterol (Dishman, NL), Distearoylphosphatidylcholine (DSPC, Avanti Polar Lipids, Alabama, US), and 1,2-Dipalmitoyl-rac-glycero-3-methylpolyoxyethylene glycol-2000 (DPG-PEG2000, NOF America Corporation, New York, US) were dissolved in anhydrous ethanol. mRNA and lipid solutions were mixed using a NanoAssemblr Ignite microfluidic mixing device and NxGen mixing cartridge from Precision Nanosystems Inc. (British Columbia, Canada). Following mixing, ethanol removal and buffer exchange was performed on the resulting LNP suspension using a discontinuous diafiltration process. LNPs were recovered from the centrifugal device and stored at 4°C for short-term use. Otherwise, LNP solutions were spiked with a 49 wt% sucrose stock solution to reach a final sucrose concentration of 9.8 wt%. LNPs were then frozen and kept at -80°C for long-term storage.

Fab design and production

For LNP-targeting Fabs, in both the mouse heavy and light chain constant domains, the native interchain disulfide-forming cysteines were mutated to serine (mouse IgG2a CH1 heavy chain C15S, mouse kappa light chain C107S). Based on sequence homology to human Fabs, similar mutations to a previous report [156] were introduced into both the heavy and light chain to enable a stabilized disulfide linkage while avoiding DSPE-PEG-maleimide conjugation (mouse IgG2a CH1 heavy chain F53C, mouse kappa light chain S69C). At the end of the mouse CH1, the human IgG1 hinge was used up to the first natural

cysteine followed by a 6-his tag (EPKSSDKTHTCHHHHHH), enabling conjugation to DSPE-PEG-maleimide and purification by IMAC.

Variable heavy and light chain amino acid sequences for anti-mouse CD3, TCR, CD8 and CD4 clones were derived from public sources (500A2 Genbank AAB81028.1, AAB81027.1; KT3 Genbank AVW80143.1; 2C11 EF063578.1; H57 PDB 1NFD, YTS105.18.10 PDB 2ARJ; YTS169.4.2.1, YTS156.7.7 and 2.43 AB030195; GK1.5 Genbank AAA51349.1, PMID 16901500). Fabs were produced in HEK, purified by IMAC, and formulated into PBS by Biointron (Taizhou, China).

Fab conjugation and LNP post-insertions

Antibody conjugations to DSPE-PEG were done similarly to previously published reports [157, 158]. DSPE-PEG(2k)-Fab conjugate was then combined with base LNPs and placed in a ThermoMixer (Eppendorf, Hamburg, Germany) at 37°C at 300 rpm for 4 hours, followed by storage at 4°C until use.

Characterization of LNPs

The LNPs were characterized to determine the average hydrodynamic diameter, zeta potential, and mRNA content (total and dye-accessible). The hydrodynamic diameter was determined by dynamic light scattering (DLS) using a Zetasizer model ZEN3600 (Malvern

Pananalytical, Malvern, UK). The zeta potential was measured in 5 mM pH 5.5 MES buffer and 5 mM pH 7.4 HEPES buffer by laser Doppler electrophoresis using the Zetasizer.

RNA content of the nanoparticles was measured using Quant-iT RiboGreen RNA Assay Kit (Thermo Fisher, Massachusetts, US). Dye-accessible RNA, which includes both non-incorporated RNA and RNA that is near the surface of the nanoparticle, was measured by diluting the nanoparticles to approximately 1 µg/mL mRNA using HEPES buffered saline, and then adding Quant-iT reagent to the mixture. Total RNA content was measured by diluting the particles to 1 µg/mL mRNA using HEPES buffered saline, disrupting the nanoparticles by heating them to 60°C for 30 minutes in HEPES buffered saline containing 0.5% Triton, and then adding Quant-iT reagent. RNA was quantified by measuring fluorescence at 485/535 nm on a SpectraMax M5 Microplate Reader (Molecular Devices, California, US) and concentration was determined relative to a contemporaneously run RNA standard curve.

BiTE detection by ELISA

anti-EphA2 x CD3 BiTE secretion was detected and quantified using a sandwich ELISA developed in-house. HEK293T cells were electroporated with varying levels of mRNA encoding the anti-EphA2 x CD3 BiTE or GFP as a negative control. 24 hours post electroporation, 2 mL of supernatants were removed and analyzed for BiTE secretion. Samples were added to a 10 kDa regenerated cellulose membrane (EMD Millipore, Massachusetts, US) and reduced to 200 µL to concentrate the samples tenfold. Immulon 2HB Flat Bottom

plates (Thermo Fisher, Massachusetts, US) were then coated with recombinant mouse EphA2 (Sino Biological, Pennsylvania, US) diluted in PBS with 100 µL per well at 3 µg/mL and incubated overnight at 4°C. After blocking the plate with ELISA BSA Block (Bio-Rad, California, US) for 1 hour, 50 µL of sample or recombinant anti-EphA2 x CD3 BiTE standard was added. After washing with TBS-T, 50 µL of biotinylated mouse anti-DYKDDDK-tag (Thermo Fisher, Massachusetts, US) diluted in ELISA BSA Block were added to the wells at 0.2 µg/mL for 2 hours. Following another wash, 50 µL of Streptavidin-HRP diluted in ELISA BSA Block (Thermo Fisher, Massachusetts, US) was added at 0.25 µg/mL and incubated in the dark for 30 minutes. After extensive washing, 100 µL of TMB Substrate solution (Thermo Fisher, Massachusetts, US) was added to each well and allowed to incubate in the dark for 5 minutes. The reaction was stopped, and ODs were determined at 450 nm using a SpectraMax M5 Microplate Reader (Molecular Devices, California, US).

Cell lines

The EphA2-positive BALB/c colon carcinoma cell line, CT26, and the EphA2-negative C57BL/6 melanoma cell line, B16-F10, were purchased from ATCC (Virginia, US). The EphA2-positive C57BL/6 colon adenocarcinoma cell line, MC38, was purchased from Creative Biolabs (New York, US). All cell lines were maintained according to the manufacturer's recommendations. CT26, B16-F10, and MC38 NucLight red cells were generated by transducing the respective WT cell lines with the NucLight Red Lentivirus (Essen Biosciences, Michigan, US) and selecting transduced cells with puromycin.

Mouse experiments

For experiments performed at Sanofi S.A., female wild-type BALB/c mice were obtained at 6 weeks of age from Jackson Laboratory (Maine, US) and housed at Charles River Accelerator and Development Lab (CRADL) (Massachusetts, US). All animal procedures were performed in accordance with the National Institutes of Health Guide for the Care and Use of Laboratory Animals and were approved by the CRADL Institutional Animal Care and Use Committee. For experiments performed at the Technical University of Denmark, female wild-type BALB/c mice were purchased at 6 weeks of age from Janvier Labs (Le Genest-Saint-Isle, France) and housed at the Department of Health Technology, Technical University of Denmark (Lyngby, Denmark). All experimental procedures were approved by the Danish National Animal Experiment Inspectorate and the Institutional Ethics Review Board.

Murine T cell generation *in vitro*

Following euthanasia by cervical dislocation spleens were harvested, cut into small fragments, and passed through a 70 µm cell strainer. Following wash in cold PBS, splenocytes were counted and $CD3^+$ or $CD8^+$ T lymphocytes were purified using direct negative magnetic isolation following the manufacturer's instructions (StemCell Technologies, Vancouver, Canada). Isolated $CD3^+$ or $CD8^+$ murine T-cells were plated in six-well plates at a concentration of $1x10^6$ cells/mL in RPMI-1640, supplemented with 10% FBS, 1X ITS, 55

µM 2-Mercaptoethanol, and 20 ng/mL recombinant murine IL-2, and 5 ng/mL recombinant murine IL-7 (Miltenyi, Bergisch Gladbach, Germany). Cells were rested for at least 2 hours at 37°C preceding treatment. For *in vitro* experiments requiring T-cell activation and expansion, isolated T-cells were stimulated by CD3/CD28 as previously described by others [178].

In vitro evaluation of CD3-, CD4-, and CD8-dependent uptake in primary T-cells

Prior to LNP treatment, isolated naïve T-cells were seeded into 96-well round bottom plates at a concentration of $1x10^6$ cells/mL. Cells were then treated by adding targeted LNPs encapsulating mRNA to the cells followed by mixing by pipetting and incubating at 37°C for 24 hours.

Cells were washed in PBS containing 0.5% BSA and 0.1% NaN_3 (FACS buffer) for cytometry analysis. After washing, cells were stained with CD4-, CD3-, and CD8-antibodies. Staining was performed at 4°C for 30 minutes prior to washing and resuspending in FACS buffer. Stained cells were acquired by flow cytometry on a Symphony (BD Biosciences, New Jersey, US) running FACSDiva software and further analyzed in FlowJo (BD Biosciences, New Jersey, US). Dead cells were excluded from analysis by using eFluor780 fixable viability dye (Thermo Fisher, Massachusetts, US).

In vitro cytotoxicity

CD3/CD28-stimulated murine $CD8^+$ T-cells were transfected as described above. Unbound LNPs were removed by washing 4 hours post-transfection, and T-cells were co-cultured with Cell Trace Violette (CTV)-stained target cells, which were either $EphA2^+$ or $EphA2^-$ cell lines as described above, at varying effector-to-target cell ratios in T-cell media (RPMI-1640, 10% FBS, 1X ITS, 55 µM 2-Mercaptoethanol, 20 ng/mL recombinant murine IL-2, and 5 ng/mL recombinant murine IL-7). After 48 hours of coculture, supernatants were removed for cytokine analysis and cells were stained with anti-CD69-antibody (BD Biosciences, New Jersey, US) and eFluor780 fixable viability dye (Thermo Fisher, Massachusetts, US) to assess levels of activation and target cell killing, respectively. Stained cells were acquired by flow cytometry on a Symphony (BD Biosciences, New Jersey, US) running FACSDiva software and further analyzed in FlowJo (BD Biosciences, New Jersey, US). The percentage of specific killing was calculated by evaluating the viability of the CTV-positive cells at the specific time point and comparing it to the viability of target cells alone.

IncuCyte Cytotoxicity assay

The IncuCyte NucLight Red Lentivirus reagent (Sartorius, Gottingen, Germany) was used to transduce CT26 cells following the manufacturer's protocol. Transduced NucLight Red positive cells were selected for using puromycin and >95% purity was confirmed by flow cytometry prior to co-culture assays. CD3/CD28-stimulated murine $CD8^+$ T-cells were

transfected as described above. Unbound LNPs were removed by washing in PBS 4 hours post-transfection. Transfected T-cells were then co-cultured with NucLight Red Lentivirus transduced CT26 cells at varying effector-to-target cell ratios in T-cell media (RPMI-1640, 10% FBS, 1X ITS, 55 µM 2-Mercaptoethanol, 20 ng/mL recombinant murine IL-2, and 5 ng/mL recombinant murine IL-7) in a 96-well flat-bottom plate. Cancer cell killing was monitored in the SX5 IncuCyte every 3 hours. The level of cytotoxicity was quantified by normalizing the count of red cells at the individual time points to the count at the initial time point.

T-cell gene expression profiles

Gene expression profiles of LNP-transfected $CD8^+$ T-cells were assessed using nCounter Mouse PanCancer Immune Profiling Panel (NanoString Technologies, Washington, US), characterizing 770 murine immunology- and cancer-related genes. Briefly, $CD8^+$ murine T-cells were isolated and transfected as described above. Cells were lysed using Buffer RLT (Qiagen, Hilden, Germany), and cell lysates were treated with Proteinase K (Thermo Fisher, Massachusetts, US) prior to hybridization following the manufacturer's instructions.

Cytokine profiling with MSD

Cytokine secretion *in vitro* and *in vivo* was analyzed by MSD (Meso Scale Diagnostics, Maryland, US). For *in vitro* analysis, supernatants were pulled from cell culture at the respective time point and a custom U-PLEX assay was used for the detection of mouse TNF-alpha and IFN-gamma following the manufacturer's instructions. For *in vivo* analysis, blood was drawn at the respective time points into 300 µL Microvette 100 EDTA tubes and centrifuged at 500 x g for 10 minutes. Plasma was then collected and analyzed using a custom U-PLEX assay for the detection of mouse IL-6, IL-12p70, TNF-alpha, and IFN-gamma following the manufacturer's instructions.

In vivo reprogramming, tissue collection, and analysis

For reprogramming T-cells *in vivo*, 0.3 mg/kg or 1 mg/kg mRNA encapsulated in LNPs was administered intravenously through the tail vein of 6 to 8-week-old female BALB/c mice.

Blood was collected into EDTA-coated collection tubes and red blood cells were lysed using Versalyse (Beckman Coulter, California, US). Cells were washed in FACS buffer and stained with CD45-, CD4-, CD3-, CD8-, CD69-, CD19-, and CD335-antibodies for 30 minutes at 4°C. Cells were washed twice in FACS buffer and acquired by flow cytometry on an LSRFortessa X-20 (BD Biosciences, New Jersey, US) running FACSDiva software and further analyzed in FlowJo. Dead cells were excluded from analysis by using eFluor780 fixable viability dye (Thermo Fisher, Massachusetts, US).

Spleens and livers were excised, weighed, and processed to single-cell suspensions before staining and acquiring by flow cytometry as described above.

Microscopic imaging

Microscopy of murine $CD8^+$ T-cells was performed on a Nikon TiE microscope with a 100X objective and analyzed on (Fiji Is Just) ImageJ software. Briefly, isolated naïve T-cells transfected with CD3/CD8-targeted GFP/DiI LNPs for 24 hours were stained with NucBlue™ Live ReadyProbes™ (Thermo Fisher, Massachusetts, US) for 20 minutes at 37°C before washing and resuspending in Live Cell Imaging Solution (Thermo Fisher, Massachusetts, US) for microscopic analysis.

Efficacy study

6–8-week-old female Balb/c mice were subcutaneously inoculated with $2.5x10^5$ CT26 cells into the right flank 7 days prior to treatment initiation. Mice were randomized into treatment groups of n=4 according to tumor size prior to the first treatment dose. Anti-mouse PD-1 (clone RMP1-14) (Bioxcell, New Hampshire, US) was administered intraperitoneally twice a week for a total of six doses at 10 mg/kg. LNPs or recombinant anti-EphA2 x CD3 BiTE were administered by intravenous injection into the tail vein once a week for a total of three doses at 0.2 mg/kg. Body weights and tumor sizes were monitored three times a week throughout the study period.

Statistical analysis

Statistical significance, comparing two samples, was evaluated using Student's *t* test. Analysis of variance (ANOVA) was used to evaluate statistical significance for multiple comparisons followed by Dunnett's posttest to compare all groups against a single control. Statistical analysis was performed using GraphPad Prism. Error bars indicate the standard deviation (SD), or the standard error of the mean (SEM) as specified in the figure legend. A *p* value less than 0.05 was considered to be statistically significant.

III.4 | Results

Designing targeted lipid nanoparticles to deliver mRNA to murine T-cells to target solid tumors

We developed a targeted mRNA delivery system to specifically introduce transient protein expression in murine T-cells using lipid nanoparticles (LNPs) (Figure III-1). The commercially available ionizable lipid DLin-KC3-DMA was combined with set ratios of phospholipid, cholesterol, and DPG-PEG and mixed via a NanoAssemblr Ignite microfluidic device with mRNA and DiIC18(5) (DiI) to form traceable LNPs (Figure III-2a-c). The base LNPs were post-inserted with anti-CD3, -CD4, and/or -CD8 Fab conjugates to form T-cell targeting LNPs.

Assessing viability, LNP association, and mRNA transfection in primary T-cells

The resulting LNPs were first verified to not cause toxicity in isolated naïve murine T-cells as opposed to transfection by electroporation. The viability was shown to be maintained in T-cells treated with targeted LNPs in comparison to untreated T-cells (Figure III-3a). Next, the association of LNPs to specific T-cell subsets was assessed by evaluating the signal of the incorporated DiI dye. 24 hours post-transfection, an increased DiI mean fluorescence intensity (MFI) signal was observed in the T-cell subset corresponding to the specific targeting moiety (Figure III-3b-e). Interestingly, by evaluating the DiI signal in the specific subsets over time, the intensity peaked at 48 hours for CD8-targeting whereas the levels were maintained at the time points tested for the CD4-targeting LNPs (Supplemental Figure III-3) indicating altered kinetics for different targets. In addition, these experiments confirm that the targeted LNPs associate with their matching T-cell subset through the targeting moieties and not non-specifically through the LNP formulation itself.

To evaluate mRNA transfection and not solely LNP association, we then assessed the ability of the targeted LNPs to deliver mRNA encoding the reporter protein enhanced green fluorescent protein (GFP) to primary T-cells. Analogous to the particle association data, increased GFP expression was observed in the targeted T-cell subsets over the subsets negative for the specific targeting moiety (Figure III-3f-i). Additionally, to investigate whether CD3 and CD8 co-targeting could work in synergy and thereby increase the mRNA delivery efficiency over CD3 and CD8 single targeting, we treated T-cells with LNPs post-inserted with both anti-CD3 and anti-CD8 Fabs. Co-targeting proved to increase GFP expression

significantly in $CD4^-$ T-cells compared to CD3 single targeting ($p < 0.001$) and CD8 single targeting ($p < 0.001$), respectively (Figure III-3h). Finally, by evaluating GFP expression over time, a peak of expression intensity could be observed at 24 hours for CD8-targeting LNPs whereas the levels for CD4-targeting were maintained throughout the time course again suggesting that the uptake kinetics are related to the targeting moiety (Supplemental Figure III-3).

CD3-targeting LNPs causes T-cell activation

To investigate whether the different targeting moieties change the state of the T-cells and thereby their phenotype we next conducted a series of experiments evaluating upregulation of activation markers, secretion of cytokines, and expression of various genes associated with T-cell activation. Here, we first observed a clear upregulation of the early activation marker, CD69, by flow cytometry in the CD3- and CD3/CD8-targeted groups but not in the CD8-targeted group (Figure III-4a). This confirms earlier findings by others demonstrating that anti-CD3-conjugated LNPs induce T-cell activation and cause a phenotypic shift [179]. Similarly, we observed increased levels of IFN-gamma and TNF-alpha in the supernatants of T-cells treated with CD3-targeting LNPs (Figure III-4b-c). Additionally, when evaluating the T-cell phenotypes 48 hours after LNP treatment, we observed a shift from naïve toward memory subsets in groups treated with CD3-targeting LNPs (Figure III-4d). Finally, we evaluated the gene expression profiles of the treated T-cells using the nCounter Mouse PanCancer Immune Profiling Panel from NanoString Technologies. Supporting the CD69 activation data described previously, we here observed upregulation of

genes associated with T-cell activation in the groups treated with CD3- or CD3/CD8-targeting LNPs compared to the group with CD8-targeting LNPs and the untreated group (Figure III-4e).

Reprogramming T-cells *in vivo*

Having verified the ability of the targeted LNPs to transfect primary T-cells *in vitro*, we next explored the *in vivo* delivery efficacy using mCherry-encoding mRNA considering that GFP has shown to be immunogenic in certain strains of wildtype mice [180]. As for the *in vitro* studies, LNPs were formulated to incorporate DiI to study the association with cells. Anti-CD3, -CD4, -CD8, -CD3/-CD8, and untargeted LNPs were intravenously injected into wildtype BALB/c mice through the tail vein at 0.3 mg/kg and 1 mg/kg. Mice were euthanized 24 hours after injection and selected tissues (blood, spleen, and liver) were harvested, processed, and stained for analysis by Flow Cytometry.

~78% of $CD3^+CD8^+$ T-cells in the blood showed LNP-association when targeted with anti-CD8 in comparison to untargeted LNPs showing <2% in the same cell population (Figure III-5a). Similarly, ~67% of the $CD3^+CD4^+$ cell population were DiI-positive in mice treated with anti-CD4-targeted LNPs in contrast to ~2% in the group treated with an equal dose of untargeted LNPs (Figure III-5b). In contrast to our *in vitro* experiments, for both the $CD3^+CD4^+$ and $CD3^+CD8^+$ cell subsets, groups treated with anti-CD3- and anti-CD3/CD8-targeted LNPs showed lower levels of DiI than anti-CD4- or anti-CD8-targeted LNPs. T-cell frequencies after treatment were shown to be reduced in the blood but not in

the liver and spleen for groups treated with anti-CD3- and anti-CD3/CD8-targeted LNPs (Supplemental Figure III-4a-c) suggesting that anti-CD3-targeted LNPs triggers T-cell depletion in the blood. To confirm our *in vitro* findings, we then investigated whether CD69, an early surface marker of T-cell activation after TCR/CD3 complex engagement, was up-regulated [181]. Here, we found that CD69 levels were increased in mice treated with anti-CD3- and anti-CD3/CD8-targeted LNPs over other groups (Supplemental Figure III-4d-f). Similarly, in the spleen, a specific targeted-dependent cell association trend was observed for all groups treated with targeted LNPs over non-targeted LNPs (Figure III-5e-f). In contrast, T-cell subsets in the liver showed higher levels of non-specific LNP association (Figure III-5i-j).

Next, we evaluated the mRNA transfection efficiency by assessing the levels of mCherry protein expression encoded in the encapsulated mRNA. Here, we observed significant transfection ($p < 0.05$) in groups treated with anti-CD3- and anti-CD3/CD8-targeted LNPs in all tissues analyzed (Figure III-5c-d, g-h, and k-l) demonstrating that mRNA can be specifically and effectively delivered to T-cells *in vivo*. Additionally, the biodistribution and thus the effect of the active targeting moiety was investigated by IVIS. From these experiments, a clear trend could be observed that active targeting enabled increased transfection in the spleen and lymph nodes, known to be common T-cell populated tissues (Supplemental Figure III-5) [178, 182].

Taken together, from assessing LNP association and mRNA transfection, the data indicate that elevated levels of specific mRNA delivery to T-cells can be achieved both *in vitro* and *in vivo*. In addition, unlike the *in vitro* data, CD3-targeting was shown to be superior to

other single receptor targeting strategies for achieving increased mRNA expression in T-cells *in vivo*.

BiTE clone selection

To demonstrate a clinical application of the delivery platform, we next designed BiTEs encoding an anti-EphA2 ScFv linked to one of three anti-CD3 scFvs derived from the 2C11, KT3, and 500A2 clones, respectively. To select a lead construct with an optimal safety profile we screened the three BiTEs in T-cells and evaluated the T-cell viability and level of cytokine secretion without target engagement. Here, we observed a drop in viability and upregulation of CD69 when treating T-cells with the KT3 clone BiTE construct (Figure III-6a-b). Additionally, we observed increased levels of IFN-gamma and TNF-alpha in the supernatants of T-cells treated with the same BiTE construct (Figure III-6c-d). The two additional constructs, derived from the 2C11 and 500A2 clones, respectively, were comparable in the parameters tested with the 2C11 clone construct showing a slight increase in CD69 expression evaluated by Flow Cytometry over the 500A2 clone construct (Figure III-6b). Taken together, these *in vitro* experiments indicate that the 500A2 clone construct has a superior safety profile over the other screened constructs.

BiTE-encoding mRNA translation and protein secretion

After establishing efficient mRNA delivery to T-cells *in vitro* and *in vivo* by evaluating reporter protein expression, BiTE-encoding mRNA was in vitro transcribed and purified by Vernal Biosciences. Since the BiTEs would likely be secreted and captured by the $CD3^+$ T-cells and not allow for protein detection in the supernatants, we decided to electroporate HEK293Ts with the naked mRNA. After electroporating HEK293T cells with varying concentrations of BiTE mRNA, supernatants were pulled and analyzed by ELISA to evaluate levels of protein secretion. Here we observed that the BiTE protein was secreted in a dose-dependent manner thus validating the ability of the designed BiTE mRNA to be translated and secreted (Figure III-6e).

BiTE-mediated target cell killing and cytokine release

Given the efficient reporter protein expression *in vitro* and *in vivo* and after having verified the ability of the BiTE mRNA to be translated and secreted, we next evaluated whether the delivery platform could drive functional BiTE-mediated target cell killing.

By co-culturing LNP-transfected T-cells secreting and capturing an anti-EphA2 x CD3 BiTE with the mouse colon carcinoma $EphA2^+$ cell line, CT26, we looked to assess specific cancer cell killing over time with the IncuCyte SX5 instrument. This was done by evaluating the number of live target cells at each scanned timepoint in each group and normalizing them to the respective T=0 timepoint. Here, we observed statistically significant ($p < 0.05$) increased killing in the BiTE groups over the corresponding non-BiTE mRNA groups

(Figure III-7). However, in the same study, we observed that CD3- and CD3/CD8-targeted LNPs encapsulating Fluc mRNA showed increased target cell killing in comparison to the untreated control groups.

BiTE-LNP drives efficacy in subcutaneous CT26 mouse model

Having shown that the targeted BiTE mRNA encapsulating LNPs could drive target-mediated killing *in vitro* we next looked to evaluate the platform in a subcutaneous CT26 efficacy model *in vivo*. Tumor-bearing mice were injected with CD3/CD8-targeted LNPs encapsulating either anti-EphA2 x CD3 BiTE mRNA or Fluc mRNA as a control once a week for a total of three doses (Figure III-8a). A separate control group was injected with recombinant anti-EphA2 x CD3 BiTE protein at a similar dose (0.2 mg/kg) and dosing schedule. Here we observed a statistically significant ($p < 0.01$) halt in tumor progression in the LNP-BiTE-treated group in comparison to the vehicle group (Figure III-8b). No other groups showed statistically significant improved survival ($p < 0.05$) in comparison to the vehicle group (Figure III-8). However, though not statistically significant, the PD-1-treated group showed a trend indicating improved efficacy over the control group.

III.5 | Discussion

While BiTEs have emerged as a promising treatment for hematologic malignancies, it is clear that several challenges remain for BiTEs to become the standard of care in various cancers and available to the broad patient population. Especially, when it comes to treating

solid tumors, the systemic infusion of recombinant BiTEs has shown low efficacy and severe systemic toxicities [163, 164, 166]. One solution could be to reprogram the patient's T-cells to become BiTE-secreting factories directly *in vivo* using in vitro transcribed (IVT) mRNA and thereby overcoming the challenges associated with the systemic administration of recombinant therapeutic proteins.

Here, we explored an mRNA delivery strategy using targeted lipid nanoparticles (LNPs) to transfect and reprogram T-cells. We demonstrate that IVT mRNA can be delivered specifically to modify T-cells *in vitro*. Additionally, we show that when administered systemically to mice, CD3-, CD4-, and CD8-targeting LNPs can be utilized to specifically deliver mRNA and thus reprogram T-cell subsets *in vivo*. Finally, we show that the systemic delivery of targeted LNPs encapsulating functional anti-EphA2 x CD3 BiTE mRNA can halt tumor progression in a subcutaneous CT26 solid tumor mouse model.

Co-targeting of CD3 and CD8 did not improve the transfection efficiency over single targeting of CD3 *in* vivo. However, a broader range of Fab densities could be assessed in the future to optimize and improve the transfection efficiency.

CD3-, CD4-, and CD8-targeting showed different expression kinetics in our time course experiments. Interestingly, this indicates that the mechanism of uptake may vary from target to target and that a depot effect – the slow release of mRNA into the cytoplasm – can be achieved for certain targets, which can result in prolonged protein expression. However, additional *in vitro* studies would be required to confirm this.

In vitro, we observed increased activation, cytokine release, and unspecific target cell killing when T-cells were transfected with CD3-targeting LNPs. The observed unspecific killing is likely a secondary event following T-cell activation rather than a result of direct interaction with the injected CD3-targeting LNPs as the targeting antibody used has been shown to be highly specific [183]. *In vivo*, we observed depletion of T-cells in the blood after treating mice with CD3-targeting LNPs, which confirms the phenomenon observed and described by others [179]. One mechanism for T-cell depletion after treatment with CD3-specific antibodies has been proposed to be activation-induced cell death. However, additional studies would be required to further conclude on this matter [184].

We chose to target EphA2 and design and encapsulate an anti-EphA2 x CD3 BiTE-encoding mRNA payload in our targeted LNPs. This was based on the strong therapeutic value of BiTEs [140, 185, 186] and the validation of EphA2 as a promising target in solid tumors [172, 173, 175, 187]. With this, we show that T-cells can be reprogrammed to secrete and capture a functional anti-EphA2 x CD3 BiTE using targeted LNPs and thereby mediate target-specific cancer cell killing. Follow-up *in vivo* studies, however, with increased numbers of mice per group and additional orthotopic cancer models, are needed to confirm this along with optimizing dosing strategies. Nevertheless, these initial proof-of-concept studies show immense potential for this as a novel anti-cancer immunotherapy strategy.

In situ reprogramming of specific cell types such as T lymphocytes is an emerging and rapidly growing field as indicated by several recently published studies [129, 133, 135, 139, 162]. However, to our knowledge, this is the first report demonstrating a targeted LNP system to specifically deliver BiTE encoding mRNA to various T-cell subsets. In

conclusion, this platform holds promise for becoming a first-in-class alternative to current BiTE therapies to treat solid tumors, overcoming significant biological barriers, and easing the patient burden associated with current BiTE treatments.

III.6 | Acknowledgements

Funding

The work in this study was supported by Sanofi S.A.

Author contributions

V.T.L., A.S., U.N., A.B., and D.D. conceived the project and designed experiments. V.T.L., A.C., C.M., B.Q., S.S., U.J.B., and D.G. performed experiments. R.A., M.M., and R.M. produced the LNPs. V.T.L., A.B., and D.D. interpreted the data. V.T.L. wrote the manuscript. All authors reviewed and edited the manuscript.

Competing interests

V.T.L., A.C., R.A., C.M., B.Q., S.S., M.M., A.S., U.N., A.B., and D.D. were employees of Sanofi at the time of the research, and A.C., B.Q., S.S., M.M., A.S., U.N., A.B., and D.D. are stockholders or hold stock options at Sanofi.

Data and material availability

The authors declare that all data supporting the results of this study are available within the paper and its supplementary information files. Source data collected in this study are available from the corresponding authors upon request.

III.7 | Figures

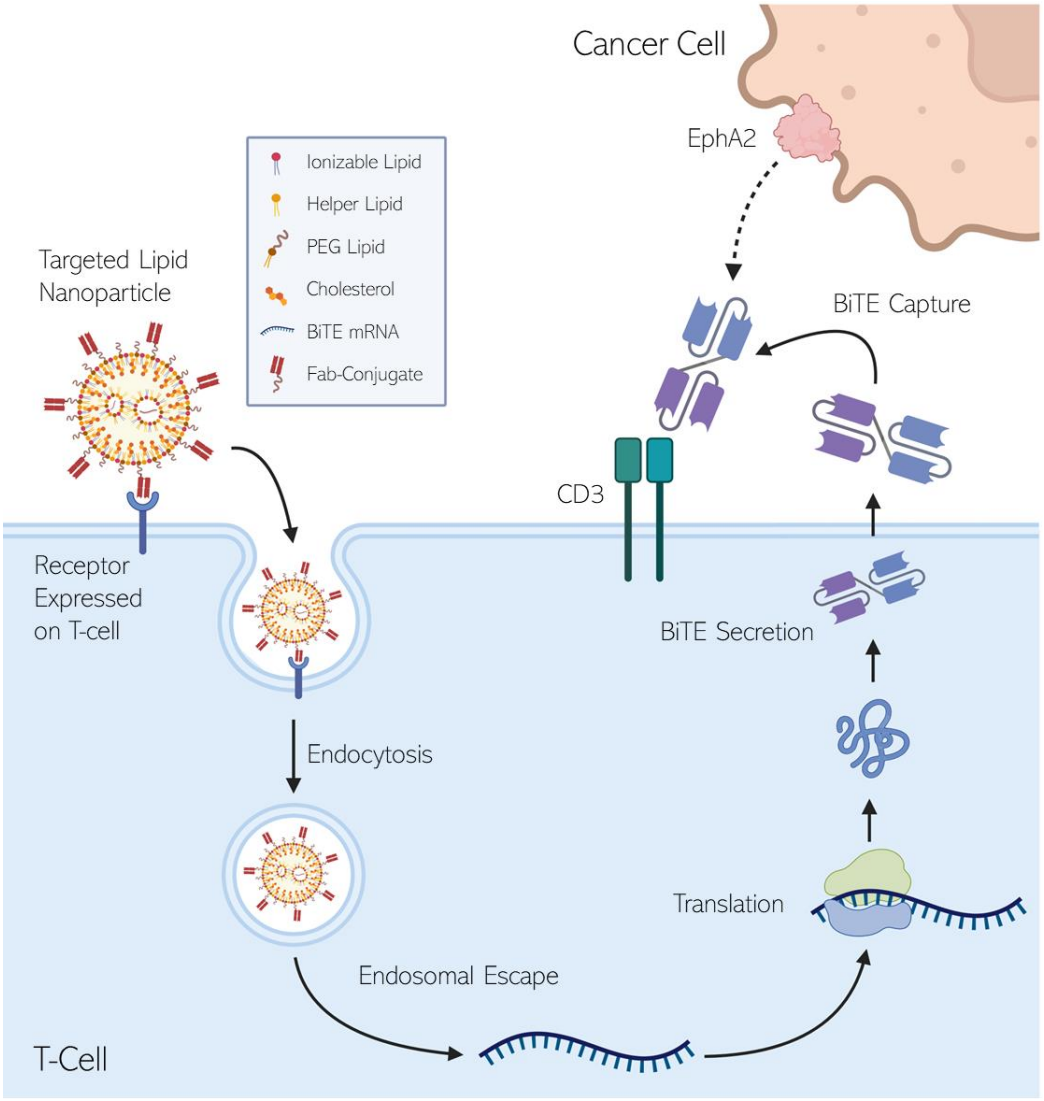

Figure III-1. Schematic of how targeted LNPs can be utilized to reprogram T-cells to secrete BiTEs.

First, LNPs engage with the T-cell through the inserted protein-based targeting moiety of interest. The target engagement allows for receptor-mediated endocytosis, which results in mRNA escape driven by the ionizable lipid. After being translated into the encoding protein, the BiTE is secreted and engages the T-cell with the target cell mediating cancer cell killing. Created with BioRender.com.

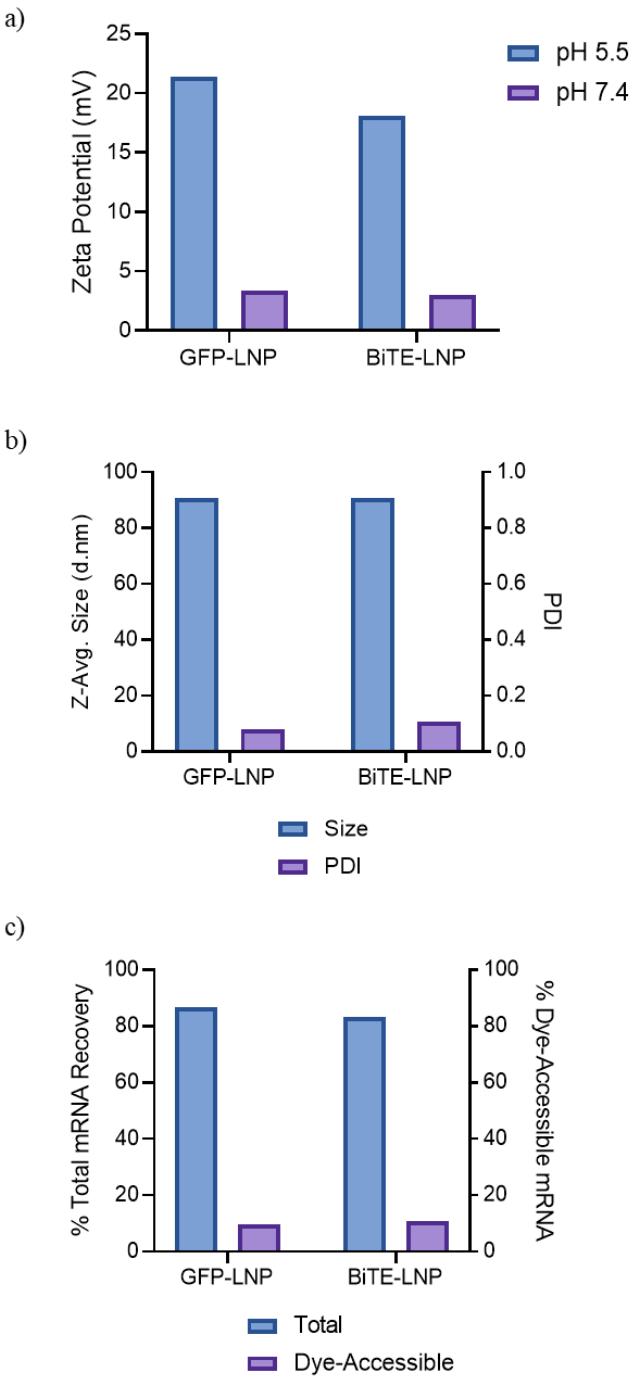

Figure III-2. LNP characterization.

a) The zeta potential, b) size-distribution, and polydispersity index (PDI) was measured using a Zetasizer. c) The RNA encapsulation efficiency was quantified using a Quant-iT RiboGreen RNA Assay Kit. Measurements were performed in triplicate. Means ± SD are depicted. GFP, enhanced green fluorescent protein.

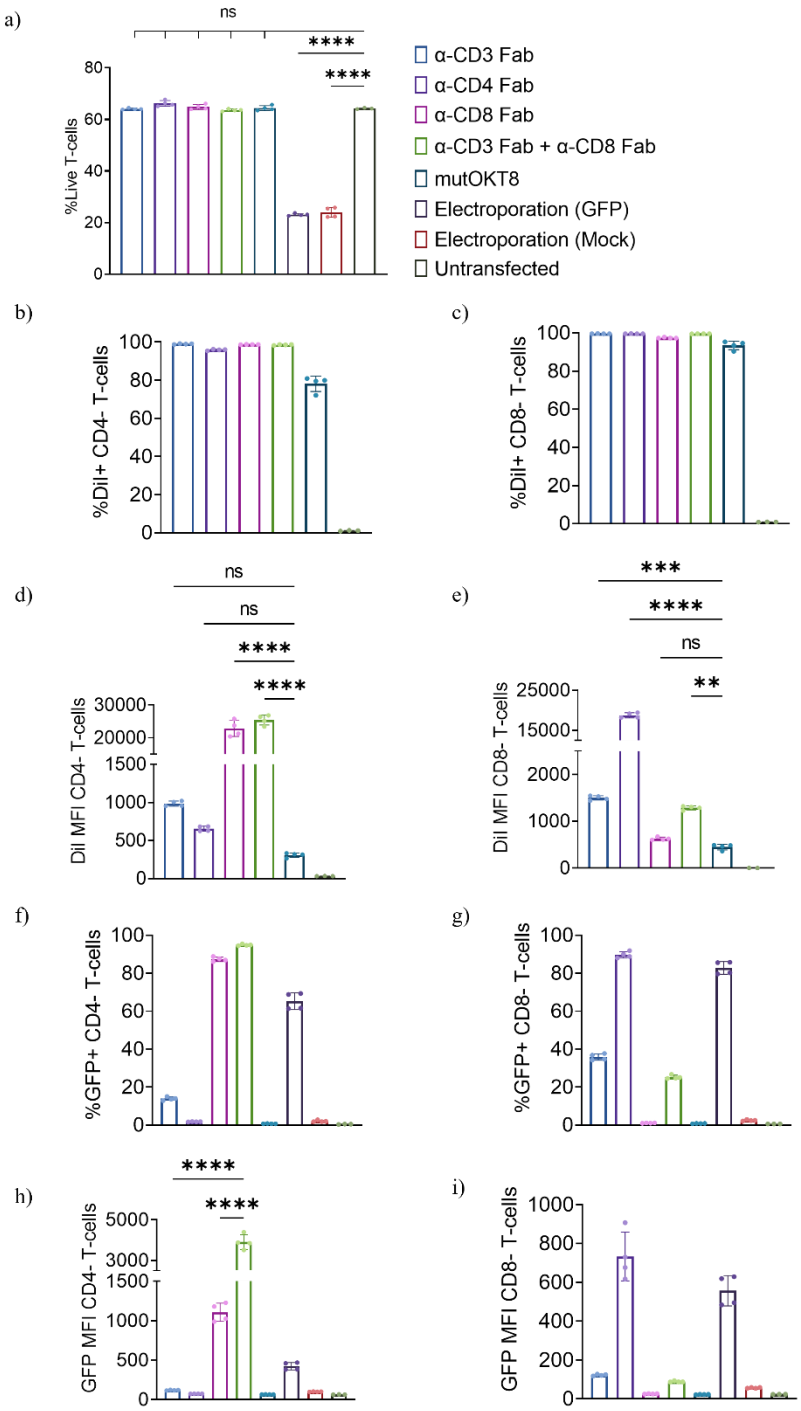

Figure III-3. T-cell transfection *in vitro*.

Naïve primary $CD3^+$ murine T-cells were treated with targeted LNPs or transfected by electroporation. a) T-cell viability, b-e) DiI association, and f-i) GFP expression was assessed 24 hours after treatment by flow cytometry. Displayed *p*-values are from one-way ANOVA $p<0.05$. Assays were performed with n = 4 biologically independent replicates. Shown are mean values ± SD.

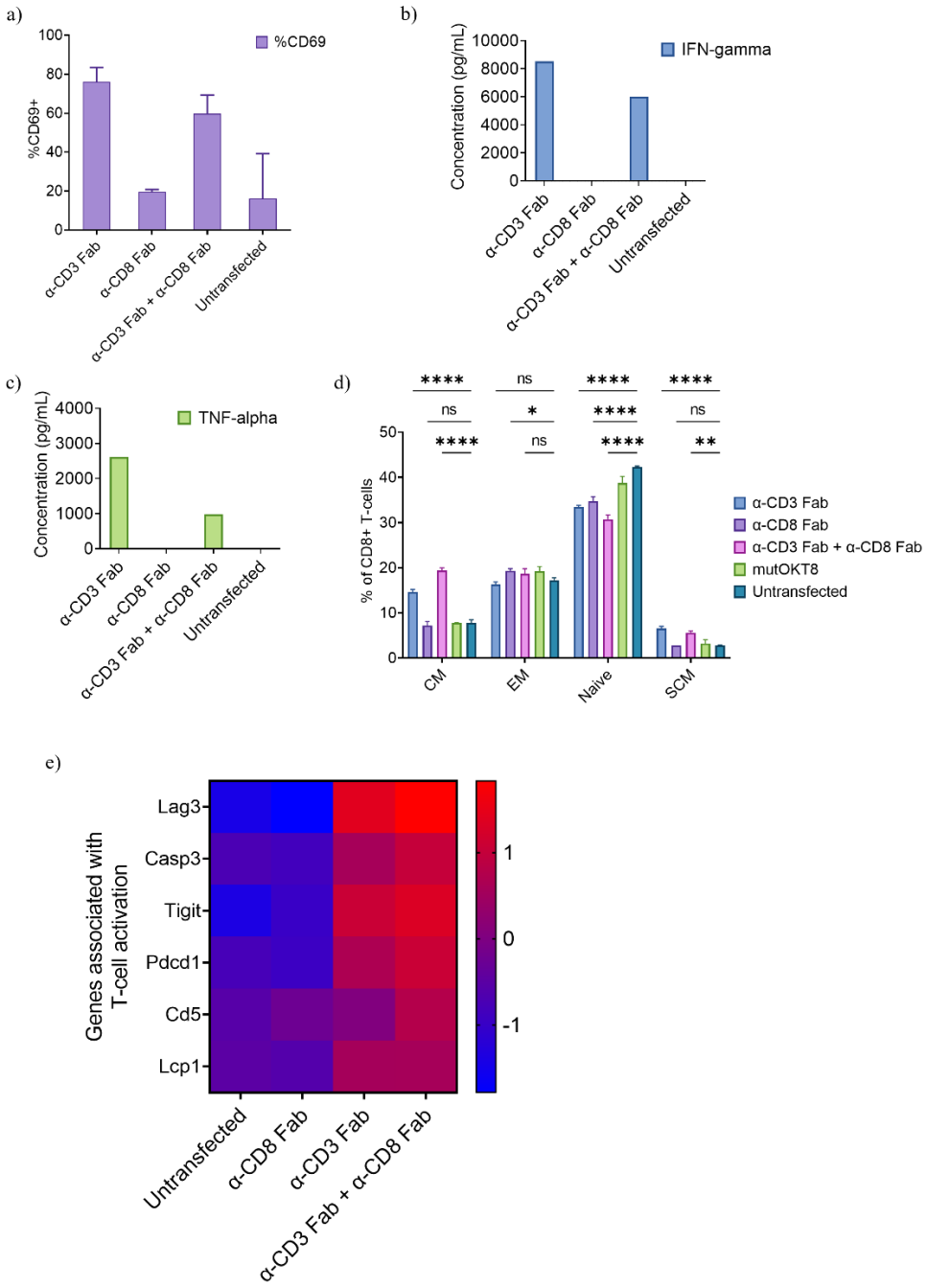

Figure III-4. Targeting effect on T-cell phenotype.

T-cell activation, cytokine release, gene expression, and phenotyping after treatment with different targeting moieties. a) The upregulation of the early activation marker, CD69, the secretion of b) IFN-gamma and c) TNF-alpha, f-i) and the gene expression was assessed after transfection with anti-CD3 and/or anti-CD8 constructs. Naïve, naïve T-cells; SCM, stem cell-like memory T-cells; CM, central memory T-cells; EM, effector memory T-cells. Displayed *p*-values are from two-way ANOVA $p<0.05$. N = 3 biologically independent samples. Data are mean ± SEM.

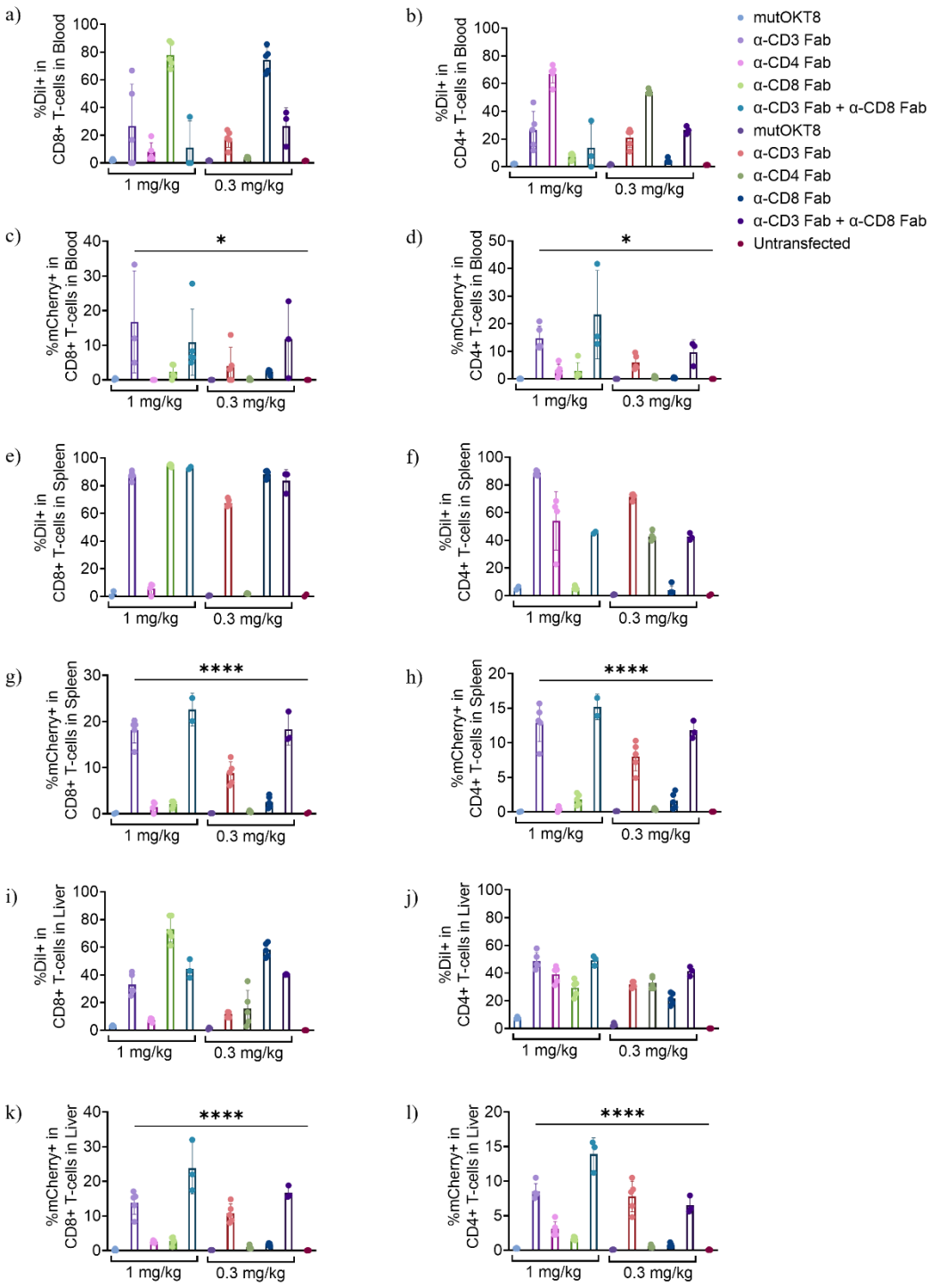

Figure III-5. LNP-mediated mRNA delivery efficiency to WT Balb/c mice.

DiI association and mCherry expression in the a-d) blood, e-h) spleen, and i-l) liver 24 hours after intravenous injection was assessed by flow cytometry. N = 4, 5 biologically independent mice per condition. Data are mean ± SEM. Displayed *p*-values are from one-way ANOVA $p<0.05$.

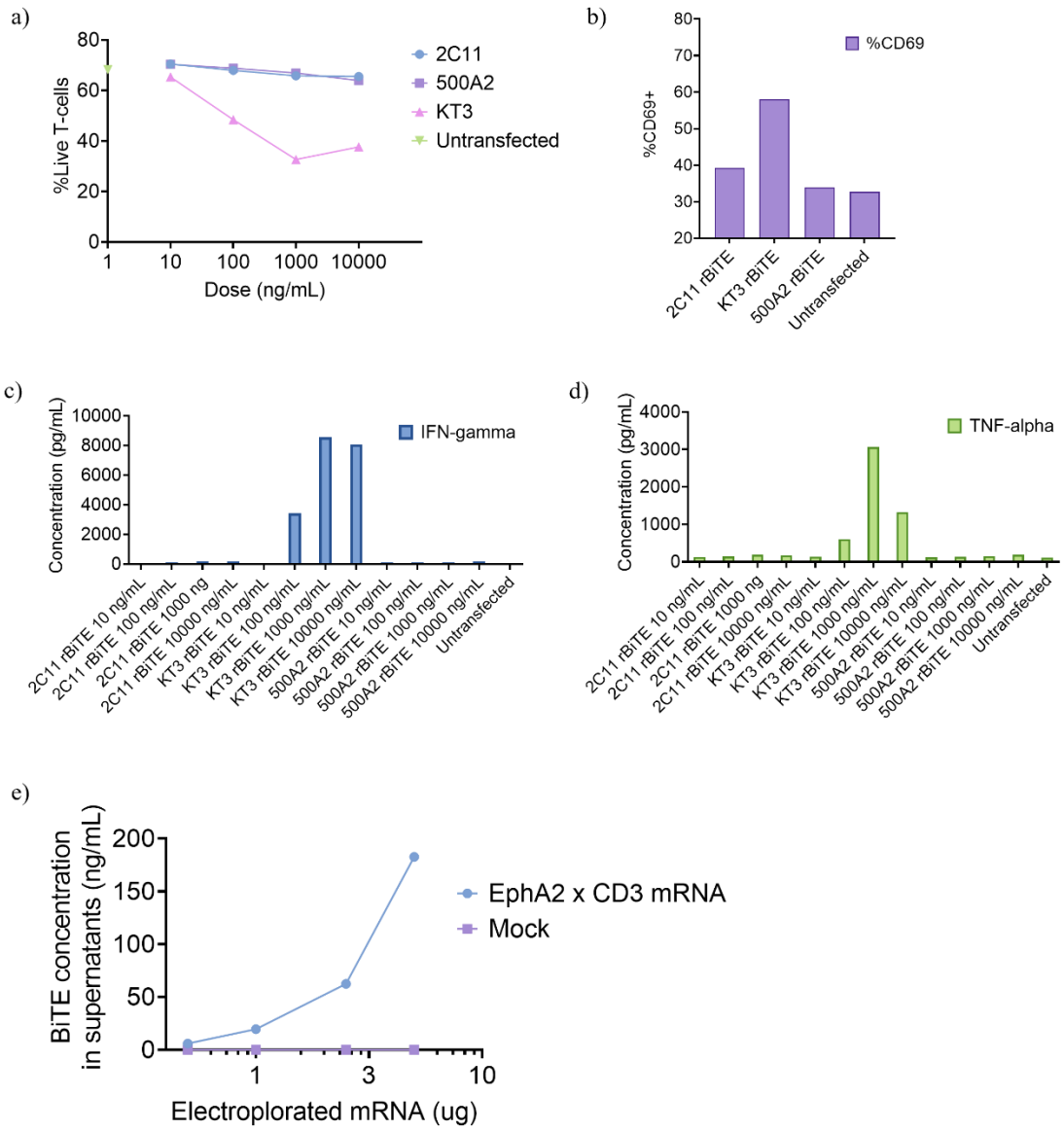

Figure III-6. BiTE construct selection.

The a) T-cell viability, b) CD69 expression, c-d) and cytokine secretion levels were evaluated after treatment with different BiTE constructs. e) The level of BiTE secretion from HEK293T cells was quantified by ELISA. Assays were performed with n = 3 biologically independent replicates. Shown are mean values ± SD.

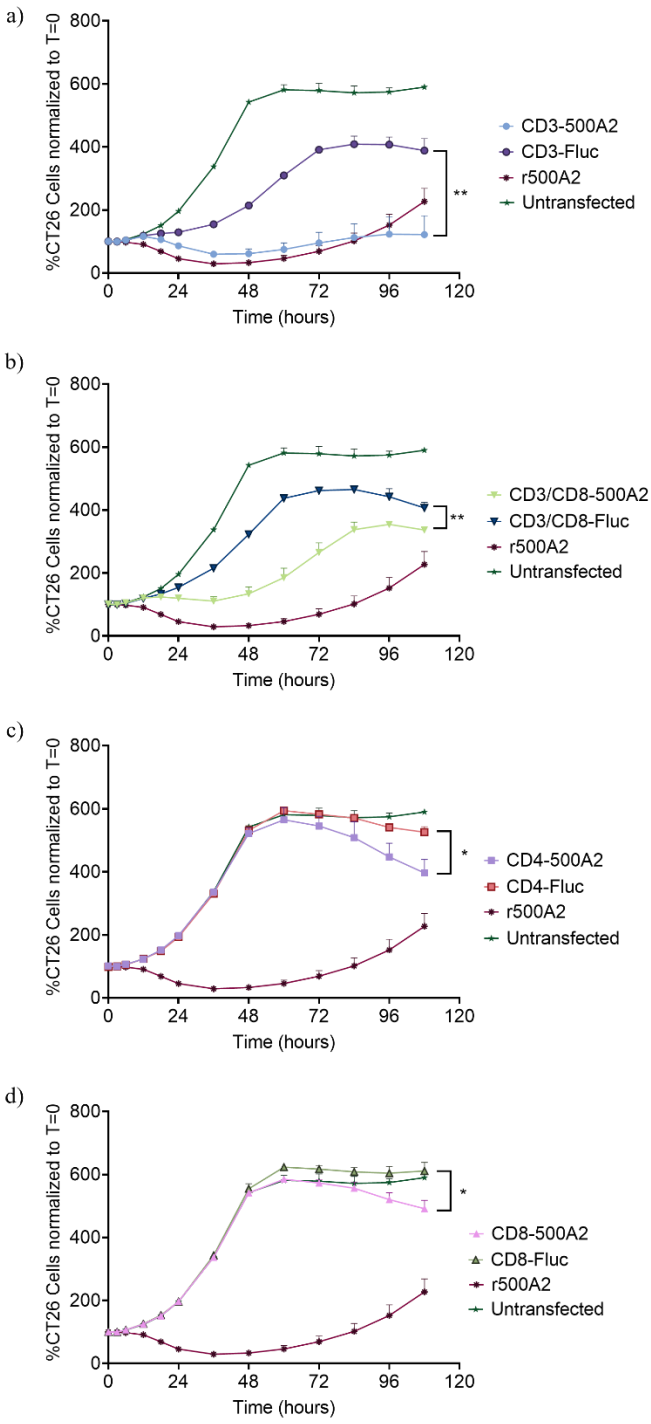

Figure III-7. *In vitro* cytotoxicity with various targeting moieties.

The level of BiTE-mediated cancer cell killing was assessed against the CT26 cell line with a) anti-CD3, b) anti-CD3/CD8, c) anti-CD4, and d) anti-CD8 mediated LNP delivery, respectively, evaluated with an SX5 IncuCyte instrument. r500A2, recombinant 500A2/EphA2 BiTE protein. Displayed *p*-values are from one-way ANOVA $p<0.05$. N = 3 biologically independent samples. Data are mean ± SEM.

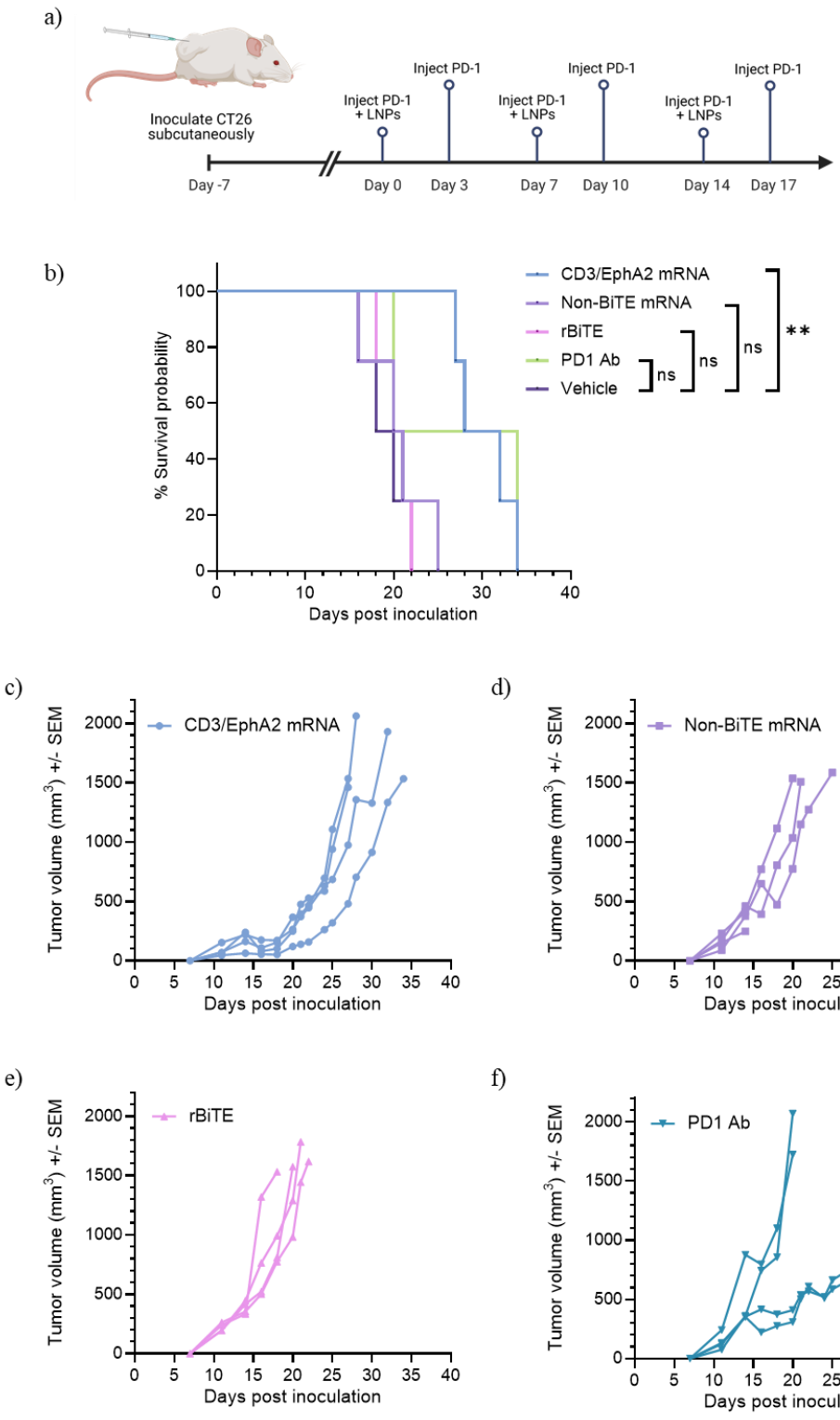
a)
Inoculate CT26 subcutaneously
Inject PD-1 + LNPs
Inject PD-1
Day -7
Day 0
Day 3
Day 7
Day 10
Day 14
Day 17
b)
% Survival probability
Days post inoculation
CD3/EphA2 mRNA
Non-BiTE mRNA
rBiTE
PD1 Ab
Vehicle
ns
**
c)
d)
e)
f)
Tumor volume (mm3) +/- SEM
Days post inoculation

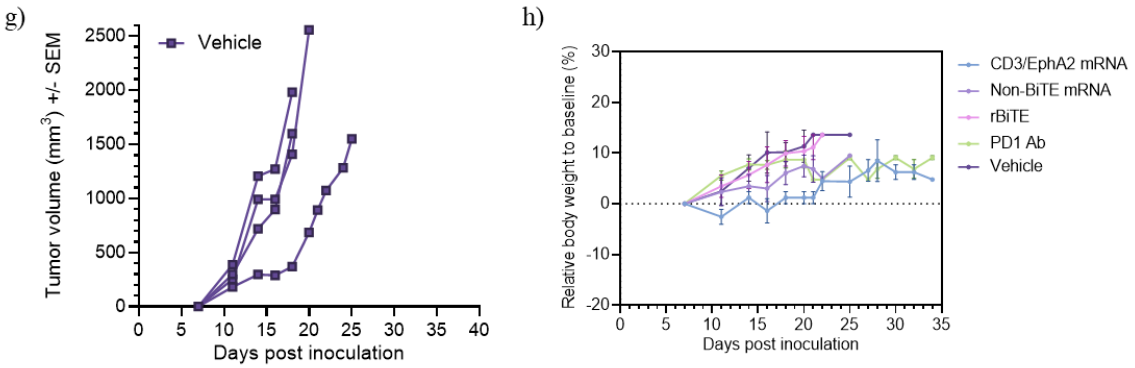

Figure III-8. Efficacy in a subcutaneous CT26 model.

a) Schematic illustrating the dosing schedule. b) The probability of survival from different treatments is illustrated in a Kaplan-Meier curve. c-g) The individual tumors were measured every 2-3 days throughout the study. h) Bodyweights were assessed every 2-3 days throughout the study. Statistical analysis was performed using the log-rank test. N = 4 biologically independent animals per group. Data are mean ± SEM. rBiTE, recombinant 500A2/EphA2 BiTE protein. Created with BioRender.com.

III.8 | Supplemental Figures

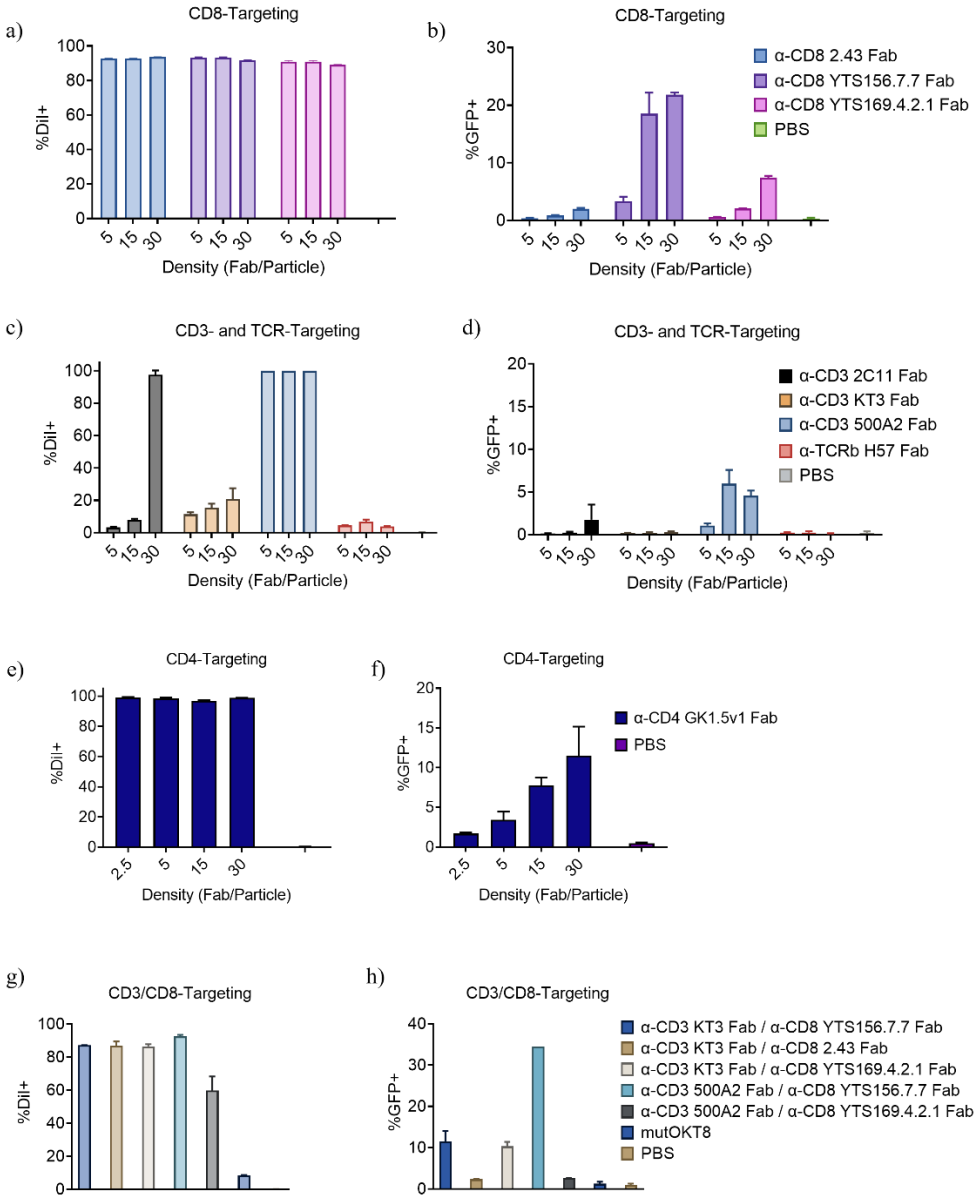

Supplemental Figure III-1. Target screening and antibody density optimization.

The targeting antibody density was optimized by transfection in isolated naïve $CD3^+$ T-cells evaluating DiI association and GFP expression for a-b) three anti-CD8 targeting clones, c-d) four anti-CD3 or anti-TCR targeting clones, e-f) one anti-CD4 targeting clone, and g-h) five anti-CD3/anti-CD8 targeting combinations. Assays were performed with n = 3 biologically independent replicates. Shown are mean values ± SD.

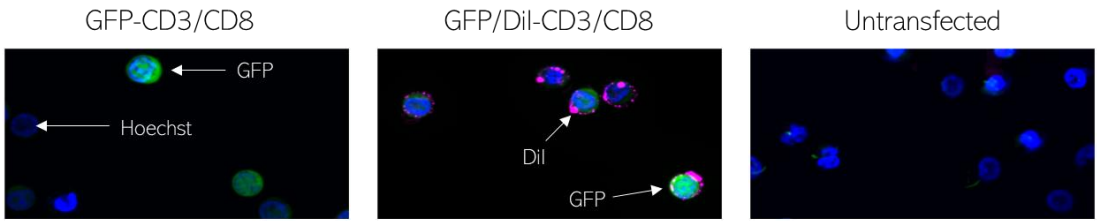

Supplemental Figure III-2. Transfection visualized by microscopy.

Microscopy was performed evaluating LNP association (pink) and GFP expression (green) in murine T-cells transfected with CD3/CD8-targeting LNPs. The nuclei were stained with Hoechst (blue).

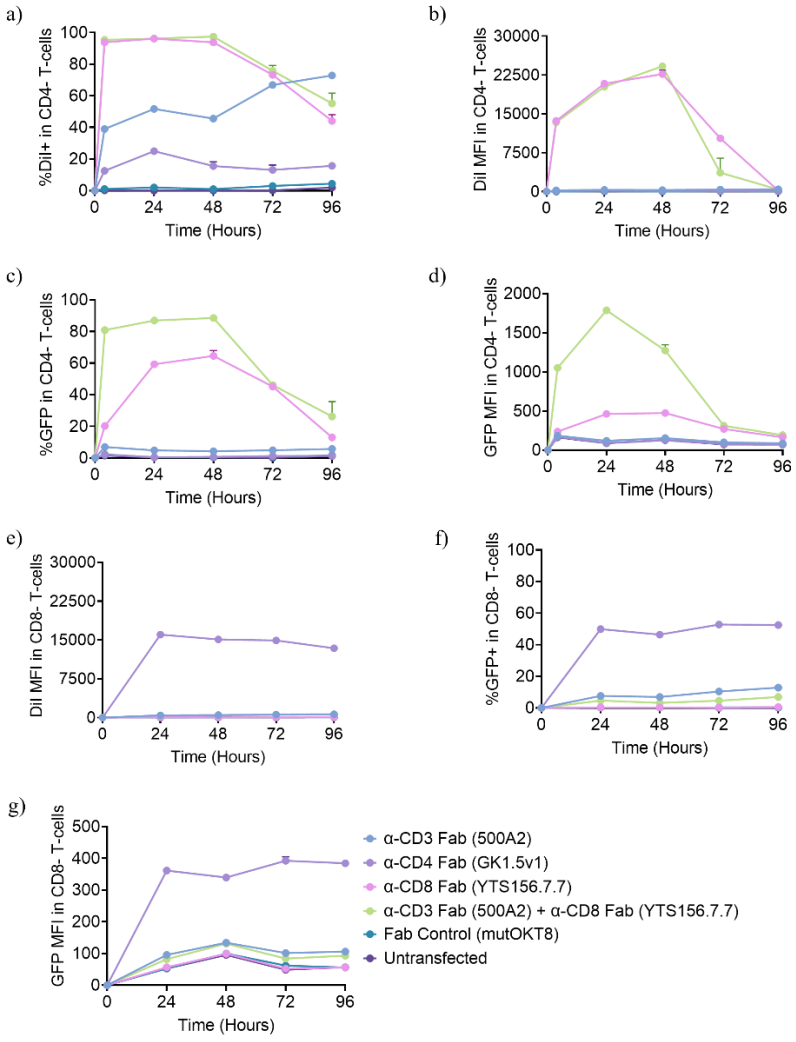
a)
%DiI+ in CD4- T-cells
Time (Hours)
b)
DiI MFI in CD4- T-cells
Time (Hours)
c)
%GFP in CD4- T-cells
Time (Hours)
d)
GFP MFI in CD4- T-cells
Time (Hours)
e)
DiI MFI in CD8- T-cells
Time (Hours)
f)
%GFP+ in CD8- T-cells
Time (Hours)
g)
GFP MFI in CD8- T-cells
Time (Hours)
α-CD3 Fab (500A2)
α-CD4 Fab (GK1.5v1)
α-CD8 Fab (YTS156.7.7)
α-CD3 Fab (500A2) + α-CD8 Fab (YTS156.7.7)
Fab Control (mutOKT8)
Untransfected

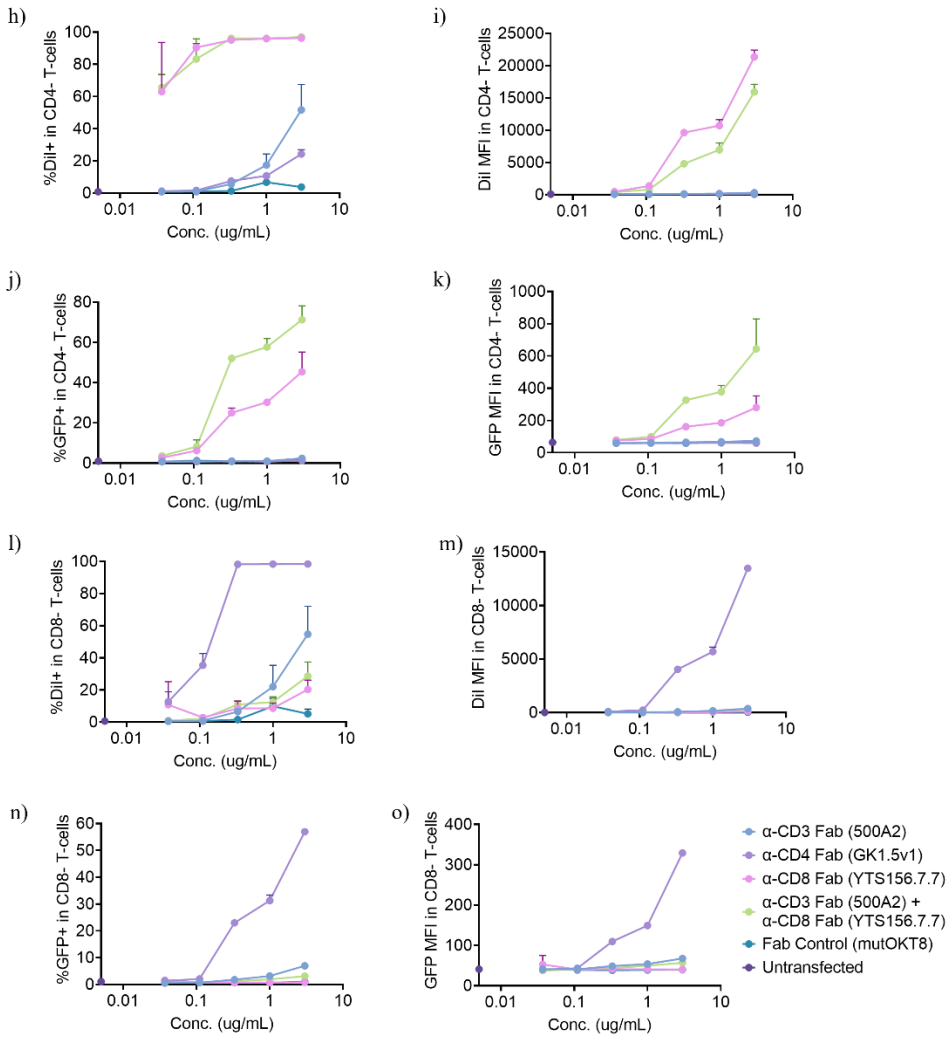

Supplemental Figure III-3. Expression time course and dose titration *in vitro*.

The lead targeting moieties were evaluated in a-g) a time course study and h-n) a dose optimization study assessing DiI association and GFP expression by Flow Cytometry. Experiments were performed with n = 3 biologically independent replicates. Shown are mean values ± SD.

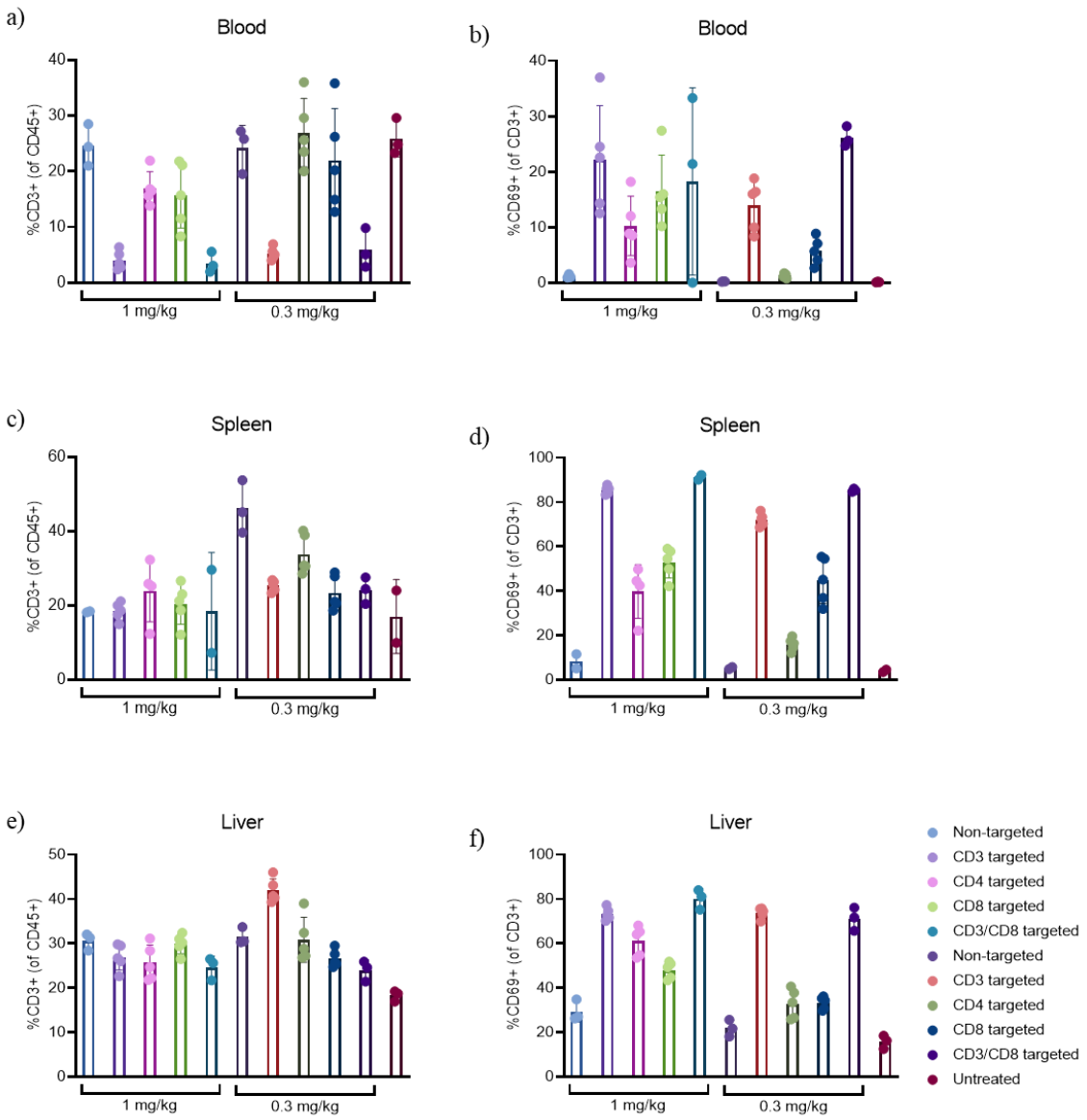

Supplemental Figure III-4. T-cell counts and activation *in vivo*.

The number of T-cells and the level of CD69 expression was assessed in a-b) the blood, c-d) the spleen, e-f) and the liver and evaluated by Flow Cytometry. N = 4, 5 biologically independent mice per condition. Data are mean ± SEM.

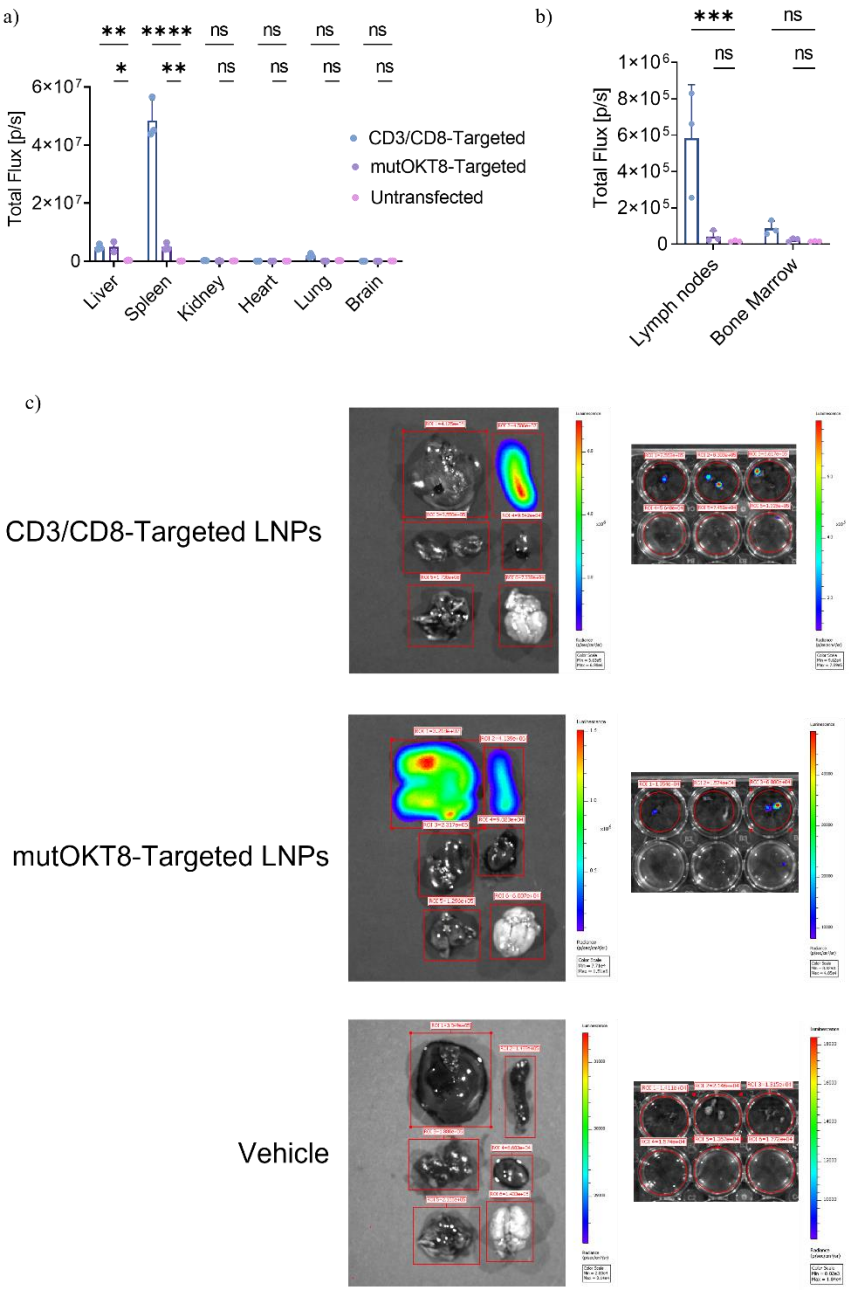

Supplemental Figure III-5. Biodistribution of CD3/CD8-targeted LNPs.

The biodistribution of anti-CD3/CD8 targeting LNPs encapsulating firefly luciferase-encoding mRNA was assessed in Balb/c WT mice. a-c) The total flux [p/s] in individual organs was evaluated and compared between groups after acquiring images ex vivo by IVIS. N = 3 biologically independent mice per condition. Data are mean ± SEM. Displayed *p*-values are from two-way ANOVA $p<0.05$.

Chapter IV | Concluding Remarks and Future Directions

Our understanding of cancer immunology is continuously improving, enabling the development of novel immunotherapeutic strategies. Immunotherapy is now a standard pillar of cancer treatment, and the modulation of the patient's own immune system has truly proven to be beneficial.

Immune checkpoint inhibitors (ICIs) and adoptive cell therapies (ACTs) are immunotherapeutic approaches for the treatment of various cancers that have received much attention in the last decade. Despite the successes and approvals of several immunotherapies, many cancer patients are non-responders, or their response is short-lived due to the development of resistance to the treatment [11, 34]. Additionally, the costs associated with currently approved immunotherapeutic drugs are substantial, which further limits access to treatment for many patients [188]. Thus, continuous efforts to engineer and develop novel immunotherapeutic strategies to overcome these barriers are needed.

Here, we developed strategies to reprogram the immune system to target cancer cells. First, we demonstrated how targeted lipid nanoparticles (LNPs) can be engineered to deliver an mRNA payload specifically to T-cells. Next, we showed how this technology can be utilized to reprogram human T-cells directly *in vivo* to express a functional chimeric antigen receptor (CAR) with the goal to treat B-cell malignancies (Chapter II). Finally, we developed a strategy to target solid tumors by reprogramming murine T-cells to secrete and capture a Bispecific T-cell Engager (BiTE) that specifically targets Ephrin receptor A2 (EphA2) (Chapter III). Thus, the immunotherapeutic strategies developed in this thesis impact multiple steps of the Cancer-Immunity Cycle both directly and indirectly (Figure I-5).

The reprogramming of T-cells to express a CAR enables tumor cell recognition and thus directly promotes cycle step 6. Additionally, BiTEs that engage T-cells with a tumor cell antigen also promote step 6 of the cycle. Finally, the CAR- and BiTE-reprogramming strategies both mediate cancer cell killing and thus significantly promote step 7, which can result in the release of neoantigens and a repeat of the Cancer-Immunity Cycle increasing the extent of the response.

Using mRNA as a strategy to achieve transient expression of a protein of interest has gained momentum following the approval of two COVID-19 vaccines. One of the challenges in the development of mRNAs for use as therapeutics in comparison to vaccines, involves achieving sufficient levels of protein expression to reach a therapeutic threshold [70]. Modifications to the mRNA that enhances the stability and expression of the encoded protein can be incorporated into the in vitro transcription (IVT) process. Such changes, including nucleotide modifications, untranslated region (UTR)- and codon optimization, 3' polyadenylation, and 5' capping have been incorporated into the mRNAs used in the work described here. However, one factor that is not included or described in this work but is of great interest to our group involves the removal of dsRNA impurities from the IVT process. Thus, significant work is currently being conducted to develop purification methods that remove residual dsRNA. With the relatively high mRNA doses required for therapeutic use compared to the use for vaccines, we believe that it is of substantial importance to remove any small traces of dsRNA that may elicit an undesired innate immune response as we are moving toward the clinic. Additionally, the possible traces of dsRNA in an mRNA vaccine may serve as a built-in adjuvant to boost the desired immune response, whereas in

a therapeutic that is administered systemically, this may trigger an unwanted innate immune response [70, 189, 190].

As previously mentioned, the use of CAR T-cells to target specific diseases has shown impressive clinical responses in patients with hematologic malignancies [16]. Thus, we believe that our strategy for reprogramming CAR-T cells *in vivo* holds promise as an off-the-shelf monotherapy for blood cancers. However, targeting solid tumors remains a significant challenge. We are interested in combining the solid tumor strategy described herein with immunotherapies targeting other cell types, as provoking an anti-tumor response in multiple immune cell subsets may prove beneficial in overcoming the suppressive tumor microenvironment (TME) [191]. Here, the approach explored to treat solid tumors may rely on a combination of the enhanced permeability and retention (EPR) effect to achieve LNP accumulation, and thus direct transfection, in the tumor and T-cell migration to the tumor site of T-cells that have been transfected in circulation. Currently, we are investigating other strategies to treat solid tumors where we aim to transfect immune cells in circulation and then facilitate increased migration of transfected cells into the TME through the mRNA payload resulting in improved anti-tumor response.

For our CAR T-cell strategy, we show promising indications that functional CAR expression can be achieved *in vivo*. However, we understand that more elaborate and appropriate efficacy studies in orthotopic animal models are needed. One model, which is commonly used to study CAR T therapies, is the B-cell non-Hodgkin lymphoma (NHL) model using Raji cells [192]. Currently, we are working to establish this model in-house to evaluate the level of target cell cytotoxicity that our platform can drive *in vivo*. Additionally, we are

currently evaluating various dosing schedules for the lead drugs to investigate what level of CAR expression can be achieved upon repeated dosing. Related to repeated dosing, we are aware of the importance of evaluating and closely monitoring the production of anti-drug and anti-PEG antibodies that may result in accelerated blood clearance of the drug (ABC phenomenon) [193-195]. Finally, a major focus of our upcoming studies will be to investigate the safety of the developed therapy. Here, we will perform dose-escalation studies to identify the lowest dose that is pharmacologically active, the maximum tolerated dose, and whether any dose-limiting toxicities are observed.

We are interested in expanding our BiTE approach to other EphA2-expressing syngeneic tumor models such as the murine Lewis carcinoma, LL-2, model and eventually translating the strategy into a human system, targeting EphA2-positive cell lines such as the ovarian cancer cell line, SKOV3 [187].

Based on our preclinical data, we believe that the platform holds promise for being utilized to treat a range of diseases in the future. However, several potential limitations will first need to be addressed. Although LNPs encapsulating mRNA have been clinically validated and broadly used as vaccines, there are still questions that remain to be answered regarding their use as therapeutics. First, the safety profile upon repeated dosing will need to be assessed through clinical trials. Additionally, clinical studies will help determine whether a therapeutic threshold that results in a desired sufficiently efficacious anti-target response can be achieved. Finally, a CMC-related challenge that is beyond the scope of this dissertation but needs to be addressed involves producing (and reproducing) the drug at scale.

Looking beyond the developed platform, messenger RNA only provides one example of how RNA can be utilized for drug development. Other strategies for delivering RNA therapeutics to immune cells exist and are currently being explored. These include small interfering RNA (siRNA) micro-RNA (miRNA), circular RNA (circRNA), and self-amplifying RNA (saRNA) [196-198]. siRNA and miRNA can be utilized to inhibit the production of disease-related proteins with an example being Onpattro, which was approved by the FDA in 2018 to treat hereditary transthyretin-mediated amyloidosis [107]. The aim of saRNA and circRNA is to increase translation and thus protein yield in comparison to linear mRNA. Companies, including Orna Therapeutics and Replicate Bioscience, are currently interested in exploring these strategies to develop drugs to treat cancers and autoimmune diseases.

Currently, LNPs are the most frequently used carrier for mRNA delivery. However, other viral- and non-viral-based strategies to deliver nucleic acids are being explored. One viral-based approach is the utilization of retroviral transduction, such as γ-retrovirus or lentivirus, to deliver a payload to the patient's cells *ex vivo*. This strategy is being exploited for all the currently FDA-approved autologous CAR products [199]. Adeno-associated viruses (AAVs), polymeric nanoparticles, and exosomes are additional examples of viral and non-viral vehicles that are currently being explored by others for CAR reprogramming *in vivo* [200, 201]. Generally, the use of non-viral vectors, such as LNPs, for nucleic acid delivery is safer than viral vectors due to the absence of immunogenic viral proteins [202, 203].

In 1945, William Woglom, director of the Cancer Institute at Columbia, accurately said: "Some may not realize how difficult the problem of [cancer] treatment really is – it is

almost, not quite, but almost as hard as finding some agent that will dissolve away the left ear, say, yet leave the right ear unharmed – so slight is the difference between the cancer cell and its normal ancestor" [204]. Thus, is important to emphasize that cancers are individual and patient-specific diseases. As cancer develops from within and with the endless number of possible genetic combinations and thus alterations, a therapy that proves successful in one cancer patient may not have the desired effect in another. Consequently, continuous efforts to develop new therapeutics are crucial to benefit a broader patient population for whom treatments are not currently available or accessible.

In conclusion, we have developed and demonstrated the effect of such therapeutics preclinically, and believe that once implemented in the clinic, these drugs will provide low-cost, practical, and broadly applicable ways to treat cancers that are not available at the time of writing this thesis. In the near term, we see our CAR-T approach having a tremendous impact on patients with B-cell malignancies for whom autologous CAR-T therapies are currently not accessible due to substantial associated treatment costs. Given that the platform is dynamic, being the ability to change the payload and the targeting moiety, we believe that our technology can lead to the development of novel modalities in the future. Thus, we predict that the technology can be used to not only treat other cancers such as solid tumors but also help patients with autoimmune- and infectious diseases and thereby be available to an even increased patient population.

References

1. Murciano-Goroff, Y.R., A.B. Warner, and J.D. Wolchok, *The future of cancer immunotherapy: microenvironment-targeting combinations.* Cell Research, 2020. **30**(6): p. 507-519.
2. Koury, J., et al., *Immunotherapies: Exploiting the Immune System for Cancer Treatment.* J Immunol Res, 2018. **2018**: p. 9585614.
3. Waldman, A.D., J.M. Fritz, and M.J. Lenardo, *A guide to cancer immunotherapy: from T cell basic science to clinical practice.* Nature Reviews Immunology, 2020. **20**(11): p. 651-668.
4. Ledford, H., H. Else, and M. Warren, *Cancer immunologists scoop medicine Nobel prize.* Nature, 2018. **562**(7725): p. 20-21.
5. Mellman, I., G. Coukos, and G. Dranoff, *Cancer immunotherapy comes of age.* Nature, 2011. **480**(7378): p. 480-489.
6. Robert, C., *A decade of immune-checkpoint inhibitors in cancer therapy.* Nature Communications, 2020. **11**(1).
7. Robert, C., et al., *Durable Complete Response After Discontinuation of Pembrolizumab in Patients With Metastatic Melanoma.* Journal of Clinical Oncology, 2018. **36**(17): p. 1668-1674.
8. Sharma, P. and J.P. Allison, *The future of immune checkpoint therapy.* Science, 2015. **348**(6230): p. 56-61.
9. O'Donnell, J.S., et al., *Resistance to PD1/PDL1 checkpoint inhibition.* Cancer Treatment Reviews, 2017. **52**: p. 71-81.
10. Cogdill, A.P., M.C. Andrews, and J.A. Wargo, *Hallmarks of response to immune checkpoint blockade.* British Journal of Cancer, 2017. **117**(1): p. 1-7.
11. Dobosz, P., et al., *Challenges of the Immunotherapy: Perspectives and Limitations of the Immune Checkpoint Inhibitor Treatment.* Int J Mol Sci, 2022. **23**(5).
12. Tan, S., D. Li, and X. Zhu, *Cancer immunotherapy: Pros, cons and beyond.* Biomed Pharmacother, 2020. **124**: p. 109821.
13. Perica, K., et al., *Adoptive T cell immunotherapy for cancer.* Rambam Maimonides Med J, 2015. **6**(1): p. e0004.
14. El-Kadiry, A.E., M. Rafei, and R. Shammaa, *Cell Therapy: Types, Regulation, and Clinical Benefits.* Front Med (Lausanne), 2021. **8**: p. 756029.
15. Hamieh, M., et al., *Programming CAR T Cell Tumor Recognition: Tuned Antigen Sensing and Logic Gating.* Cancer Discovery, 2023: p. OF1-OF15.
16. June, C.H. and M. Sadelain, *Chimeric Antigen Receptor Therapy.* New England Journal of Medicine, 2018. **379**(1): p. 64-73.
17. Morotti, M., et al., *Promises and challenges of adoptive T-cell therapies for solid tumours.* British Journal of Cancer, 2021. **124**(11): p. 1759-1776.
18. Kirtane, K., et al., *Adoptive cellular therapy in solid tumor malignancies: review of the literature and challenges ahead.* J Immunother Cancer, 2021. **9**(7).
19. Abreu, T.R., et al., *Current challenges and emerging opportunities of CAR-T cell therapies.* Journal of Controlled Release, 2020. **319**: p. 246-261.
20. Wolf, B., et al., *Safety and Tolerability of Adoptive Cell Therapy in Cancer.* Drug Safety, 2019. **42**(2): p. 315-334.

21. Yang, J.C., *Toxicities Associated With Adoptive T-Cell Transfer for Cancer.* Cancer J, 2015. **21**(6): p. 506-9.
22. Sukari, A., N. Abdallah, and M. Nagasaka, *Unleash the power of the mighty T cells-basis of adoptive cellular therapy.* Critical Reviews in Oncology/Hematology, 2019. **136**: p. 1-12.
23. Hanahan, D. and R.A. Weinberg, *The Hallmarks of Cancer.* Cell, 2000. **100**(1): p. 57-70.
24. Hanahan, D. and Robert, *Hallmarks of Cancer: The Next Generation.* Cell, 2011. **144**(5): p. 646-674.
25. Hanahan, D., *Hallmarks of Cancer: New Dimensions.* Cancer Discov, 2022. **12**(1): p. 31-46.
26. Motz, G. and G. Coukos, *Deciphering and Reversing Tumor Immune Suppression.* Immunity, 2013. **39**(1): p. 61-73.
27. Chen, D. and I. Mellman, *Oncology Meets Immunology: The Cancer-Immunity Cycle.* Immunity, 2013. **39**(1): p. 1-10.
28. Zhu, Y., et al., *STING: a master regulator in the cancer-immunity cycle.* Molecular Cancer, 2019. **18**(1): p. 152.
29. Ramachandran, M., A. Dimberg, and M. Essand, *The cancer-immunity cycle as rational design for synthetic cancer drugs: Novel DC vaccines and CAR T-cells.* Seminars in Cancer Biology, 2017. **45**: p. 23-35.
30. Calmeiro, J., et al., *Dendritic Cell Vaccines for Cancer Immunotherapy: The Role of Human Conventional Type 1 Dendritic Cells.* Pharmaceutics, 2020. **12**(2).
31. Williams, M.A., A.J. Tyznik, and M.J. Bevan, *Interleukin-2 signals during priming are required for secondary expansion of CD8+ memory T cells.* Nature, 2006. **441**(7095): p. 890-3.
32. Sun, Z., et al., *A next-generation tumor-targeting IL-2 preferentially promotes tumor-infiltrating CD8+ T-cell response and effective tumor control.* Nature Communications, 2019. **10**(1): p. 3874.
33. Peterson, C., N. Denlinger, and Y. Yang, *Recent Advances and Challenges in Cancer Immunotherapy.* Cancers (Basel), 2022. **14**(16).
34. Esfahani, K., et al., *A review of cancer immunotherapy: from the past, to the present, to the future.* Curr Oncol, 2020. **27**(Suppl 2): p. S87-S97.
35. Li, Y., et al., *Immune Cycle-Based Strategies for Cancer Immunotherapy.* Advanced Functional Materials, 2021. **31**(50): p. 2107540.
36. Subklewe, M., M. von Bergwelt-Baildon, and A. Humpe, *Chimeric Antigen Receptor T Cells: A Race to Revolutionize Cancer Therapy.* Transfus Med Hemother, 2019. **46**(1): p. 15-24.
37. Ahmad, A., S. Uddin, and M. Steinhoff, *CAR-T Cell Therapies: An Overview of Clinical Studies Supporting Their Approved Use against Acute Lymphoblastic Leukemia and Large B-Cell Lymphomas.* Int J Mol Sci, 2020. **21**(11).
38. Schuster, S.J., et al., *Chimeric Antigen Receptor T Cells in Refractory B-Cell Lymphomas.* New England Journal of Medicine, 2017. **377**(26): p. 2545-2554.
39. Park, J.H., et al., *Long-Term Follow-up of CD19 CAR Therapy in Acute Lymphoblastic Leukemia.* New England Journal of Medicine, 2018. **378**(5): p. 449-459.
40. Wang, M., et al., *KTE-X19 CAR T-Cell Therapy in Relapsed or Refractory Mantle-Cell Lymphoma.* New England Journal of Medicine, 2020. **382**(14): p. 1331-1342.
41. Berdeja, J.G., et al., *Ciltacabtagene autoleucel, a B-cell maturation antigen-directed chimeric antigen receptor T-cell therapy in patients with relapsed or refractory multiple myeloma (CARTITUDE-1): a phase 1b/2 open-label study.* The Lancet, 2021. **398**(10297): p. 314-324.

42. Abramson, J.S., et al., *Lisocabtagene maraleucel for patients with relapsed or refractory large B-cell lymphomas (TRANSCEND NHL 001): a multicentre seamless design study.* The Lancet, 2020. **396**(10254): p. 839-852.
43. Munshi, N.C., et al., *Idecabtagene Vicleucel in Relapsed and Refractory Multiple Myeloma.* New England Journal of Medicine, 2021. **384**(8): p. 705-716.
44. Sadelain, M., R. Brentjens, and I. Rivière, *The promise and potential pitfalls of chimeric antigen receptors.* Curr Opin Immunol, 2009. **21**(2): p. 215-23.
45. Sadelain, M., R. Brentjens, and I. Rivière, *The Basic Principles of Chimeric Antigen Receptor Design.* Cancer Discovery, 2013. **3**(4): p. 388-398.
46. Guedan, S., et al., *Engineering and Design of Chimeric Antigen Receptors.* Molecular Therapy - Methods & Clinical Development, 2019. **12**: p. 145-156.
47. Guest, R.D., et al., *The Role of Extracellular Spacer Regions in the Optimal Design of Chimeric Immune Receptors: Evaluation of Four Different scFvs and Antigens.* Journal of Immunotherapy, 2005. **28**(3).
48. Hudecek, M., et al., *The nonsignaling extracellular spacer domain of chimeric antigen receptors is decisive for in vivo antitumor activity.* Cancer Immunology Research, 2015. **3**(2): p. 125-135.
49. Kochenderfer, J.N., et al., *Construction and Preclinical Evaluation of an Anti-CD19 Chimeric Antigen Receptor.* Journal of Immunotherapy, 2009. **32**(7): p. 689-702.
50. Sadelain, M., I. Rivière, and R. Brentjens, *Targeting tumours with genetically enhanced T lymphocytes.* Nature Reviews Cancer, 2003. **3**(1): p. 35-45.
51. Germain, R.N. and I. Stefanová, *THE DYNAMICS OF T CELL RECEPTOR SIGNALING: Complex Orchestration and the Key Roles of Tempo and Cooperation.* Annual Review of Immunology, 1999. **17**(1): p. 467-522.
52. Maher, J., et al., *Human T-lymphocyte cytotoxicity and proliferation directed by a single chimeric TCRζ /CD28 receptor.* Nature Biotechnology, 2002. **20**(1): p. 70-75.
53. Marin, V., et al., *Cytokine-induced killer cells for cell therapy of acute myeloid leukemia: improvement of their immune activity by expression of CD33-specific chimeric receptors.* Haematologica, 2010. **95**(12): p. 2144-52.
54. Chmielewski, M. and H. Abken, *TRUCKs: the fourth generation of CARs.* Expert Opin Biol Ther, 2015. **15**(8): p. 1145-54.
55. Chmielewski, M. and H. Abken, *TRUCKS, the fourth-generation CAR T cells: Current developments and clinical translation.* ADVANCES IN CELL AND GENE THERAPY, 2020. **3**(3): p. e84.
56. Kagoya, Y., et al., *A novel chimeric antigen receptor containing a JAK–STAT signaling domain mediates superior antitumor effects.* Nature Medicine, 2018. **24**(3): p. 352-359.
57. Kim, D.W. and J.-Y. Cho, *Recent Advances in Allogeneic CAR-T Cells.* Biomolecules, 2020. **10**(2): p. 263.
58. Sterner, R.C. and R.M. Sterner, *CAR-T cell therapy: current limitations and potential strategies.* Blood Cancer Journal, 2021. **11**(4): p. 69.
59. Wang, Z. and W. Han, *Biomarkers of cytokine release syndrome and neurotoxicity related to CAR-T cell therapy.* Biomark Res, 2018. **6**: p. 4.
60. Neelapu, S.S., et al., *Axicabtagene Ciloleucel CAR T-Cell Therapy in Refractory Large B-Cell Lymphoma.* New England Journal of Medicine, 2017. **377**(26): p. 2531-2544.
61. Maude, S.L., et al., *Tisagenlecleucel in Children and Young Adults with B-Cell Lymphoblastic Leukemia.* New England Journal of Medicine, 2018. **378**(5): p. 439-448.

62. Marofi, F., et al., *CAR T cells in solid tumors: challenges and opportunities.* Stem Cell Research & Therapy, 2021. **12**(1): p. 81.
63. Patel, U., et al., *CAR T cell therapy in solid tumors: A review of current clinical trials.* eJHaem, 2022. **3**(S1): p. 24-31.
64. Fiorenza, S., et al., *Value and affordability of CAR T-cell therapy in the United States.* Bone Marrow Transplantation, 2020. **55**(9): p. 1706-1715.
65. Choi, G., G. Shin, and S. Bae, *Price and Prejudice? The Value of Chimeric Antigen Receptor (CAR) T-Cell Therapy.* Int J Environ Res Public Health, 2022. **19**(19).
66. Ciotti, M., et al., *The COVID-19 pandemic.* Critical Reviews in Clinical Laboratory Sciences, 2020. **57**(6): p. 365-388.
67. Anand, P. and V.P. Stahel, *The safety of Covid-19 mRNA vaccines: a review.* Patient Safety in Surgery, 2021. **15**(1).
68. Baden, L.R., et al., *Efficacy and Safety of the mRNA-1273 SARS-CoV-2 Vaccine.* New England Journal of Medicine, 2021. **384**(5): p. 403-416.
69. Polack, F.P., et al., *Safety and Efficacy of the BNT162b2 mRNA Covid-19 Vaccine.* New England Journal of Medicine, 2020. **383**(27): p. 2603-2615.
70. Rohner, E., et al., *Unlocking the promise of mRNA therapeutics.* Nature Biotechnology, 2022. **40**(11): p. 1586-1600.
71. Pormohammad, A., et al., *Efficacy and Safety of COVID-19 Vaccines: A Systematic Review and Meta-Analysis of Randomized Clinical Trials.* Vaccines (Basel), 2021. **9**(5).
72. Ghazy, R.M., et al., *Efficacy and Effectiveness of SARS-CoV-2 Vaccines: A Systematic Review and Meta-Analysis.* Vaccines (Basel), 2022. **10**(3).
73. Thomas, S.J., et al., *Safety and Efficacy of the BNT162b2 mRNA Covid-19 Vaccine through 6 Months.* New England Journal of Medicine, 2021. **385**(19): p. 1761-1773.
74. DeRosa, F., et al., *Therapeutic efficacy in a hemophilia B model using a biosynthetic mRNA liver depot system.* Gene Therapy, 2016. **23**(10): p. 699-707.
75. Chen, C.-Y., et al., *Treatment of Hemophilia A Using Factor VIII Messenger RNA Lipid Nanoparticles.* Molecular Therapy - Nucleic Acids, 2020. **20**: p. 534-544.
76. Mulligan, M.J., et al., *Phase I/II study of COVID-19 RNA vaccine BNT162b1 in adults.* Nature, 2020. **586**(7830): p. 589-593.
77. Sun, H., et al. *mRNA-Based Therapeutics in Cancer Treatment*. Pharmaceutics, 2023. **15**, DOI: 10.3390/pharmaceutics15020622.
78. Qin, S., et al., *mRNA-based therapeutics: powerful and versatile tools to combat diseases.* Signal Transduction and Targeted Therapy, 2022. **7**(1): p. 166.
79. Beck, J.D., et al., *mRNA therapeutics in cancer immunotherapy.* Molecular Cancer, 2021. **20**(1): p. 69.
80. Weng, Y., et al., *The challenge and prospect of mRNA therapeutics landscape.* Biotechnology Advances, 2020. **40**: p. 107534.
81. Beckert, B. and B. Masquida, *Synthesis of RNA by In Vitro Transcription*, in *RNA: Methods and Protocols*, H. Nielsen, Editor. 2011, Humana Press: Totowa, NJ. p. 29-41.
82. Henderson, J.M., et al., *Correction: Cap 1 Messenger RNA Synthesis with Co-transcriptional CleanCap® Analog by In Vitro Transcription.* Current Protocols, 2021. **1**(12): p. e336.
83. Mu, X. and S. Hur, *Immunogenicity of In Vitro-Transcribed RNA.* Accounts of Chemical Research, 2021. **54**(21): p. 4012-4023.
84. Ramanathan, A., G.B. Robb, and S.-H. Chan, *mRNA capping: biological functions and applications.* Nucleic Acids Research, 2016. **44**(16): p. 7511-7526.

85. Grier, A.E., et al., *pEVL: A Linear Plasmid for Generating mRNA IVT Templates With Extended Encoded Poly(A) Sequences.* Molecular Therapy - Nucleic Acids, 2016. **5**: p. e306.
86. Gallie, D.R., *The cap and poly(A) tail function synergistically to regulate mRNA translational efficiency.* Genes & Dev, 1991.
87. Holtkamp, S., et al., *Modification of antigen-encoding RNA increases stability, translational efficacy, and T-cell stimulatory capacity of dendritic cells.* Blood, 2006. **108**(13): p. 4009-4017.
88. Suknuntha, K., et al., *Optimization of Synthetic mRNA for Highly Efficient Translation and its Application in the Generation of Endothelial and Hematopoietic Cells from Human and Primate Pluripotent Stem Cells.* Stem Cell Rev Rep, 2018. **14**(4): p. 525-534.
89. Sahin, U., K. Karikó, and Ö. Türeci, *mRNA-based therapeutics — developing a new class of drugs.* Nature Reviews Drug Discovery, 2014. **13**(10): p. 759-780.
90. Gustafsson, C., S. Govindarajan, and J. Minshull, *Codon bias and heterologous protein expression.* Trends in Biotechnology, 2004. **22**(7): p. 346-353.
91. Kariko, K., et al., *Incorporation of pseudouridine into mRNA yields superior nonimmunogenic vector with increased translational capacity and biological stability.* Mol Ther, 2008. **16**(11): p. 1833-40.
92. Andries, O., et al., *N(1)-methylpseudouridine-incorporated mRNA outperforms pseudouridine-incorporated mRNA by providing enhanced protein expression and reduced immunogenicity in mammalian cell lines and mice.* J Control Release, 2015. **217**: p. 337-44.
93. Baiersdörfer, M., et al., *A Facile Method for the Removal of dsRNA Contaminant from In Vitro-Transcribed mRNA.* Molecular Therapy - Nucleic Acids, 2019. **15**: p. 26-35.
94. Hartmann, G., *Nucleic Acid Immunity*. 2017, Elsevier. p. 121-169.
95. Piao, X., et al., *Double-stranded RNA reduction by chaotropic agents during in vitro transcription of messenger RNA.* Molecular Therapy - Nucleic Acids, 2022. **29**: p. 618-624.
96. Karikó, K., et al., *Generating the optimal mRNA for therapy: HPLC purification eliminates immune activation and improves translation of nucleoside-modified, protein-encoding mRNA.* Nucleic Acids Res, 2011. **39**(21): p. e142.
97. Weissman, D., et al., *HPLC purification of in vitro transcribed long RNA.* Methods Mol Biol, 2013. **969**: p. 43-54.
98. Kowalski, P.S., et al., *Delivering the Messenger: Advances in Technologies for Therapeutic mRNA Delivery.* Molecular Therapy, 2019. **27**(4): p. 710-728.
99. Houseley, J. and D. Tollervey, *The Many Pathways of RNA Degradation.* Cell, 2009. **136**(4): p. 763-776.
100. Hou, X., et al., *Lipid nanoparticles for mRNA delivery.* Nature Reviews Materials, 2021. **6**(12): p. 1078-1094.
101. Loughrey, D. and J.E. Dahlman, *Non-liver mRNA Delivery.* Accounts of Chemical Research, 2022. **55**(1): p. 13-23.
102. Schoenmaker, L., et al., *mRNA-lipid nanoparticle COVID-19 vaccines: Structure and stability.* Int J Pharm, 2021. **601**: p. 120586.
103. Cheng, X. and R.J. Lee, *The role of helper lipids in lipid nanoparticles (LNPs) designed for oligonucleotide delivery.* Adv Drug Deliv Rev, 2016. **99**(Pt A): p. 129-137.
104. Semple, S.C., et al., *Rational design of cationic lipids for siRNA delivery.* Nature Biotechnology, 2010. **28**(2): p. 172-176.
105. Hajj, K.A. and K.A. Whitehead, *Tools for translation: non-viral materials for therapeutic mRNA delivery.* Nature Reviews Materials, 2017. **2**(10): p. 17056.

106. Meng, C., et al., *Nanoplatforms for mRNA Therapeutics.* Advanced Therapeutics, 2021. **4**(1): p. 2000099.
107. Akinc, A., et al., *The Onpattro story and the clinical translation of nanomedicines containing nucleic acid-based drugs.* Nature Nanotechnology, 2019. **14**(12): p. 1084-1087.
108. Yonezawa, S., H. Koide, and T. Asai, *Recent advances in siRNA delivery mediated by lipid-based nanoparticles.* Advanced Drug Delivery Reviews, 2020. **154-155**: p. 64-78.
109. Maier, M.A., et al., *Biodegradable lipids enabling rapidly eliminated lipid nanoparticles for systemic delivery of RNAi therapeutics.* Mol Ther, 2013. **21**(8): p. 1570-8.
110. Sabnis, S., et al., *A Novel Amino Lipid Series for mRNA Delivery: Improved Endosomal Escape and Sustained Pharmacology and Safety in Non-human Primates.* Molecular Therapy, 2018. **26**(6): p. 1509-1519.
111. Han, X., et al., *An ionizable lipid toolbox for RNA delivery.* Nature Communications, 2021. **12**(1): p. 7233.
112. Swingle, K.L., A.G. Hamilton, and M.J. Mitchell, *Lipid Nanoparticle-Mediated Delivery of mRNA Therapeutics and Vaccines.* Trends in Molecular Medicine, 2021. **27**(6): p. 616-617.
113. Miao, L., et al., *Synergistic lipid compositions for albumin receptor mediated delivery of mRNA to the liver.* Nature Communications, 2020. **11**(1): p. 2424.
114. Fenton, O.S., et al., *Bioinspired Alkenyl Amino Alcohol Ionizable Lipid Materials for Highly Potent In Vivo mRNA Delivery.* Advanced Materials, 2016. **28**(15): p. 2939-2943.
115. Tam, Y.Y.C., S. Chen, and P.R. Cullis *Advances in Lipid Nanoparticles for siRNA Delivery*. Pharmaceutics, 2013. **5**, 498-507 DOI: 10.3390/pharmaceutics5030498.
116. Sebastiani, F., et al., *Apolipoprotein E Binding Drives Structural and Compositional Rearrangement of mRNA-Containing Lipid Nanoparticles.* ACS Nano, 2021. **15**(4): p. 6709-6722.
117. Chen, D., et al., *The role of apolipoprotein- and vitronectin-enriched protein corona on lipid nanoparticles for in vivo targeted delivery and transfection of oligonucleotides in murine tumor models.* Nanoscale, 2019. **11**(40): p. 18806-18824.
118. Akinc, A., et al., *Targeted delivery of RNAi therapeutics with endogenous and exogenous ligand-based mechanisms.* Mol Ther, 2010. **18**(7): p. 1357-64.
119. Johnson, L.T., et al., *Lipid Nanoparticle (LNP) Chemistry Can Endow Unique In Vivo RNA Delivery Fates within the Liver That Alter Therapeutic Outcomes in a Cancer Model.* Molecular Pharmaceutics, 2022. **19**(11): p. 3973-3986.
120. Witzigmann, D., et al., *Lipid nanoparticle technology for therapeutic gene regulation in the liver.* Advanced Drug Delivery Reviews, 2020. **159**: p. 344-363.
121. Kularatne, R.N., R.M. Crist, and S.T. Stern, *The Future of Tissue-Targeted Lipid Nanoparticle-Mediated Nucleic Acid Delivery.* Pharmaceuticals (Basel), 2022. **15**(7).
122. Veiga, N., Y. Diesendruck, and D. Peer, *Targeted nanomedicine: Lessons learned and future directions.* Journal of Controlled Release, 2023. **355**: p. 446-457.
123. Dahlman, J.E., et al., *Barcoded nanoparticles for high throughput in vivo discovery of targeted therapeutics.* Proceedings of the National Academy of Sciences, 2017. **114**(8): p. 2060-2065.
124. Cheng, Q., et al., *Selective organ targeting (SORT) nanoparticles for tissue-specific mRNA delivery and CRISPR–Cas gene editing.* Nature Nanotechnology, 2020. **15**(4): p. 313-320.
125. Nakamura, T., et al., *The Effect of Size and Charge of Lipid Nanoparticles Prepared by Microfluidic Mixing on Their Lymph Node Transitivity and Distribution.* Mol Pharm, 2020. **17**(3): p. 944-953.

126. Álvarez-Benedicto, E., et al., *Optimization of phospholipid chemistry for improved lipid nanoparticle (LNP) delivery of messenger RNA (mRNA).* Biomaterials Science, 2022. **10**(2): p. 549-559.
127. Dilliard, S.A., Q. Cheng, and D.J. Siegwart, *On the mechanism of tissue-specific mRNA delivery by selective organ targeting nanoparticles.* Proc Natl Acad Sci U S A, 2021. **118**(52).
128. Veiga, N., Y. Diesendruck, and D. Peer, *Targeted lipid nanoparticles for RNA therapeutics and immunomodulation in leukocytes.* Advanced Drug Delivery Reviews, 2020. **159**: p. 364-376.
129. Veiga, N., et al., *Cell specific delivery of modified mRNA expressing therapeutic proteins to leukocytes.* Nature Communications, 2018. **9**(1).
130. Kedmi, R., et al., *A modular platform for targeted RNAi therapeutics.* Nature Nanotechnology, 2018. **13**(3): p. 214-219.
131. Rosenblum, D., et al., *CRISPR-Cas9 genome editing using targeted lipid nanoparticles for cancer therapy.* Science Advances. **6**(47): p. eabc9450.
132. Shin, S., et al., *Nanoparticle-Based Chimeric Antigen Receptor Therapy for Cancer Immunotherapy.* Tissue Engineering and Regenerative Medicine, 2023.
133. Tombácz, I., et al., *Highly efficient CD4+ T cell targeting and genetic recombination using engineered CD4+ cell-homing mRNA-LNPs.* Molecular Therapy, 2021. **29**(11): p. 3293-3304.
134. Rurik, J.G., et al., *CAR T cells produced in vivo to treat cardiac injury.* Science, 2022. **375**(6576): p. 91-96.
135. Ramishetti, S., et al., *Systemic Gene Silencing in Primary T Lymphocytes Using Targeted Lipid Nanoparticles.* ACS Nano, 2015. **9**(7): p. 6706-6716.
136. Parhiz, H., et al., *PECAM-1 directed re-targeting of exogenous mRNA providing two orders of magnitude enhancement of vascular delivery and expression in lungs independent of apolipoprotein E-mediated uptake.* Journal of Controlled Release, 2018. **291**: p. 106-115.
137. Shi, D., S. Toyonaga, and D.G. Anderson, *In Vivo RNA Delivery to Hematopoietic Stem and Progenitor Cells via Targeted Lipid Nanoparticles.* Nano Letters, 2023. **23**(7): p. 2938-2944.
138. Parayath, N.N., et al., *In vitro-transcribed antigen receptor mRNA nanocarriers for transient expression in circulating T cells in vivo.* Nature Communications, 2020. **11**(1).
139. Smith, T.T., et al., *In situ programming of leukaemia-specific T cells using synthetic DNA nanocarriers.* Nature Nanotechnology, 2017. **12**(8): p. 813-820.
140. Zhang, F., et al., *Genetic programming of macrophages to perform anti-tumor functions using targeted mRNA nanocarriers.* Nature Communications, 2019. **10**(1).
141. Bain, S., *Sanofi acquires Tidal Therapeutics, adding innovative mRNAbased research platform with applications in oncology, immunology, and other disease areas*. 2021.
142. Fidler, B., *'In vivo' cell therapy: expanding beyond CAR-T*, in *BioPharmaDive*. 2022.
143. June, C.H., et al., *CAR T cell immunotherapy for human cancer.* Science, 2018. **359**(6382): p. 1361-1365.
144. Labanieh, L., R.G. Majzner, and C.L. Mackall, *Programming CAR-T cells to kill cancer.* Nature Biomedical Engineering, 2018. **2**(6): p. 377-391.
145. Neelapu, S.S., et al., *Chimeric antigen receptor T-cell therapy — assessment and management of toxicities.* Nature Reviews Clinical Oncology, 2018. **15**(1): p. 47-62.
146. Bonifant, C.L., et al., *Toxicity and management in CAR T-cell therapy.* Molecular therapy oncolytics, 2016. **3**: p. 16011-16011.

147. Bouchkouj, N., et al., *FDA Approval Summary: Axicabtagene Ciloleucel for Relapsed or Refractory Large B-cell Lymphoma.* Clinical Cancer Research, 2019. **25**(6): p. 1702-1708.
148. Vormittag, P., et al., *A guide to manufacturing CAR T cell therapies.* Current Opinion in Biotechnology, 2018. **53**: p. 164-181.
149. Riley, R.S., et al., *Delivery technologies for cancer immunotherapy.* Nature Reviews Drug Discovery, 2019. **18**(3): p. 175-196.
150. Steinle, H., et al., *Concise Review: Application of In Vitro Transcribed Messenger RNA for Cellular Engineering and Reprogramming: Progress and Challenges.* Stem Cells, 2017. **35**(1): p. 68-79.
151. Guan, S. and J. Rosenecker, *Nanotechnologies in delivery of mRNA therapeutics using nonviral vector-based delivery systems.* Gene Therapy, 2017. **24**(3): p. 133-143.
152. Anderson, E.J., et al., *Safety and Immunogenicity of SARS-CoV-2 mRNA-1273 Vaccine in Older Adults.* New England Journal of Medicine, 2020. **383**(25): p. 2427-2438.
153. Rosenblum, D., et al., *Progress and challenges towards targeted delivery of cancer therapeutics.* Nature Communications, 2018. **9**(1).
154. Blanco, E., H. Shen, and M. Ferrari, *Principles of nanoparticle design for overcoming biological barriers to drug delivery.* Nature Biotechnology, 2015. **33**(9): p. 941-951.
155. Carrasco, M.J., et al., *Ionization and structural properties of mRNA lipid nanoparticles influence expression in intramuscular and intravascular administration.* Communications Biology, 2021. **4**(1).
156. Drummond, D.C., et al., *DISULFIDE - STABILIZED FABS*, U. Patent, Editor. 2018, Merrimack Pharmaceuticals Inc: United States.
157. Béduneau, A., et al., *Design of targeted lipid nanocapsules by conjugation of whole antibodies and antibody Fab' fragments.* Biomaterials, 2007. **28**(33): p. 4978-4990.
158. Hermanson, G.T., *Chapter 18 - PEGylation and Synthetic Polymer Modification*, in *Bioconjugate Techniques (Third Edition)*, G.T. Hermanson, Editor. 2013, Academic Press: Boston. p. 787-838.
159. Müller, T., et al., *Expression of a CD20-specific chimeric antigen receptor enhances cytotoxic activity of NK cells and overcomes NK-resistance of lymphoma and leukemia cells.* Cancer Immunology, Immunotherapy, 2008. **57**(3): p. 411-423.
160. Lee, D.W., et al., *T cells expressing CD19 chimeric antigen receptors for acute lymphoblastic leukaemia in children and young adults: a phase 1 dose-escalation trial.* The Lancet, 2015. **385**(9967): p. 517-528.
161. Kochenderfer, J.N., et al., *B-cell depletion and remissions of malignancy along with cytokine-associated toxicity in a clinical trial of anti-CD19 chimeric-antigen-receptor–transduced T cells.* Blood, 2012. **119**(12): p. 2709-2720.
162. McKinlay, C.J., et al., *Enhanced mRNA delivery into lymphocytes enabled by lipid-varied libraries of charge-altering releasable transporters.* Proceedings of the National Academy of Sciences, 2018. **115**(26): p. E5859-E5866.
163. Goebeler, M.-E. and R.C. Bargou, *T cell-engaging therapies — BiTEs and beyond.* Nature Reviews Clinical Oncology, 2020. **17**(7): p. 418-434.
164. Zhou, S., et al., *The landscape of bispecific T cell engager in cancer treatment.* Biomarker Research, 2021. **9**(1).
165. Huang, C., et al., *Lipid Nanoparticle Delivery System for mRNA Encoding B7H3-redirected Bispecific Antibody Displays Potent Antitumor Effects on Malignant Tumors.* Adv Sci (Weinh), 2023. **10**(3): p. e2205532.

166. Suurs, F.V., et al., *A review of bispecific antibodies and antibody constructs in oncology and clinical challenges.* Pharmacology & Therapeutics, 2019. **201**: p. 103-119.
167. Yuraszeck, T., S. Kasichayanula, and J. Benjamin, *Translation and Clinical Development of Bispecific T-cell Engaging Antibodies for Cancer Treatment.* Clinical Pharmacology & Therapeutics, 2017. **101**(5): p. 634-645.
168. Godbersen-Palmer, C., et al., *Toxicity Induced by a Bispecific T Cell–Redirecting Protein Is Mediated by Both T Cells and Myeloid Cells in Immunocompetent Mice.* The Journal of Immunology, 2020. **204**(11): p. 2973-2983.
169. Stein, A., et al., *Benefit–Risk Assessment of Blinatumomab in the Treatment of Relapsed/Refractory B-Cell Precursor Acute Lymphoblastic Leukemia.* Drug Safety, 2019. **42**(5): p. 587-601.
170. Topp, M.S., et al., *Safety and activity of blinatumomab for adult patients with relapsed or refractory B-precursor acute lymphoblastic leukaemia: a multicentre, single-arm, phase 2 study.* The Lancet Oncology, 2015. **16**(1): p. 57-66.
171. Wilson, K., E. Shiuan, and D.M. Brantley-Sieders, *Oncogenic functions and therapeutic targeting of EphA2 in cancer.* Oncogene, 2021. **40**(14): p. 2483-2495.
172. Wykosky, J. and W. Debinski, *The EphA2 Receptor and EphrinA1 Ligand in Solid Tumors: Function and Therapeutic Targeting.* Molecular Cancer Research, 2008. **6**(12): p. 1795-1806.
173. Xiao, T., et al., *Targeting EphA2 in cancer.* Journal of Hematology & Oncology, 2020. **13**(1).
174. Kinch, M.S., M.B. Moore, and D.H. Harpole, Jr., *Predictive value of the EphA2 receptor tyrosine kinase in lung cancer recurrence and survival.* Clin Cancer Res, 2003. **9**(2): p. 613-8.
175. Hammond, S.A., et al., *Selective Targeting and Potent Control of Tumor Growth Using an EphA2/CD3-Bispecific Single-Chain Antibody Construct.* Cancer Research, 2007. **67**(8): p. 3927-3935.
176. Iwahori, K., et al., *Engager T Cells: A New Class of Antigen-specific T Cells That Redirect Bystander T Cells.* Molecular Therapy, 2015. **23**(1): p. 171-178.
177. Hao, S., et al., *BiTE secretion from in situ-programmed myeloid cells results in tumor-retained pharmacology.* J Control Release, 2022. **342**: p. 14-25.
178. Lewis, M.D., et al., *A reproducible method for the expansion of mouse CD8+ T lymphocytes.* J Immunol Methods, 2015. **417**: p. 134-138.
179. Kheirolomoom, A., et al., *In situ T-cell transfection by anti-CD3-conjugated lipid nanoparticles leads to T-cell activation, migration, and phenotypic shift.* Biomaterials, 2022. **281**: p. 121339.
180. Ansari, A.M., et al., *Cellular GFP Toxicity and Immunogenicity: Potential Confounders in in Vivo Cell Tracking Experiments.* Stem Cell Reviews and Reports, 2016. **12**(5): p. 553-559.
181. Ziegler, S.F., F. Ramsdell, and M.R. Alderson, *The activation antigen CD69.* Stem Cells, 1996. **12**(5): p. 456-465.
182. Bousso, P., *T-cell activation by dendritic cells in the lymph node: lessons from the movies.* Nature Reviews Immunology, 2008. **8**(9): p. 675-684.
183. Loubaki, L., T. Tremblay, and R. Bazin, *In vivo depletion of leukocytes and platelets following injection of T cell-specific antibodies into mice.* Journal of Immunological Methods, 2013. **393**(1): p. 38-44.
184. Chatenoud, L., *CD3-specific antibody-induced active tolerance: from bench to bedside.* Nature Reviews Immunology, 2003. **3**(2): p. 123-132.

185. Zhu, M., et al., *Blinatumomab, a Bispecific T-cell Engager (BiTE®) for CD-19 Targeted Cancer Immunotherapy: Clinical Pharmacology and Its Implications.* Clinical Pharmacokinetics, 2016. **55**(10): p. 1271-1288.
186. Arvedson, T., et al., *Targeting Solid Tumors with Bispecific T Cell Engager Immune Therapy.* Annual Review of Cancer Biology, 2022. **6**(1): p. 17-34.
187. Kamoun, W.S., et al., *Antitumour activity and tolerability of an EphA2-targeted nanotherapeutic in multiple mouse models.* Nature Biomedical Engineering, 2019. **3**(4): p. 264-280.
188. Ventola, C.L., *Cancer Immunotherapy, Part 3: Challenges and Future Trends.* P t, 2017. **42**(8): p. 514-521.
189. Kobiyama, K. and K.J. Ishii, *Making innate sense of mRNA vaccine adjuvanticity.* Nature Immunology, 2022. **23**(4): p. 474-476.
190. Li, C., et al., *Mechanisms of innate and adaptive immunity to the Pfizer-BioNTech BNT162b2 vaccine.* Nature Immunology, 2022. **23**(4): p. 543-555.
191. Datta, M., et al., *Reprogramming the Tumor Microenvironment to Improve Immunotherapy: Emerging Strategies and Combination Therapies.* American Society of Clinical Oncology Educational Book, 2019(39): p. 165-174.
192. Wen, H., et al., *Pre-clinical efficacy of CD20-targeted chimeric antigen receptor T cells for non-Hodgkin's lymphoma.* Discover Oncology, 2022. **13**(1): p. 122.
193. Kozma, G.T., et al., *Anti-PEG antibodies: Properties, formation, testing and role in adverse immune reactions to PEGylated nano-biopharmaceuticals.* Advanced Drug Delivery Reviews, 2020. **154-155**: p. 163-175.
194. Ishida, T., et al., *Accelerated clearance of PEGylated liposomes in rats after repeated injections.* Journal of Controlled Release, 2003. **88**(1): p. 35-42.
195. Dams, E.T., et al., *Accelerated blood clearance and altered biodistribution of repeated injections of sterically stabilized liposomes.* J Pharmacol Exp Ther, 2000. **292**(3): p. 1071-9.
196. Lundstrom, K., *Self-Replicating RNA Viruses for RNA Therapeutics.* Molecules, 2018. **23**(12): p. 3310.
197. Tarab-Ravski, D., L. Stotsky-Oterin, and D. Peer, *Delivery strategies of RNA therapeutics to leukocytes.* Journal of Controlled Release, 2022. **342**: p. 362-371.
198. Chen, R., et al., *Engineering circular RNA for enhanced protein production.* Nature Biotechnology, 2023. **41**(2): p. 262-272.
199. Kulkarni, J.A., et al., *The current landscape of nucleic acid therapeutics.* Nature Nanotechnology, 2021. **16**(6): p. 630-643.
200. Nawaz, W., et al., *AAV-mediated in vivo CAR gene therapy for targeting human T-cell leukemia.* Blood Cancer Journal, 2021. **11**(6): p. 119.
201. Xin, T., et al., *In-Vivo Induced CAR-T Cell for the Potential Breakthrough to Overcome the Barriers of Current CAR-T Cell Therapy.* Front Oncol, 2022. **12**: p. 809754.
202. Zhao, Y. and L. Huang, *Lipid nanoparticles for gene delivery.* Adv Genet, 2014. **88**: p. 13-36.
203. Yin, H., et al., *Non-viral vectors for gene-based therapy.* Nature Reviews Genetics, 2014. **15**(8): p. 541-555.
204. Wright, J.C., *Cancer Chemotherapy: Past, Present, and Future - Part I.* Journal of the National Medical Association, 1984. **76**.